

TEXAS
TRANSPORTATION
INSTITUTE

TEXAS
HIGHWAY
DEPARTMENT

COOPERATIVE
RESEARCH

**BEARING CAPACITY PREDICTION BY WAVE
EQUATION ANALYSIS--STATE
OF THE ART**

in cooperation with the
Department of Transportation
Federal Highway Administration

**RESEARCH REPORT 125-8F
STUDY 2-5-67-125
BEARING CAPACITY FOR AXIALLY LOADED PILES**

1. Report No.		2. Government Accession No.		3. Recipient's Catalog No.	
4. Title and Subtitle BEARING CAPACITY PREDICTION BY WAVE EQUATION ANALYSIS - STATE OF THE ART				5. Report Date August 1973	
7. Author(s) Harry M. Coyle, Richard E. Bartoskewitz and William J. Berger				6. Performing Organization Code	
9. Performing Organization Name and Address Texas Transportation Institute Texas A & M University College Station, Texas 77843				8. Performing Organization Report No. Research Report 125-8 F	
12. Sponsoring Agency Name and Address Texas Highway Department 11th and Brazos Austin, Texas 78701				10. Work Unit No.	
				11. Contract or Grant No. Research Study 2-5-67-125	
15. Supplementary Notes Research performed in cooperation with DOT, FHWA Research Study Title: "Bearing Capacity for Axially Loaded Piles"				13. Type of Report and Period Covered Final - September 1967 August 1973	
				14. Sponsoring Agency Code	
16. Abstract A procedure for predicting the bearing capacity of an axially loaded pile is presented herein. Field data consisting of measured dynamic forces and static loads are correlated with predicted results obtained from wave equation analyses. The field data are obtained from five full-scale instrumented pile tests in clay and sand. Soil quake values and soil damping values are determined for both clay and sand. Application of wave equation analysis for predicting bearing capacity and driving stresses is discussed. Conclusions and recommendations are presented to summarize the state-of-the-art.					
17. Key Words Wave Equation Analyses, Predicted Bearing Capacity, Predicted Driving Stresses, Soil Quake, Soil Damping, Dynamic Pile Tests, Static Pile Tests, Piles in Clay, Piles in Sand				18. Distribution Statement	
19. Security Classif. (of this report) Unclassified		20. Security Classif. (of this page) Unclassified		21. No. of Pages 134	22. Price

BEARING CAPACITY PREDICTION BY WAVE
EQUATION ANALYSIS - STATE OF THE ART

By

Harry M. Coyle
Research Engineer

Richard E. Bartoskewitz
Engineering Research Associate

and

William J. Berger
Research Assistant

Research Report Number 125-8 (Final)

Bearing Capacity for Axially Loaded Piles
Research Study Number 2-5-67-125

Sponsored by
The Texas Highway Department
In Cooperation with the
U. S. Department of Transportation
Federal Highway Administration

August 1973

TEXAS TRANSPORTATION INSTITUTE
Texas A&M University
College Station, Texas

Disclaimer

The contents of this report reflect the views of the authors who are responsible for the facts and the accuracy of the data presented herein. The contents do not necessarily reflect the official views or policies of the Federal Highway Administration. This report does not constitute a standard, specification, or regulation.

ABSTRACT

A procedure for predicting the bearing capacity of an axially loaded pile is presented herein. Field data consisting of measured dynamic forces and static loads are correlated with predicted results obtained from wave equation analyses. The field data are obtained from five full-scale instrumented pile tests in clay and sand. Soil quake values and soil damping values are determined for both clay and sand. Application of wave equation analysis for predicting bearing capacity and driving stresses is discussed. Conclusions and recommendations are presented to summarize the state-of-the-art.

KEY WORDS: Wave Equation Analyses, Predicted Bearing Capacity, Predicted Driving Stresses, Soil Quake, Soil Damping, Dynamic Pile Tests, Static Pile Tests, Piles in Clay, Piles in Sand

SUMMARY

The information presented in this report was developed during the sixth and final year of Research Study 2-5-67-125 which was a cooperative research study entitled "Bearing Capacity for Axially Loaded Piles" sponsored jointly by the Texas Highway Department and the Federal Highway Administration.

A brief history of the one-dimensional wave equation application to the pile driving problem is presented in this final report. Simulation techniques for the pile-hammer and pile-soil systems are discussed.

Results of static load tests on five instrumented test piles are tabulated and load vs. settlement curves are plotted. Physical descriptions of the test piles and soil profiles at the test sites are given and the driving records are summarized.

Static load test data are used to compute normalized load transfer and tip load vs. movement curves for sand and clay, and soil quake values are determined for each soil type for loading and unloading conditions. Dynamic force vs. time data from the head of each test pile were recorded during driving and re-driving eight to eleven days later. The dynamic data are used to determine friction damping and point damping values for sand and clay which produce the best overall correlation between measured and computed pile stresses and blow counts. The procedure for predicting pile bearing capacity by wave equation analysis is described. A bearing graph is produced for

each test pile and the predicted capacities are tabulated and compared with the capacities measured by load test.

Applications of wave equation analysis to several common pile driving problems are illustrated. Field control of driving stresses, development of bearing capacity versus depth curves, and comparison of various hammer types are considered.

IMPLEMENTATION STATEMENT

The findings of this study as presented in this state-of-the-art report on bearing capacity of axially loaded piles are recommended for immediate implementation by concerned personnel. Unqualified use of the data given in this report should be limited to applications where- in the soil conditions are essentially the same as those surrounding the piles tested during the research study. Different soil conditions should warrant one or more load tests to validate the adequacy of the findings of this report for the existing situation.

TABLE OF CONTENTS

	PAGE
INTRODUCTION	1
Historical Background	1
Research Objectives	2
WAVE EQUATION ANALYSIS	4
Pile-Hammer Simulation	4
Pile-Soil Simulation	6
INSTRUMENTED TEST PILES	11
Port Arthur Test Piles	11
Corpus Christi Test Pile	14
Harlingen Test Piles	15
ANALYSIS OF TEST PILE DATA	22
General Method of Analysis	22
Dynamic Forces and Static Loads	24
Soil Quake	26
Soil Damping	41
Pile Stresses	43
Bearing Capacity	49
APPLICATIONS OF WAVE EQUATION ANALYSIS	61
CONCLUSIONS AND RECOMMENDATIONS	73
Conclusions	73
Recommendations	74
APPENDIX I - REFERENCES	76
APPENDIX II - FIELD TEST AND COMPUTER INPUT DATA	78

LIST OF TABLES

TABLE		PAGE
1	SUMMARY OF STATIC LOAD TEST RESULTS FOR TEST PILES	20
2	SUMMARY OF LOADING SOIL QUAKE VALUES FOR TEST PILES	35
3	SUMMARY OF PILE STRESSES AND BLOW COUNTS FOR CORPUS CHRISTI INITIAL USING DIFFERENT SOIL DAMPING VALUES, FORCE-TIME DATA AND Q-SIDE = 0.2, Q-POINT = 0.4	44
4	SUMMARY OF SOIL DAMPING VALUES FOR ALL FIVE TEST PILES . .	43
5	SUMMARY OF DYNAMIC PEAK COMPRESSIVE FORCES FOR PORT ARTHUR PILES	46
6	SUMMARY OF DYNAMIC PEAK COMPRESSIVE FORCES FOR CORPUS CHRISTI TEST PILE	47
7	SUMMARY OF DYNAMIC PEAK COMPRESSIVE FORCES FOR HARLINGEN TEST PILES	48
8	SUMMARY OF PREDICTED BEARING CAPACITY RESULTS FOR TEST PILES	59

LIST OF FIGURES

FIGURE		PAGE
1	HAMMER-PILE SYSTEM	5
2	PILE-SOIL SYSTEM	7
3	LOAD-DEFORMATION CHARACTERISTIC OF PILE-SOIL MODEL . . .	9
4	SOIL PROFILE FOR PORT ARTHUR TEST PILE NO. 1	12
5	SOIL PROFILE FOR PORT ARTHUR TEST PILE NO. 2	13
6	SOIL PROFILE FOR CORPUS CHRISTI TEST PILE	16
7	SOIL PROFILE FOR HARLINGEN TEST PILE 99R	18
8	SOIL PROFILE FOR HARLINGEN TEST PILE 4L	19
9	LOAD TRANSFER VS. MOVEMENT CURVES PORT ARTHUR PILE NO. 1 TEST NO. 1	27
10	LOAD TRANSFER VS. MOVEMENT CURVES CORPUS CHRISTI TEST PILE - INITIAL TEST	29
11	LOAD TRANSFER VS. MOVEMENT CURVES FOR CLAY	30
12	POINT LOAD VS. MOVEMENT CURVES FOR CLAY	31
13	LOAD TRANSFER VS. MOVEMENT CURVES FOR SAND	32
14	POINT LOAD VS. MOVEMENT CURVES FOR SAND	33
15	PERCENT LOAD TRANSFER VS. MOVEMENT FOR CLAY	36
16	PERCENT POINT LOAD VS. MOVEMENT FOR CLAY	37
17	PERCENT LOAD TRANSFER VS. MOVEMENT FOR SAND	38
18	PERCENT POINT LOAD VS. MOVEMENT FOR SAND	39
19	SOIL LOAD-DEFORMATION CURVES	51
20	RUT VS. BLOW COUNT CURVES FOR PORT ARTHUR NO. 1	54
21	RUT VS. BLOW COUNT CURVES FOR PORT ARTHUR NO. 2	55

LIST OF FIGURES - CONTINUED

FIGURE		PAGE
22	RUT VS. BLOW COUNT CURVES FOR CORPUS CHRISTI TEST PILE	56
23	RUT VS. BLOW COUNT CURVES FOR HARLINGEN 99R	57
24	RUT VS. BLOW COUNT CURVES FOR HARLINGEN 4L	58
25	MAXIMUM TENSILE STRESS AND BLOW COUNT VS. SOIL RESISTANCE	65
26	MINIMUM ALLOWABLE BLOW COUNT FOR PREVENTION OF CRITICAL TENSILE STRESS	66
27	DETERMINATION OF BEARING CAPACITY VS. DEPTH FROM DRIVING RECORD	68

ACKNOWLEDGEMENTS

Throughout the six-year period of this research study many persons and agencies, both individually and collectively, rendered inestimable assistance towards the completion of the study objectives. The authors sincere thanks and appreciation are extended to the Federal Highway Administration and the Texas Highway Department, whose cooperative sponsorship made the research possible.

The greatest debt of gratitude is owed to the personnel of the Texas Highway Department for their assistance during the entire study. Particular thanks are accorded to Messrs. Wayne Henneberger, Farland Bundy, Clarence Rea, H. D. Butler, Horace Hoy, and Chet Safe for their cooperation and support. Sincere appreciation is also expressed to the personnel of Texas Highway Department Districts 16 (Corpus Christi), 20 (Beaumont), and 21 (Pharr), and to the Resident Engineers and their assistants within those districts, who worked so diligently to coordinate the field tests and ensure their success.

Recognition is also given to Heldenfels Bros. of Corpus Christi, and Baass Bros. Concrete Co. of Victoria, for their interest and spirited cooperation during the installation of instrumentation in concrete piling.

Grateful acknowledgement is given to Messrs. T. J. Hirsch, Lee L. Lowery, Jr., Lionel J. Milberger, and Thomas C. Bennett, of the Texas Transportation Institute, for their technical assistance, counsel, and support. The contributions of Research Assistants Gary C. Gibson,

Kenneth W. Korb, Joseph D. Rehmert, George W. Perdue, Dirk A. van Reenen,
and Graduate Student Robert Foye, Jr., are especially acknowledged.

INTRODUCTION

Historical Background. - Over the years, the use of piles for foundations of heavy structures and the use of new pile driving methods has created more and more interest in finding a reliable method to predict pile bearing capacity. Issacs (11)* is credited in 1931 with first noting the applicability of the one-dimensional wave equation to the piling behavior problem. In 1932, Fox (6) proposed an exact solution for the piling behavior problem, which was later verified by Glanville (10) in 1938. However, the solution was very complex and, since electronic computers were not available, many simplifying assumptions had to be made. In 1940, Cummings (3) reviewed the earlier work and noted the long and complicated mathematical expressions involved in the solutions. Smith (19) made a real contribution in 1950 by developing a solution to the wave equation based on a discrete element idealization of the actual hammer-pile-soil system. Then, in 1960 Smith (18) published a paper which dealt exclusively with the application of wave theory to the investigation of piling behavior during driving.

The research effort on wave equation analysis of piling behavior began at Texas A&M University in 1962. The Texas Highway Department at that time was experiencing difficulty involving the cracking of long prestressed concrete piles. Consequently the main research effort

*Numbers in parentheses refer to the references listed in Appendix I.

during the period 1962 to 1967 was directed towards the development of good driving practices which would prevent the cracking of these piles. From 1967 to the present, the main research effort has been directed towards the prediction of pile bearing capacity by wave equation analysis. For the past several years a number of instrumented pile tests have been conducted at actual bridge sites and the field test data have been used to determine improved soil parameters for use in predicting bearing capacity.

Research Objectives. - Because this is a final report covering the research accomplishments since 1967, it is appropriate to state the objectives of the study. The broad objective of the study was to develop a procedure using wave equation analysis whereby the bearing capacity of an axially loaded pile could be predicted for any hammer-pile-soil system. To accomplish this broad objective the study was divided into three phases as follows:

Phase I - The objective of this phase was to conduct laboratory tests on a variety of soils in order to study dynamic soil properties, and to develop and test a miniature test pile in preparation for full-scale instrumented pile tests.

Phase II - The objective of this phase was to develop and test full-scale instrumented test piles at actual bridge sites, and correlate dynamic and static resistance using the field test data.

Phase III - The objective of this phase was to accomplish the final analysis and correlation of the field test data and develop the most current design procedure for predicting the bearing capacity of an axially loaded pile by wave equation analysis.

This is the final state-of-the-art report for this research study. It contains the information necessary to satisfy the objective of Phase III. In addition to this report there have been seven other research progress reports published. Research reports 125-1 (9), 125-2 (12), and 125-3 (17) cover the research progress made under Phase I. Research reports 125-4 (16), 125-5 (1), 125-6 (20), and 125-7 (7) cover the research progress made during Phase II.

WAVE EQUATION ANALYSIS

Pile-Hammer Simulation. - The accomplishments of the research effort on wave equation analysis during the period 1962-1967 are published in research report 33-13 (14). The state-of-the-art report covers in some detail the numerical solution of the wave equation, the recommended methods of simulation for the various pile driving hammers, and the recommended load-deformation properties for the various cushion and capblock materials. Also, research report 33-9 contains a listing of the wave equation computer program and a utilization manual.

A generalized simulation of the hammer-pile system is shown in Fig. 1. The various computer input parameters required for the hammer-pile simulation include initial impact velocity, the weights of the different components, the stiffnesses and coefficients of restitution of the various materials, and a slack parameter which equals explosive force for diesel hammers or is used to specify the ability to transmit tension for other hammers. The wave equation computer program has been formulated to handle drop hammers; single, double, and differential acting steam hammers; and diesel hammers. The hammer-pile simulation would differ for each hammer type and would not necessarily be the same as represented in Fig. 1. The simulation of the different type hammers is given in detail in Appendix B of research report 33-13 (14).

The hammer-pile simulation shown in Fig. 1 is representative of the driving components used for a prestressed concrete pile. The instrumented

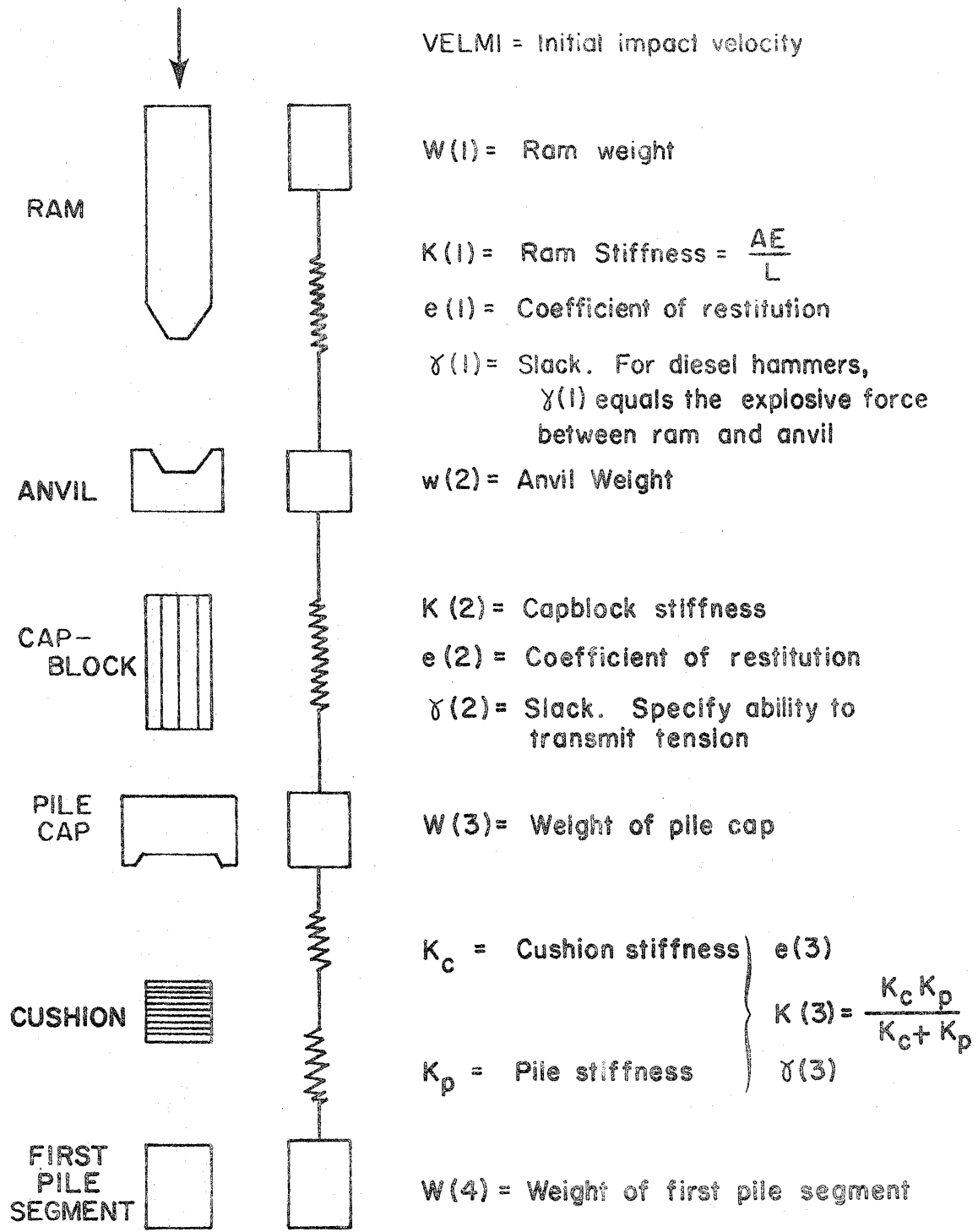


FIG.1 - HAMMER - PILE SYSTEM

piles which were tested during this research study included both prestressed concrete and steel pipe piles. In the case of the steel pipe pile, the hammer-pile simulation would normally involve steel-on-steel impact between the pile cap (adapter) and the pile. The simulation shown in Fig. 1 would be changed by replacing the pile cap with an adapter and removing the cushion. Consequently, the stiffness $K(3)$ of Fig. 1 would represent the stiffness of the first pile segment only. As was reported in research report 125-7 (7), it was necessary to make changes in the stiffness values in order to match measured and computed force-time data for the instrumented test piles. These changes in stiffness values are discussed and justified in research report 125-7 (7), and in this report in the section on analysis of test pile data.

Pile-Soil Simulation. The state-of-the-art accomplishments of this research effort on wave equation analysis during the period 1967-present are mainly concerned with the pile-soil system. This report covers in some detail the methods of instrumenting the test piles and the procedures used to conduct the field load tests. The section on analysis of test pile data covers the correlation of dynamic and static resistance using the data obtained from the field tests. Also, the application of wave equation analysis for use in predicting bearing capacity and driving stresses is reviewed and recommended design procedures are given.

The pile-soil system simulation used in the wave equation analysis is given in Fig. 2. The computer input parameters needed for the pile-soil simulation include the static soil resistance, the soil quake, and the soil damping. The static soil resistance is input as

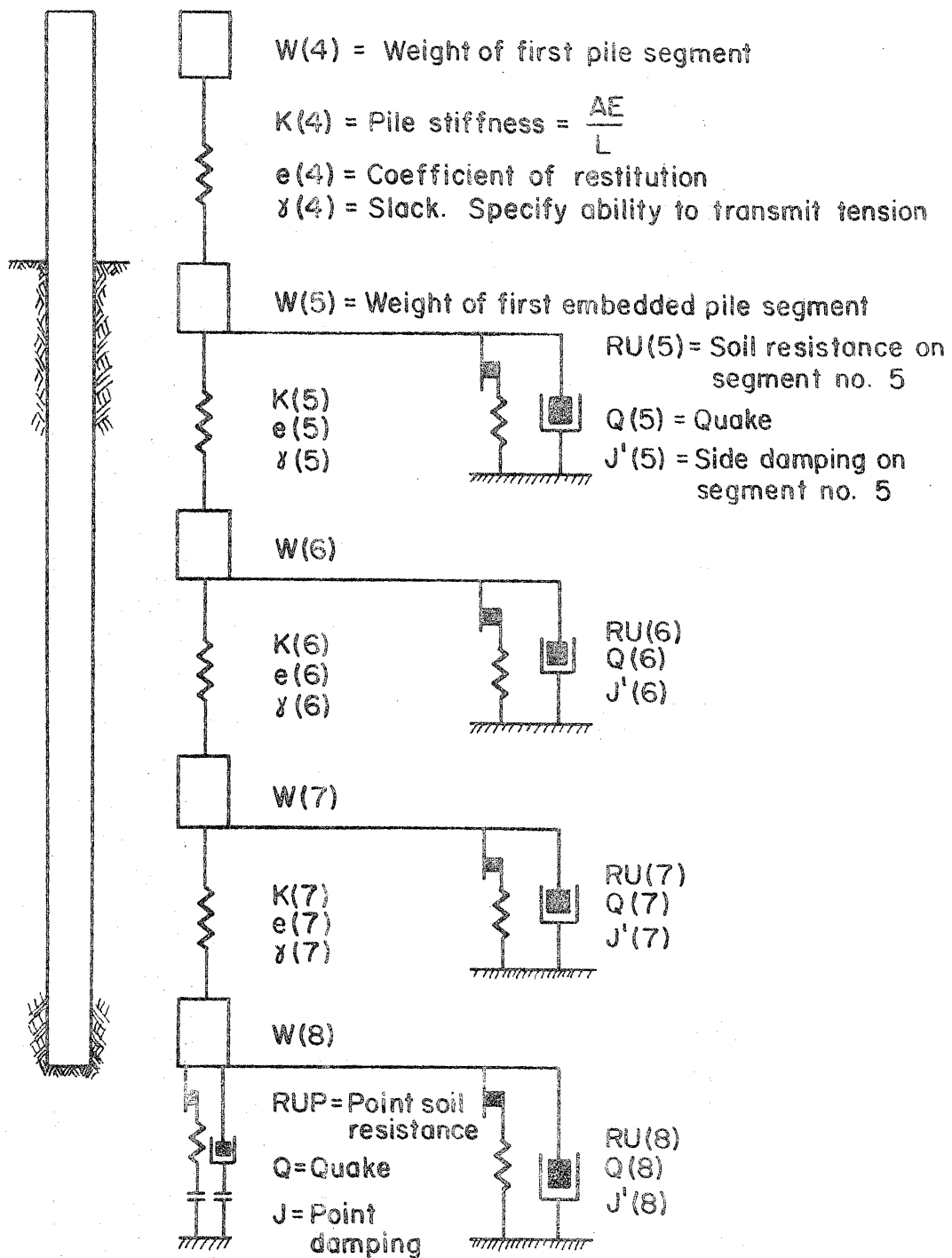


FIG. 2 — PILE — SOIL SYSTEM

point resistance-RUP and the side resistance-RU, which can be distributed uniformly or in accordance with any variation in the soil profile. The total soil resistance-RUT is the sum of the side resistance and the point resistance. Soil quake-Q, which is the amount of static deformation the soil will experience before failure as shown in Fig. 3a, is input both along the side and at the point of the pile. The magnitude of the quake can be different for different soil types, and the loading and unloading value can differ. The soil damping, which accounts for the dynamic soil behavior, is input as side damping-J' and point damping-J. The magnitude of the soil damping can be different for different soil types and the values of side damping and point damping can differ.

The soil load-deformation relationship used in the wave equation analysis is shown in Fig. 3a, and the pile-soil model is shown in Fig. 3b. The soil resistance mobilized during dynamic loading is determined using the equation given in Fig. 3b. The terms appearing in this equation are defined as follows:

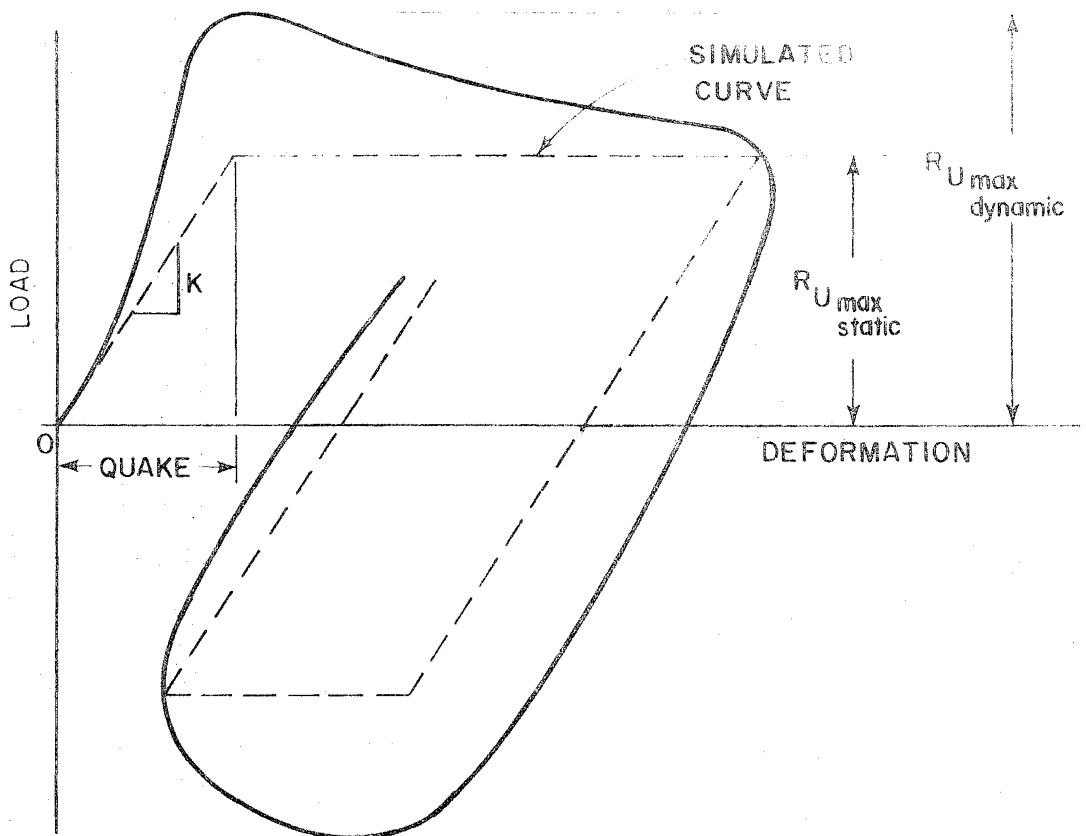
R_u = dynamic or static soil resistance, pounds;

J = a damping constant for the soil at the point of the pile, seconds per foot;

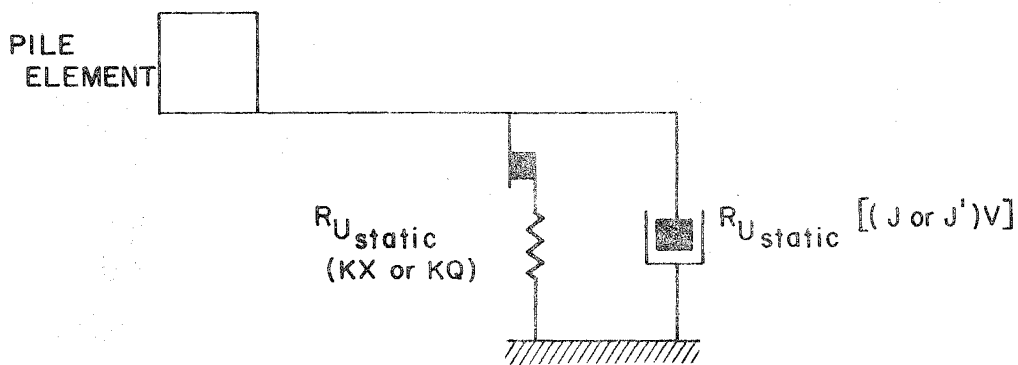
J' = a damping constant for the soil along the side of the pile, seconds per foot; and

V = the instantaneous velocity of a segment of the pile at a given time, feet per second.

As a result of the laboratory tests conducted in 1968 by Gibson (9) and the model tests conducted in 1969 by Korb (12), this equation was modified by raising the velocity term to a power N, where $0 < N \leq 1.0$. Later studies using some of the initial field test data were made by



(a) LOAD - DEFORMATION CURVE



$$R_{U\ dynamic} = R_{U\ static} [1 + (J\ or\ J')V] \quad \text{DEFORMATION} < Q$$

$$R_{U\ dynamic} = R_{U\ static} + R_{U\max\ static} (J\ or\ J')V \quad \text{ONCE DEFORMATION EXCEEDS } Q \text{ AND THERE AFTER}$$

(b) PILE - SOIL MODEL

FIG. 3 - LOAD - DEFORMATION CHARACTERISTIC OF PILE - SOIL MODEL

Bartoskewitz (1) in 1970 and VanReenen (20) in 1971. These studies showed that, at the higher velocities experienced in the field, the damping parameters J and J' were constant for velocity raised to the power $N = 1.0$. Therefore, the equation shown in Fig. 3b was used in the wave equation analysis of all field test piles.

It is important to note at this point in this final report that the reliability of predicted bearing capacity and predicted driving stresses is primarily a function of the correctness of the soil parameters used in the wave equation analysis. The main research effort during the past year has been directed towards the determination of appropriate soil parameters. The static test data from five instrumented field test piles have been used to determine appropriate values of soil quake for sand and clay. Using measured dynamic force-time data as input at the pile head from the five test piles and the appropriate static soil quake values, a satisfactory combination of side and point damping has been determined. The correctness of the soil parameters has been verified by comparing computed bearing capacities and pile stresses with measured test pile data. These soil parameters are applicable to soil and driving conditions which approximate those which existed at the time the data were acquired from which the parameters were derived. For wave equation analysis of piles under dissimilar conditions it will be recommended that at least one load test be performed to either substantiate the suitability of the parameters for the given conditions, or establish new parameters by correlation of theoretical and measured test loads in a manner consonant with the procedures discussed in the "Analysis of Test Pile Data" section of this report.

INSTRUMENTED TEST PILES

Port Arthur Test Piles. - During November, 1969, two instrumented test piles were driven and load tested at the Intracoastal Canal Bridge on State Highway 87, south of Port Arthur, Texas. Both piles were 16-in. OD, 3/8 in. wall thickness, closed end steel pipe piles driven by a Link Belt 520 diesel hammer. Test pile No. 1 (PA 1) had a total length of 67 feet and an embedded length of 62 ft. Test pile No. 2 (PA 2) had a total length of 78 ft and was embedded 74 ft. Both piles were statically load tested using the Texas Highway Department Quick-Load Test Method (8). The initial load test was conducted within two hours after driving and the final load test was conducted 11 days after driving. The piles were re-driven approximately 5 ft upon completion of the 11 day static load tests.

Strain gage bridges at the pile head and tip were used to determine the total static soil resistance (RUF) and the point-bearing resistance (RUP) during each load test. Dynamic force-time data for each strain gage bridge location were recorded during initial driving and final re-driving. Soil profiles and locations of strain gage bridges for the Port Arthur piles are shown in Figs. 4 and 5. The predominant soil formation at Port Arthur was Beaumont Clay overlain by recent river deposits. The water table was approximately 3 ft below the ground surface.

DEPTH (FT)	STRAIN GAGE BRIDGE LOCATIONS	SOIL SYMBOL	DESCRIPTION OF STRATUM	DRY DENSITY LB/CU FT.	MOISTURE CONTENT %	LIQUID LIMIT	PLASTIC LIMIT	UNCONFINED SHEAR STR. (PSF)
0	☒							
10			DARK ORGANIC CLAY		* FIELD VANE SHEAR VALUES			* 300 * 240 * 360 * 1000
20	☒		WET TAN & GRAY SILTY CLAY	92.6	22.6	78.9	18.2	2820
30			WET TAN & GRAY CLAYEY SILT	90.5	30.5	78.4	31.3	1480
40	☒		WET GRAY CLAY WITH SOME SHELL	84.5	42.6	85.5	30.7	2510
50			WET TAN & GRAY SILTY CLAY					
60	☒			105.4	18.4	67.8	18.8	1675
	☒		PLASTIC GRAY CLAY	112.1	16.2	50	17.9	1870

FIG.4 - SOIL PROFILE FOR PORT ARTHUR TEST PILE NO.1

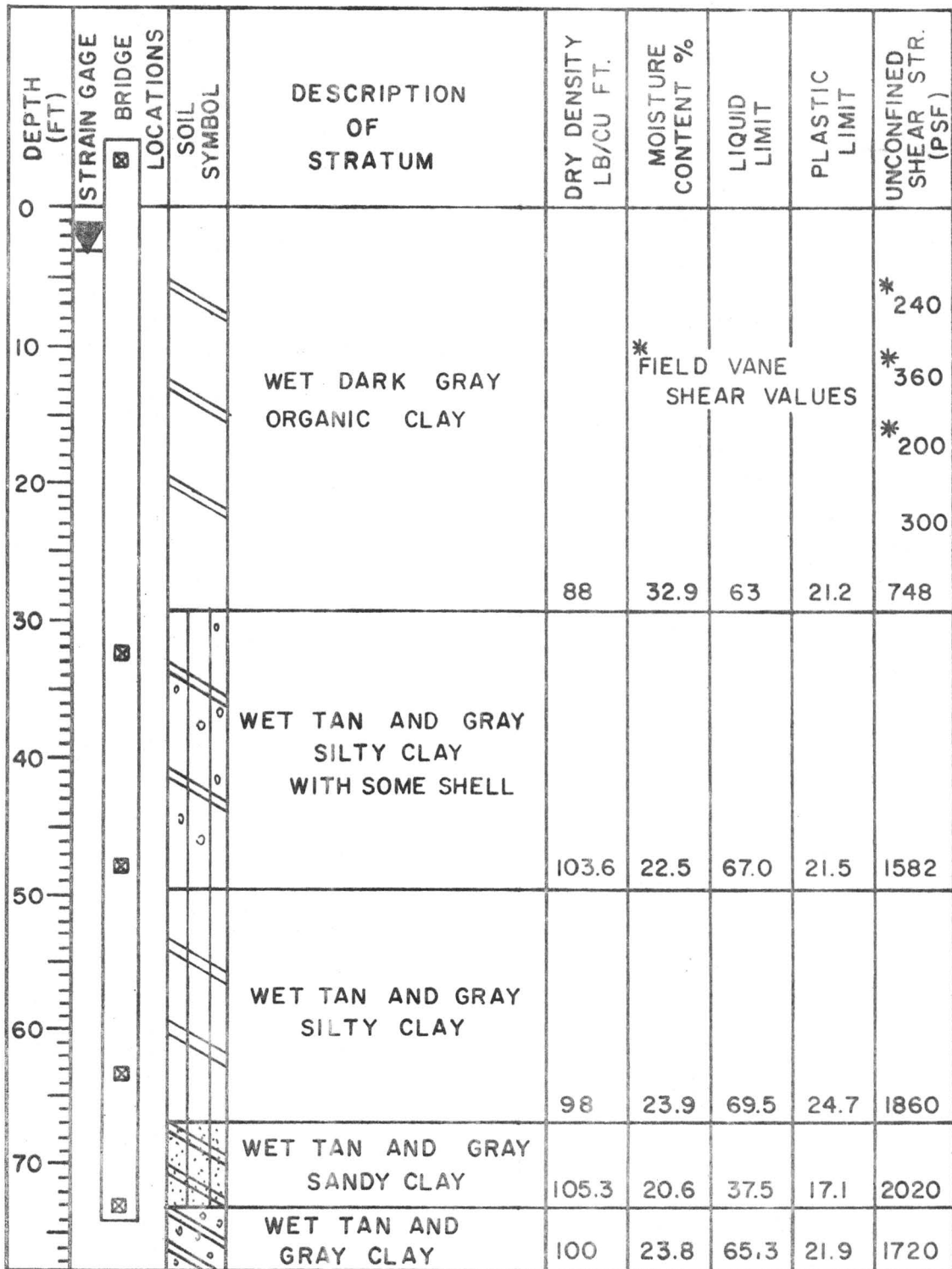


FIG.-5 -SOIL PROFILE FOR PORT ARTHUR TEST PILE NO.2

Blow counts of 16 blows per foot for PA 1 at initial driving (PA 1-Initial) and 18 blows per foot for PA 2 at initial driving (PA 2-Initial) were recorded for the last foot of driving. The blow counts for PA 1 Final (final re-driving) and PA 2-Final (final re-driving) were determined by averaging the relatively constant blow counts encountered after the piles were broken loose and moving relative to the soil. The re-driving blow count for PA 1-Final was 72 blows per foot and for PA 2-Final it was 200 blows per foot. The load settlement curves, static load test data, driving records, and computer input data used in wave equation analyses are given in Appendix II.

Corpus Christi Test Pile. - During May, 1971, a 16 in. square prestressed concrete pile was driven and statically load tested at Park Road 22 on the Intracoastal Waterway near Corpus Christi, Texas. A Delmag D-22 diesel hammer was used to drive the pile to an embedded depth of 28.5 ft. The total length of the test pile was 38 ft. Static load tests were conducted using the Quick-Load Test Method within 1 1/2 hours after completion of initial driving, 7 days later, and again at 10 days. The pile was re-driven approximately 4 ft upon the completion of the 10 day test.

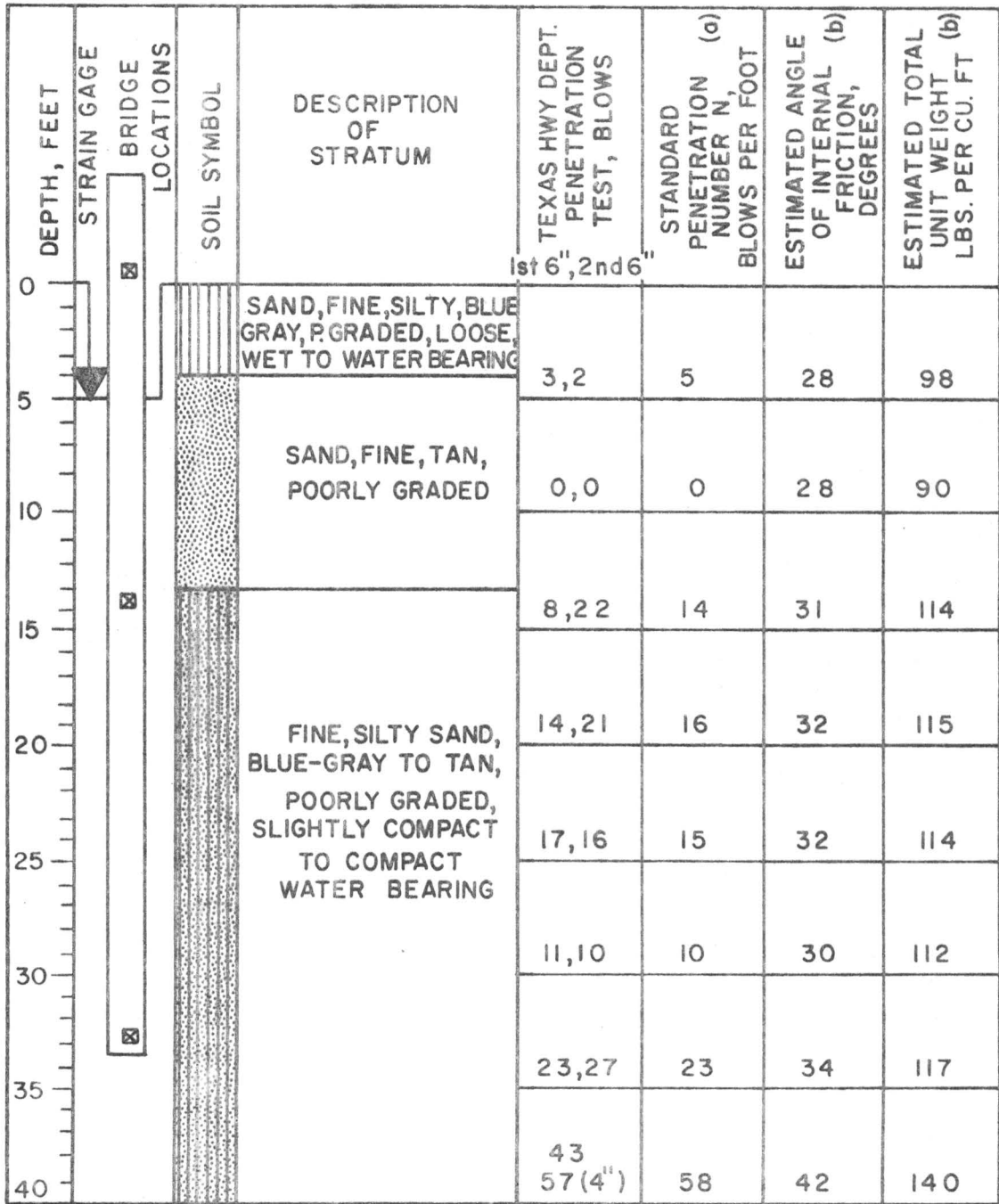
The same set of measurements was obtained for the Corpus Christi test pile as previously discussed for the Port Arthur test piles. Strain gages bridges were employed near the pile head and tip to measure RUT and RUP during static load tests and to obtain dynamic force-time data at each gage location during initial driving

(CC Initial) and final re-driving (CC-Final). The soil profile and location of the strain gage bridges for the Corpus Christi pile are shown in Fig. 6. The soil profile shows the test pile to be entirely embedded in saturated sand with the water table at a depth of 5 ft below the ground surface. The load-settlement curves and static load test data are given in Appendix II.

Blow counts were recorded in the field for the Corpus Christi test pile at initial driving and final re-driving. The average blow count over the last foot of driving for the initial test (CC-Initial) was 48 blows per foot. The average blow count for the first six inches of final re-driving (CC-Final) was 84 blows per foot. The driving records and computer input data are given in Appendix II.

Harlingen Test Piles. - Two test piles were driven and statically load tested near Harlingen, Texas during June, 1972, along U.S. Highway 77 at the North Floodway. The two test piles were 16 in. square prestressed concrete piles driven by a Link Belt 520 diesel hammer. Test pile No. 99R had a total length of 20 ft and an embedded length of 14.5 ft. Test pile No. 4L had a total length of 24 ft and was embedded 17.5 ft. Both piles were statically load tested using the Quick-Load Test Method within one hour after driving and again 8 days later. Both piles were re-driven approximately 3 ft upon completion of the 8-day static load test.

Strain gage bridges were used to record both static soil resistance and dynamic force-time data. The soil profiles and the locations of the strain gage bridges for the Harlingen test piles are



(a) STANDARD PENETRATION NUMBER N OBTAINED FROM TEXAS HIGHWAY DEPARTMENT TEST DATA.

(b) ESTIMATED FROM STANDARD PENETRATION NUMBER N.

FIG. 6 - SOIL PROFILE FOR CORPUS CHRISTI TEST PILE

shown in Figs. 7 and 8. These piles were driven through clay into sand. The water table is located at a depth of approximately 16 ft. Load-settlement curves and static load test data are given in Appendix II.

The blow counts for 99R, as recorded in the field, were 85 blows per foot for initial driving (99R-Initial) and 120 blows per foot for final re-driving (99R-Final). A determination of the blow counts for 4L was a problem as the pile evidently encountered a pocket of loose sand during initial driving. An inspection of the driving record in Appendix II shows that for the last foot of initial driving the blow count dropped, while for the final re-driving the blow count increased after the first 4 inches of re-driving. As a result, the blow counts used for this investigation were determined to be 43 blows per foot for initial driving (4L-Initial) and 48 blows per foot for final re-driving (4L-Final) based on the similarity of the initial and final static load tests. The driving records and computer input data are given in Appendix II.

A summary of the static load test results for all five test piles is given in Table 1. The total soil resistance-RUT (load measured at pile head) for each test is tabulated in columns 2 and 3. The point resistance-RUP (load measured at pile point) for each test is tabulated in columns 4 and 5. It is significant to note that the point resistance did not change much between the initial and final load tests. An increase in total soil resistance between the initial and final load test is indicated in column 6 as soil

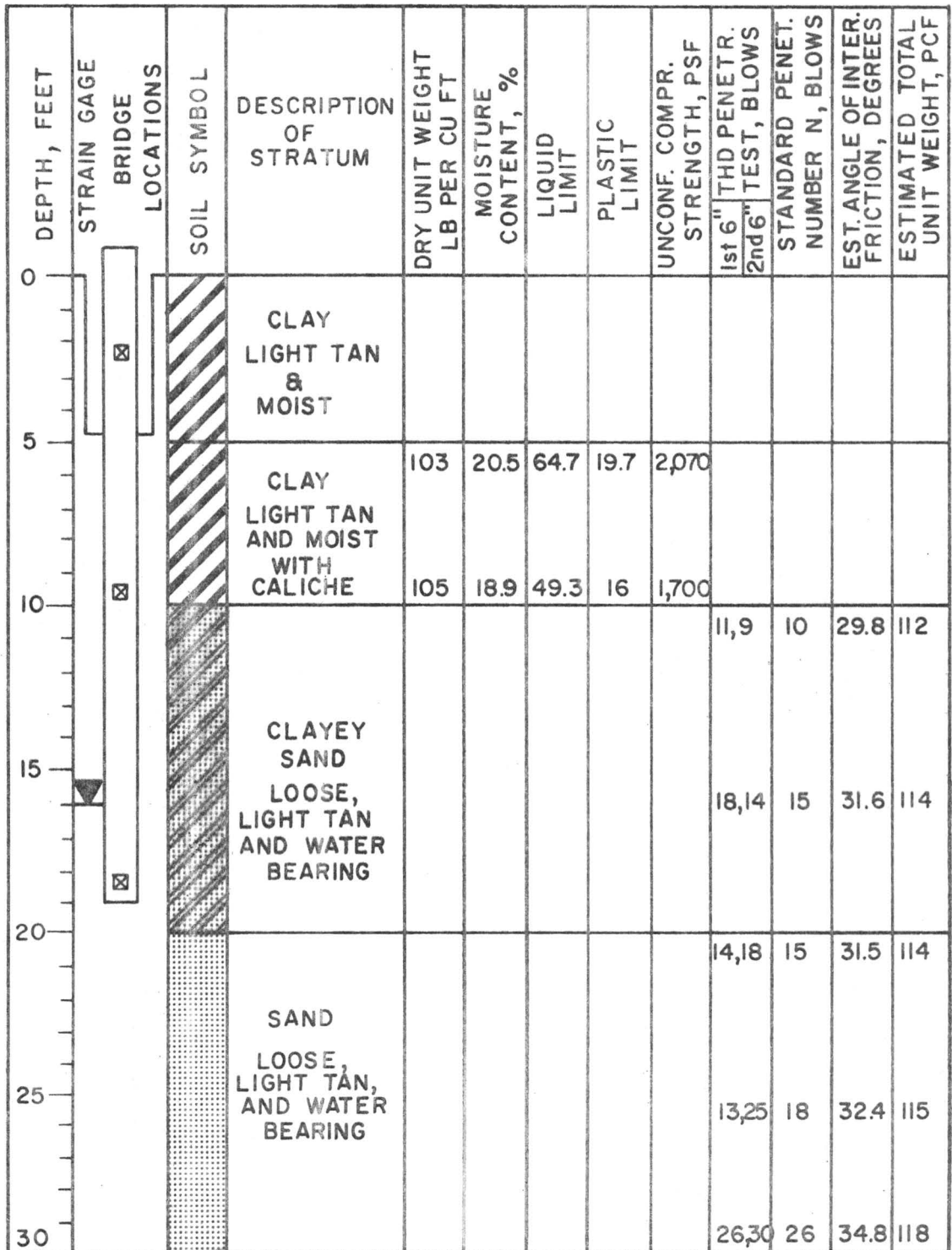


FIG. 7 - SOIL PROFILE FOR HARLINGEN TEST PILE 99R

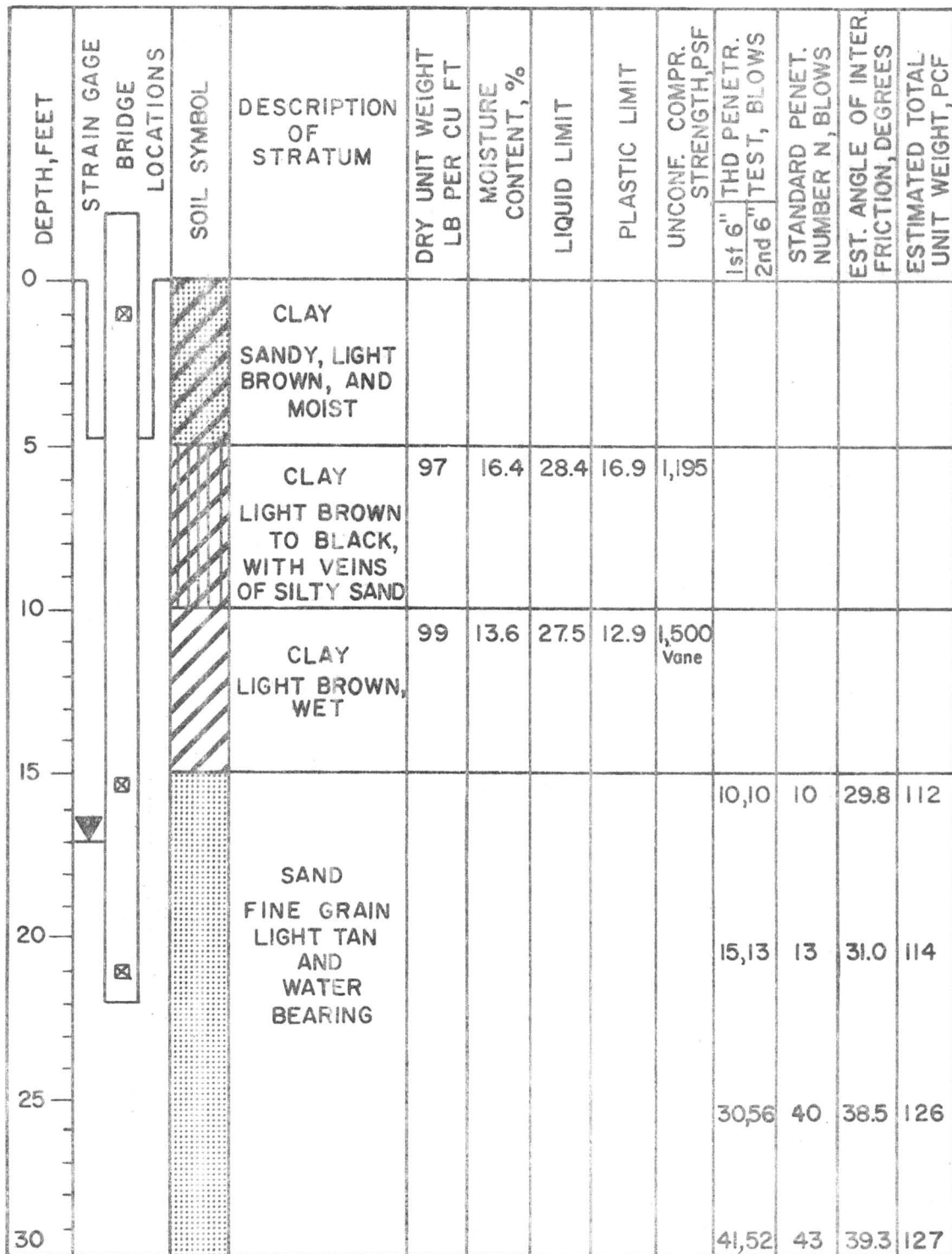


FIG. 8 - SOIL PROFILE FOR HARLINGEN TEST PILE 4L

TABLE 1.

SUMMARY OF STATIC LOAD TEST RESULTS FOR TEST PILES

Test Pile No. (1)	Static Soil Resistance (RUT), tons		Point-Bearing Resistance (RUP), tons		Soil "Set-Up" $\frac{\text{col (3)}}{\text{col (2)}} \text{ (6)}$	$\frac{\text{RUP}}{\text{RUT}}$	
	Initial Test (2)	Final Test (3)	Initial Test (4)	Final Test (5)		Initial Test (7)	Final Test (8)
PA 1	46.0	100.0	9.0	5.0	2.17	0.195	0.050
PA 2	54.0	131.0	8.0	10.0	2.43	0.148	0.076
CC	134.0	157.0	106.0	112.0	1.17	0.791	0.713
HAR 99R	185.0	199.0	116.0	118.0	1.07	0.627	0.593
HAR 4L	129.0	133.0	81.0	88.0	1.03	0.628	0.662

"set-up" or "freeze". The Port Arthur piles, which were embedded entirely in clay, experienced a considerable amount of "set-up". The ratio of point resistance to total resistance for each test pile, which is a measure of the amount of total load carried at the point, is tabulated in columns 7 and 8. These ratios indicate that the Port Arthur test piles are friction piles since only 5% to 20% of the total load is carried at the point. However, the Corpus Christi and Harlingen test piles, with the point embedded in sand, are point bearing piles since 60% to 80% of the total load is carried at the point. A complete set of static load test data is given in Appendix II for each load test. Since these data were measured, the static load distribution is known and was used with the pile-soil simulation for the wave equation analysis of each test pile.

ANALYSIS OF TEST PILE DATA

General Method of Analysis. - The general method or procedure used in the analysis of the test pile data was similar to the procedure used by Foye (7). Known computer input parameters were used where possible and unknown computer input parameters were varied in order to obtain the best possible agreement between the measured and computed stresses and bearing capacity for each of the test piles. Unknown parameters are defined as those which are required input for the computer program but for which no field data are available for direct evaluation. In this study, the unknown parameters are the side damping - J' and the point damping - J .

In the initial analysis of the Port Arthur and Corpus Christi data, Foye used hammer input data which included computed cushion and pile segment stiffness values based on the geometry and mechanical properties of these components. The computed stresses were found to be significantly larger than the measured stresses. By adjusting the stiffness ($\frac{AE}{L}$) value at the head of each pile the peak stress at that point was made to agree with the measured value. The adjusted stiffness value was then used to determine the best value of side damping - J' using the measured blow count as the criterion. The adjusted stiffness values together with the best value of J' required for matching computed and measured blow counts with hammer input data yielded a reasonably good correlation between computed and measured stresses. The limiting factor throughout Foye's investigation was the assumption

that, in all cases, the soil quake $Q = 0.1$ in. and point damping $J = 0.0$. During this past year the work started by Foye was continued without the constraint of a constant Q and J .

The basic plan for analysis of the data was to first determine appropriate values for soil quake - Q from the static load test data. Then, having appropriate values for Q and using measured dynamic force time data as input at the pile head, a parameter study was conducted to evaluate J and J' . With Q , J , and J' thus established, hammer simulation data were used to determine the value of $\frac{AE}{L}$ at the head of the pile which yielded the best correlation between measured and computed stresses. Finally, bearing graphs were developed to allow an assessment of the correlation between computed and measured bearing capacity based on the previously determined values of Q , J , J' , and $\frac{AE}{L}$.

Although Foye's general data analysis procedures were used, a few minor changes were made in the basic simulation for the hammer-pile and pile-soil systems. Three of the most significant changes were:

1. For each test pile, 2-ft pile segments were used, whereas Foye had used 5-ft segments.
2. The ram of the pile hammer was simulated by a single mass, or segment, whereas Foye had used three segments.
3. For those computer analyses where hammer simulation data were used, the program-computed value for the critical time interval $1/\Delta t$ was used, whereas Foye had used a manual input

value for $1/\Delta t$. (The critical time interval is the time allowed for the stress wave to progress along the pile at the rate of one segment per time interval.)

Dynamic Forces and Static Loads. - A previous section of this report (Instrumented Test Piles) gives details on the location of the strain gage bridges along each test pile. Also, it was noted that the test sequence involved initial driving of the pile; static load testing as soon as possible after initial driving; static load testing after an elapsed time of 8 to 11 days; and re-driving after the final static load test. Dynamic data were recorded from the strain gage bridge outputs during the last 3 to 5 ft of initial driving and the first 3 to 5 ft of re-driving (until the pile was moving relative to the soil and/or a constant re-driving blow count was achieved). A calibrated load cell was used for the acquisition of dynamic data during the Port Arthur tests only. The outputs of the strain gage bridges during the dynamic tests were mechanically recorded on paper. This provided a permanent record of the load in the pile as a function of time at each bridge location for every blow of the hammer throughout the time the data were being recorded. The force-time data at the top of the pile are particularly valuable from a wave equation analysis standpoint because these data can be used as input to the computer program. In so doing, all the uncertainties connected with simulating the hammer-pile system are eliminated. A partial listing of the uncertainties thus eliminated (see Fig. 1) would include ram impact velocity (which is also a measure of hammer efficiency);

coefficients of restitution for various elements above the pile head; dynamic stiffness values for the hammer elements; the explosive force in the chamber for diesel hammers; and others. With force-time input, there is no need for a mathematical model which will predict or calculate the dynamic force applied to the pile. This force is known with a measured degree of accuracy. Therefore any discrepancies between computed and measured quantities below the hammer-pile interface can be charged to an inadequacy in the pile-soil simulation.

For the static load tests the calibrated load cell was used for every test. The strain gage bridges were located along the pile at points selected to yield the desired information. The bridge at the head of the pile, along with the load cell, measured the total static force being applied to the pile during any load increment. The bridge at the point of the pile measured the load being supported by the pile in end bearing. The ratio of point load to total load must be known for wave equation analysis purposes. Interior strain gage bridges were placed so that they would be as close as possible to the interface of major soil stratum changes at the end of the initial driving. In this manner it was possible to determine the load transfer, in tons per linear foot of pile, for each stratum. Again, this information is useful for wave equation analysis purposes since it is possible to input soil parameters in accordance with the actual (measured) distribution for each layer of soil.

The nature of the static load test is such that the load is applied incrementally to the pile and the corresponding settlement is

measured for each load increment. This incremental loading, together with a judicious choice of strain gage bridge locations, makes it possible to determine the elastic behavior, or quake, of the soil.

Soil Quake. - The soil quake - Q has been defined earlier as the amount of soil deformation or movement which must occur before the soil reaches a state of plastic failure. This concept has been shown graphically in Fig. 3a. The deliberate placement of strain gage bridges and the incremental nature of the static load test made it possible to develop load transfer versus movement curves for each stratum between bridges. Similarly, the data were used to construct a tip load versus tip movement curve for the soil beneath the tip of the pile. The details of the procedure used to develop these curves can be found in a paper by Coyle and Sulaiman (2). By developing these curves from the static load test data it is possible to evaluate quake - Q .

Basically the procedure for obtaining the load versus movement curves consists of first obtaining the load transfer between an adjacent pair of strain gage bridges at each increment of load. A strain gage bridge measures the total load in the pile at the location of the bridge. The difference between the readings of two adjacent bridges shows the amount of load which has been removed from the pile and is now being carried by the soil, hence the use of the term load transfer. A sketch of one of the Port Arthur instrumented piles is shown in Fig. 9. The numbers along the side of the pile designate strain gage bridge locations and the letters refer to pile

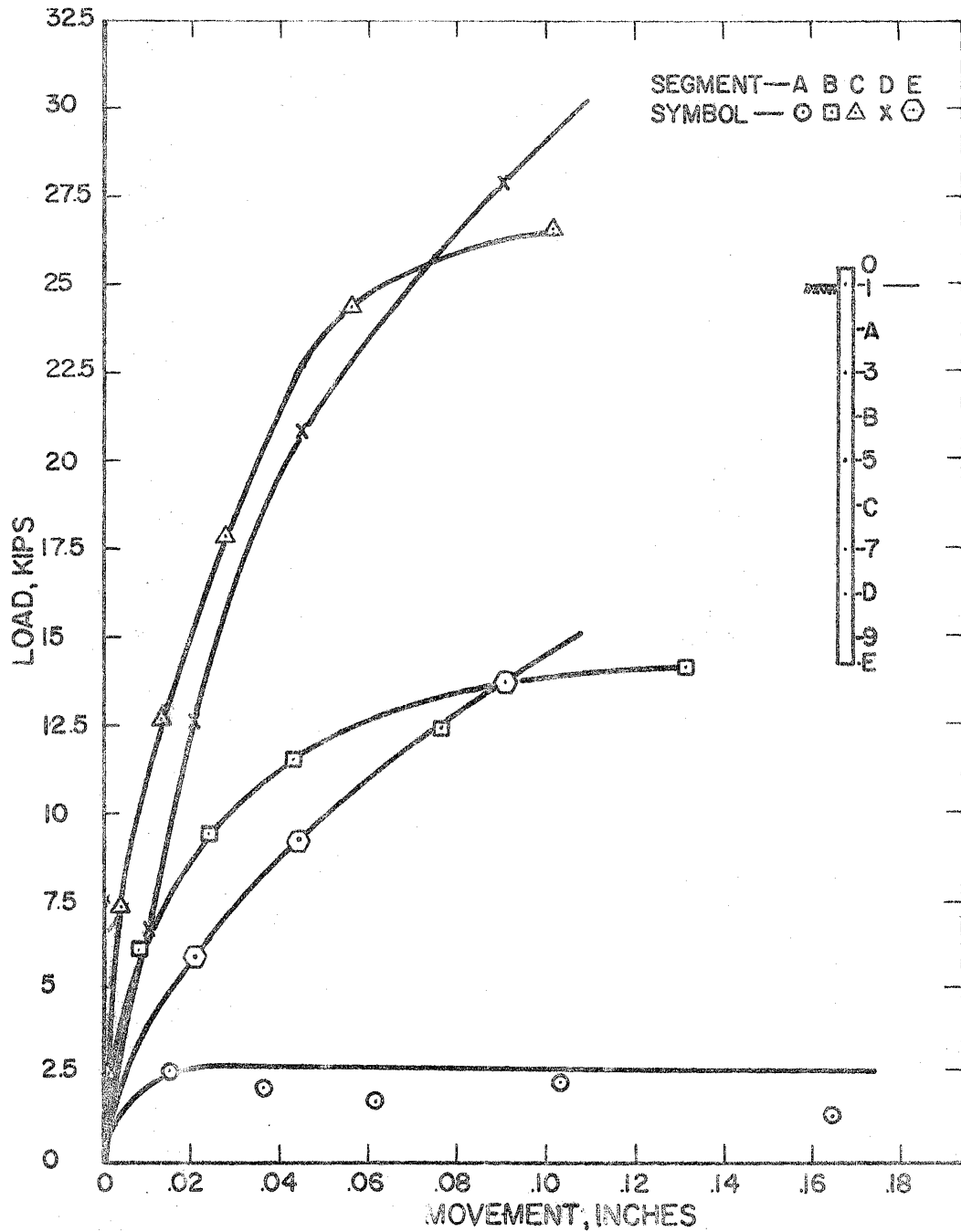


FIG.9 -LOAD TRANSFER vs. MOVEMENT CURVES
 PORT ARTHUR PILE NO.1 TEST NO.1

segments between adjacent bridge locations. The load transfer for segment A is equal to the difference in readings of bridges 1 and 3. For any segment the load transfer is associated with some amount of movement of the segment. For each load increment the gross settlement at the top of the pile is recorded (see Load-Settlement Curves in Appendix II). The elastic compression of the pile can be calculated from the known physical and geometric properties of the pile and the known load at bridge locations. The movement at any bridge location for a given load increment equals the observed settlement at the top of the pile minus the elastic compression between the top of the pile and the bridge location. The movement associated with a particular segment is the movement which occurs at the mid-point of the segment. Assuming a linear load transfer between adjacent bridges, the movement at the mid-point of the segment equals the average of the movement at the top and bottom of the segment.

Presented in Fig. 9 are the load transfer versus movement curves for the initial test on Port Arthur Pile No. 1. Fig. 10 presents load transfer versus movement curves for the initial Corpus Christi pile test. For the determination of soil quake - Q , the load transfer versus movement data from all pile tests were grouped into four categories to include load transfer versus movement for clay; point load versus movement for clay; load transfer versus movement for sand; and point load versus movement for sand. The grouped data are presented in Figs. 11 through 14.

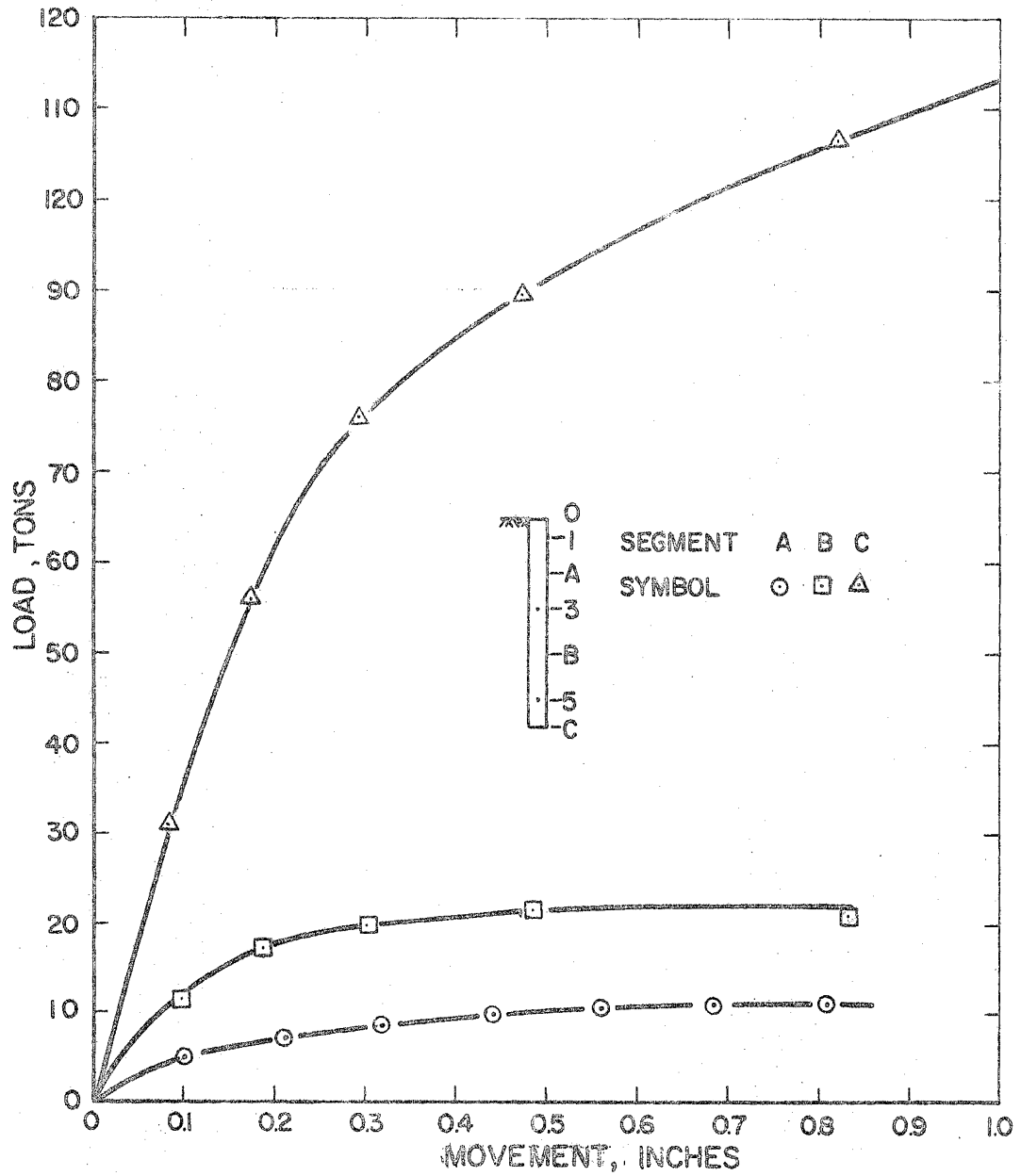


FIG. 10—LOAD TRANSFER vs. MOVEMENT CURVES
CORPUS CHRISTI TEST PILE—INITIAL TEST

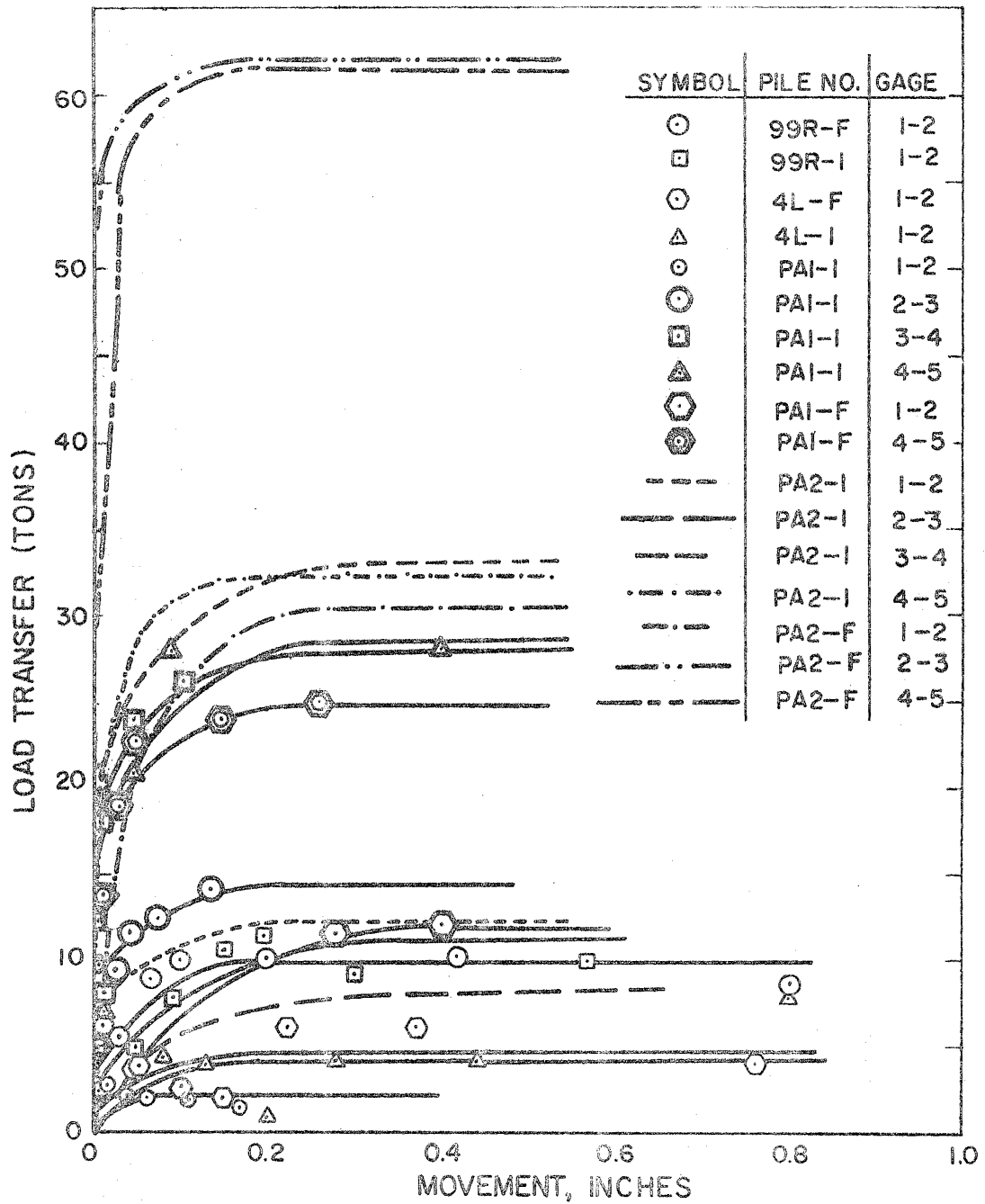


FIG. II - LOAD TRANSFER vs. MOVEMENT CURVES FOR CLAY

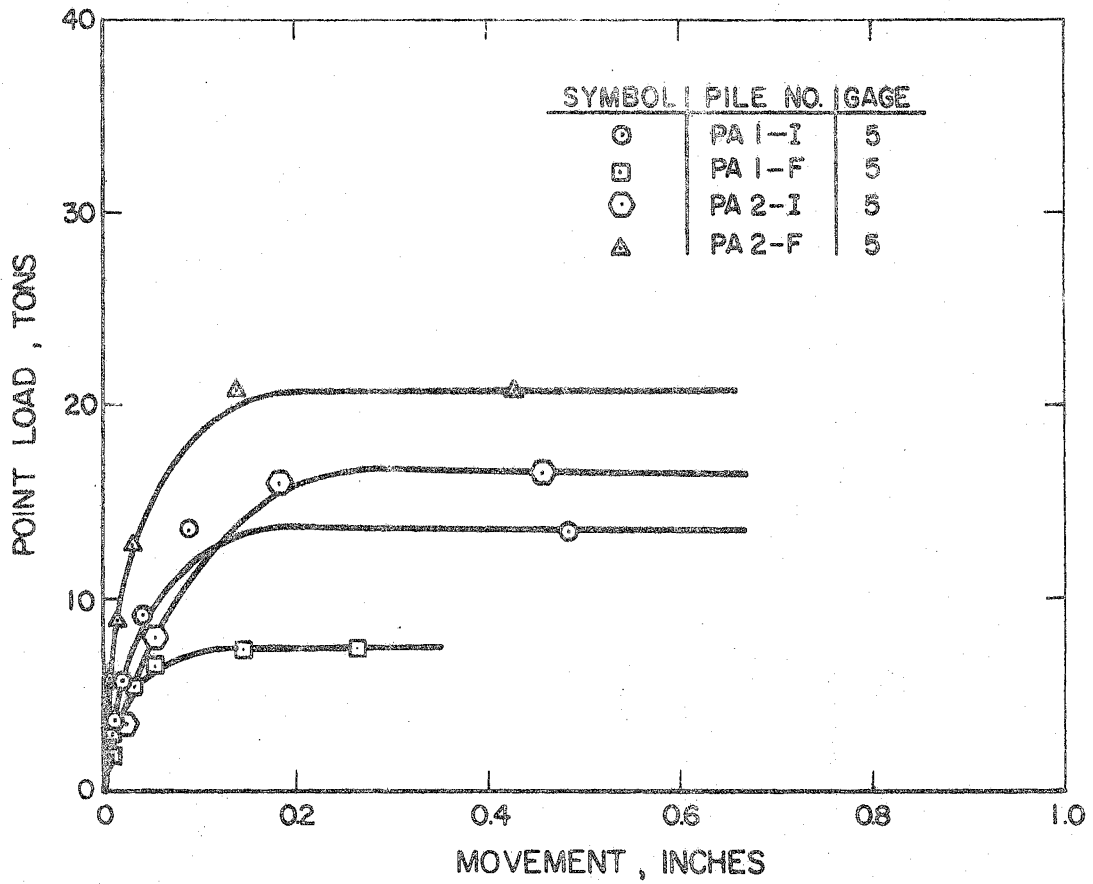


FIG.12— POINT LOAD vs. MOVEMENT CURVES FOR CLAY

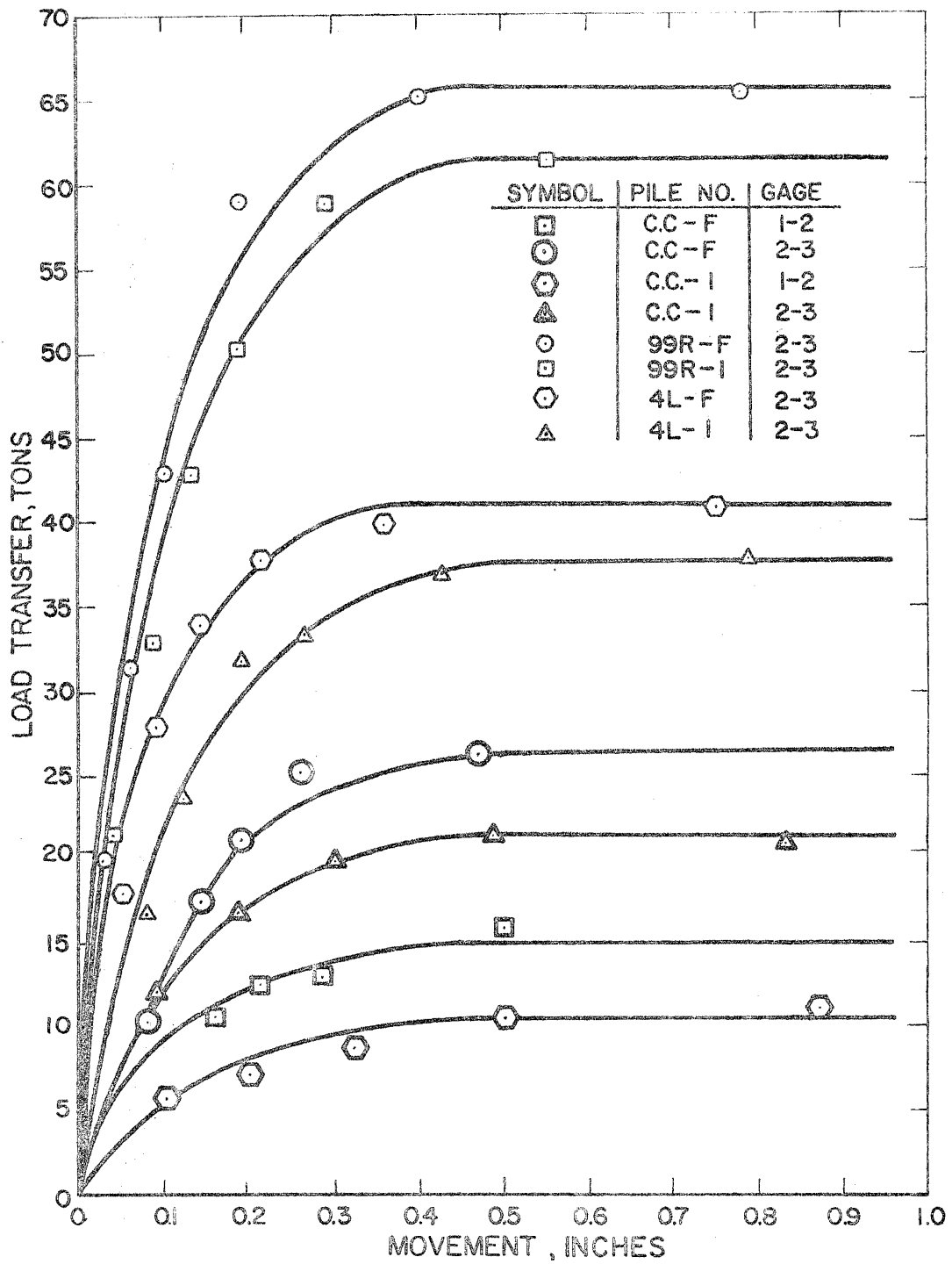


FIG.13-LOAD TRANSFER vs. MOVEMENT CURVES FOR SAND

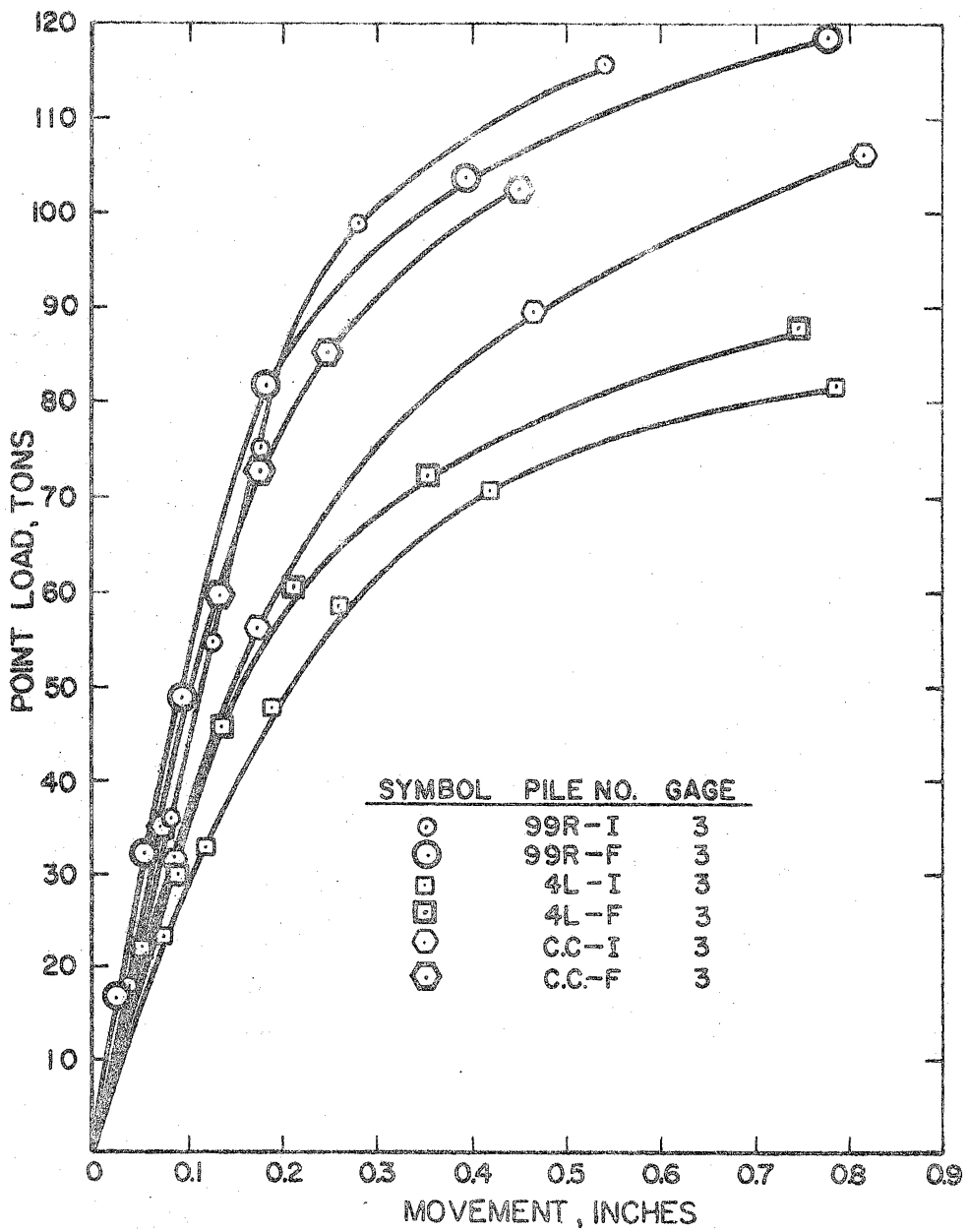


FIG. 14-- POINT LOAD vs. MOVEMENT CURVES
FOR SAND

The ultimate load transfer or point load for a pile may not always be unequivocally established by the static load test data. Ultimate load transfer as used herein means the maximum load transfer that occurred regardless of how much movement occurs. For piles in clay which have been loaded until a plunging failure occurs, a maximum calculated load transfer can be determined. The test piles in this investigation which were in clay were loaded until a plunging or near-plunging failure occurred, as evidenced by the load-settlement curves given in Appendix II. For piles in sand, plunging failures are less common and more difficult to attain. The determination of an ultimate load under these conditions may be ambiguous. This was found to be especially true during this investigation for point loads in sand (see Fig. 14).

The ultimate loads represented by the data of Figs. 11 through 14 vary throughout an average range of approximately 50 tons, except for the point load versus movement curves for clay which has an ultimate load range of 13 tons. For example, the load transfer versus movement data for clay involves ultimate loads as low as 2 tons and as high as 62 tons. To represent all the data within a particular category by a single curve, the data of Figs. 11 through 14 were normalized with respect to load transfer and point load. Each load transfer and point load value for an individual curve was divided by the ultimate value for that curve, and the resulting quotient was expressed as a percentage. For the data of Fig. 14, the maximum observed point load value was taken to be the ultimate value for that curve.

The piles from which the data were obtained were similar in the dimension perpendicular to the longitudinal axis (16-in. diam. metal shell or 16-in. sq concrete). Therefore, the effect of the lateral dimension of pile size on the magnitude of Q could not be studied in this investigation. However, the values of quake as determined in this investigation are considered appropriate for use by the Texas Highway Department because all piles tested were common sizes in current use for bridge foundations.

The data normalized with respect to load transfer and point load were then plotted. A reasonable amount of data scatter was present. For each of the four categories a curve similar to the static curve in Fig. 3a was obtained by drawing the linear elastic and linear plastic lines which appeared to best approximate the non-linear data. The linear elastic-plastic plots are shown in Figs. 15 through 18. The intersection of the linear elastic and plastic lines determines the value of quake - Q which is believed to be representative for each of the four categories. These values are shown in Table 2.

TABLE 2.

SUMMARY OF LOADING SOIL QUAKE VALUES FOR TEST PILES

Soil Type	Side Quake Q	Point Quake Q
Sand	0.2	0.4
Clay	0.1	0.1

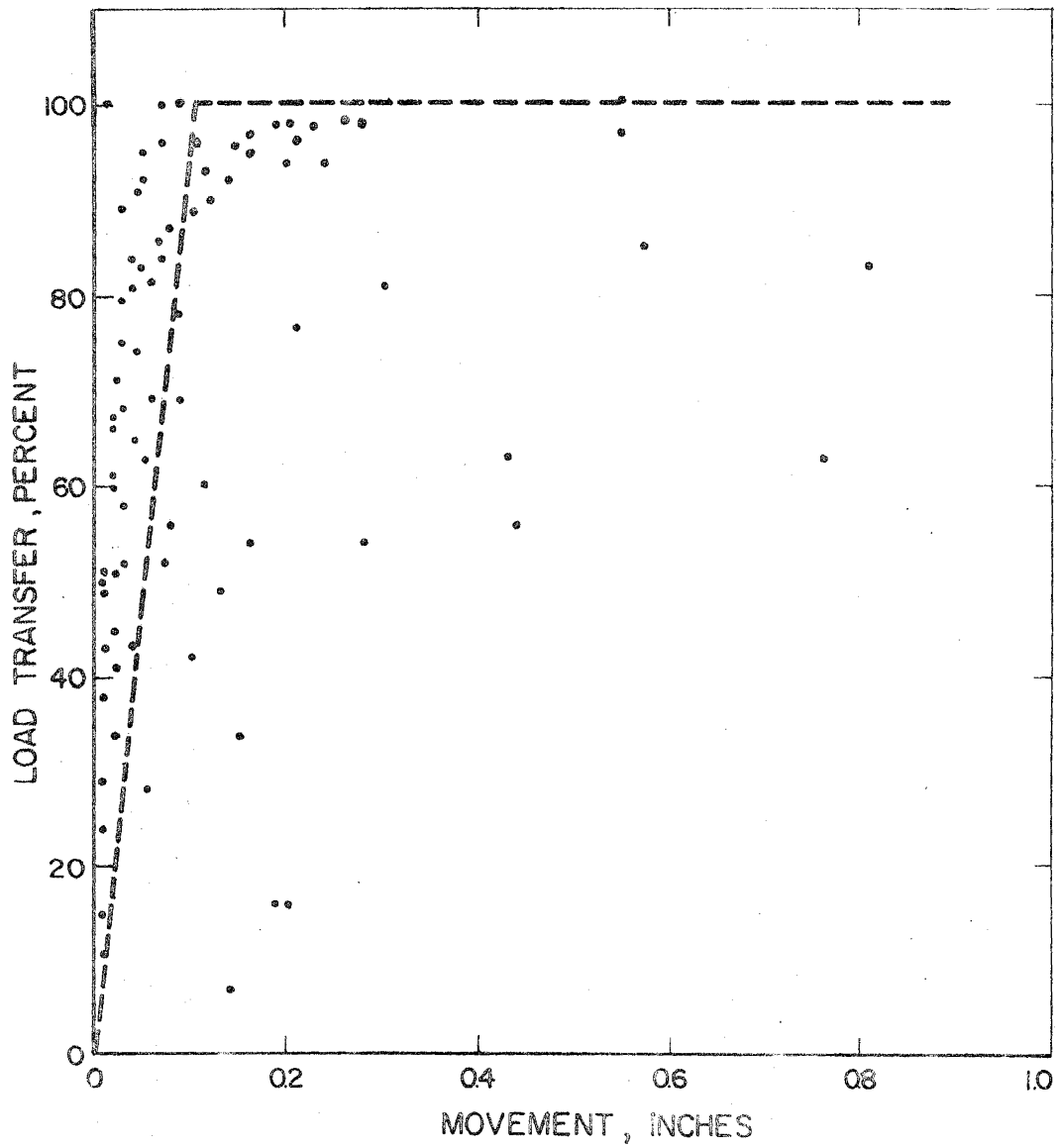


FIG. 15—PERCENT LOAD TRANSFER vs. MOVEMENT FOR CLAY

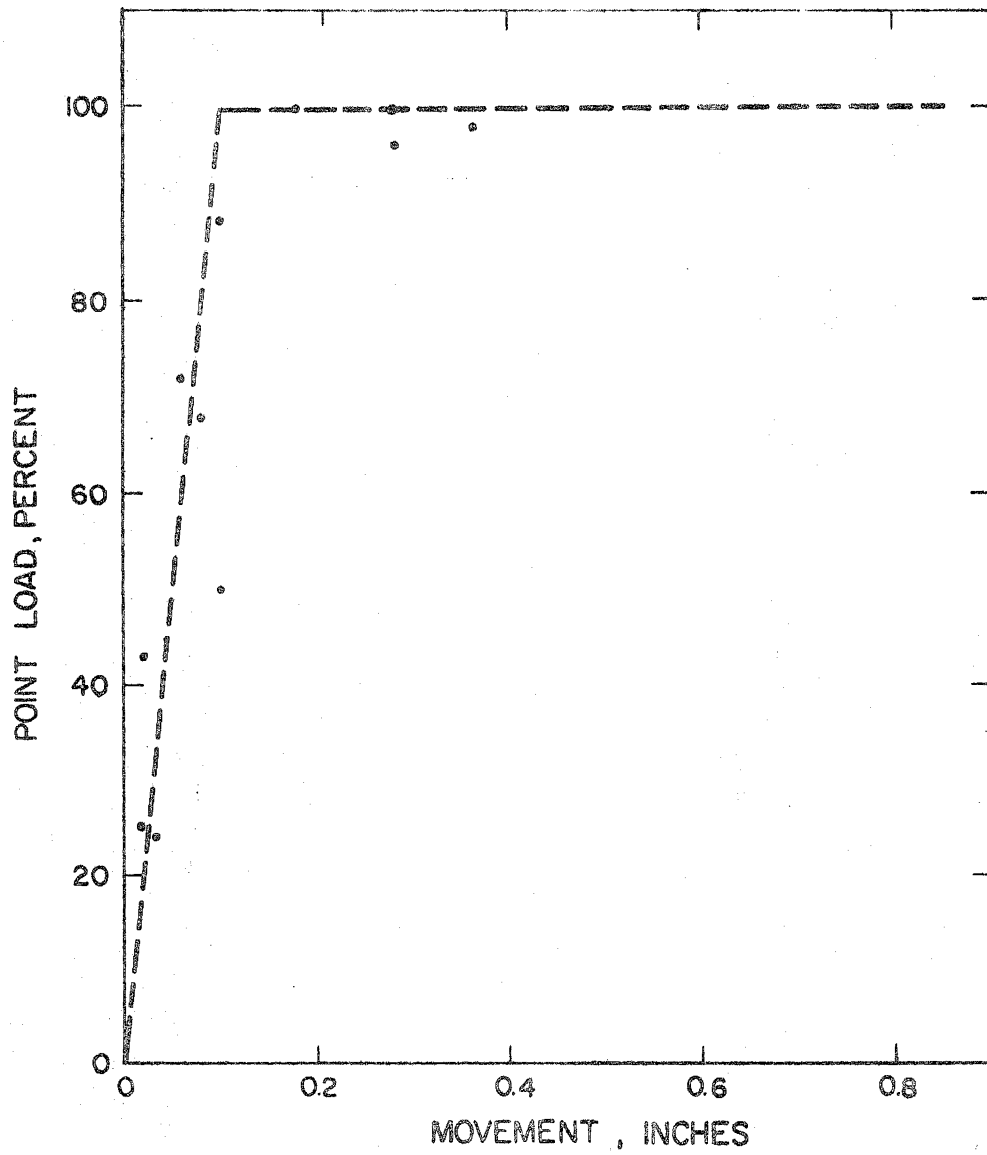


FIG. 16—PERCENT POINT LOAD vs. MOVEMENT FOR CLAY

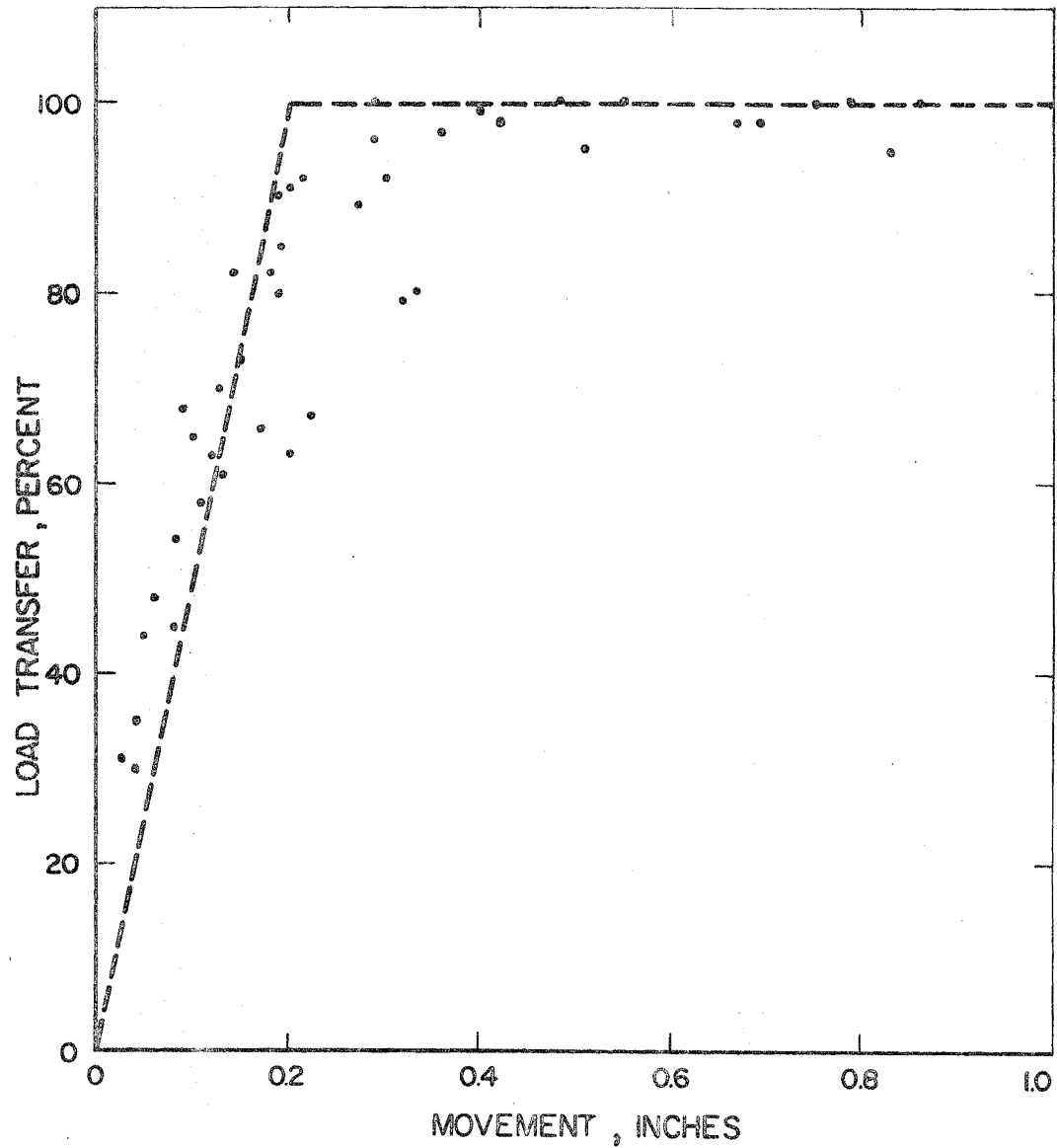


FIG. 17—PERCENT LOAD TRANSFER vs. MOVEMENT FOR SAND

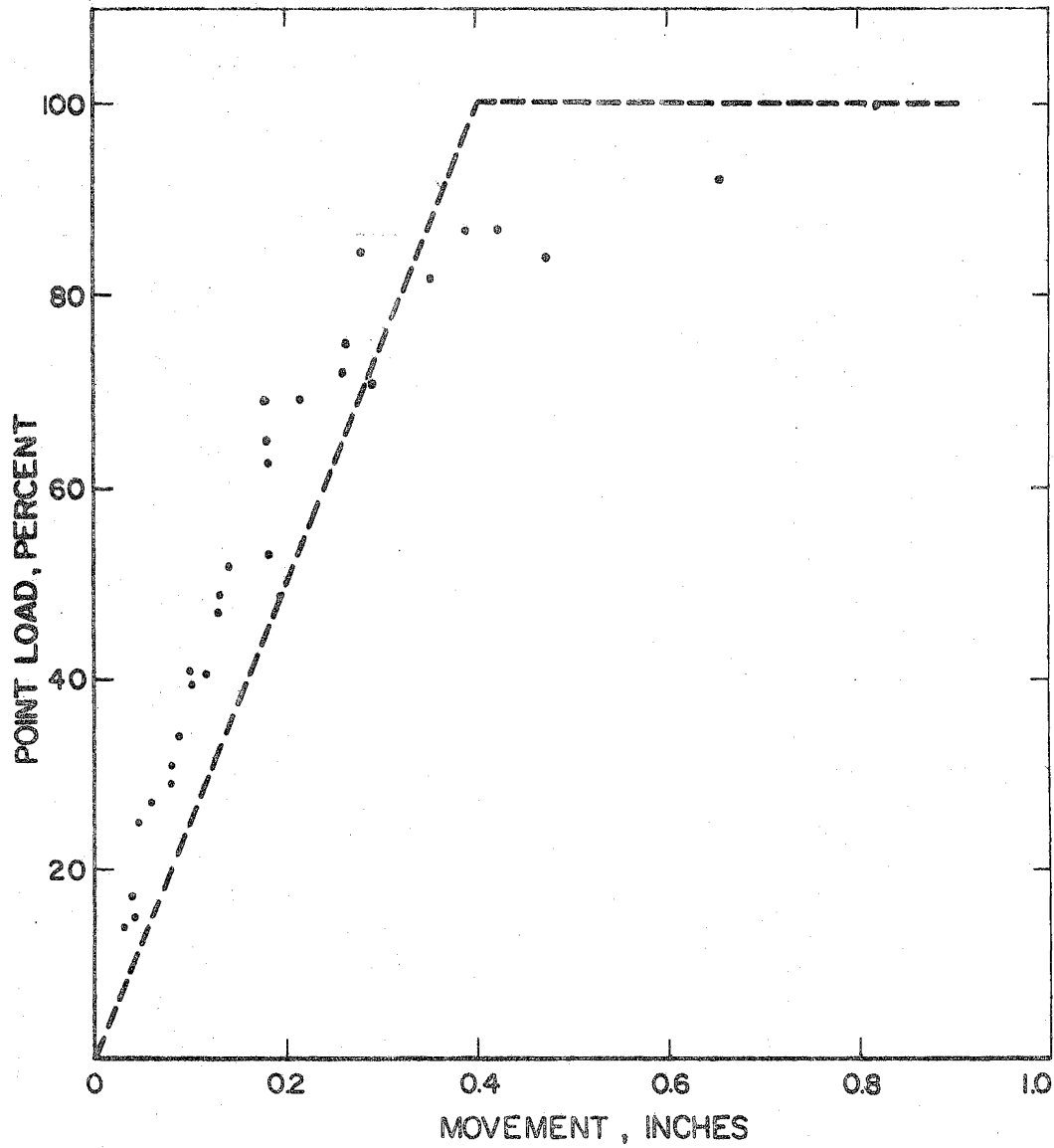


FIG. 18—PERCENT POINT LOAD vs. MOVEMENT FOR SAND

The quake values in Table 2 are designated as loading quakes because the values were derived from loading tests on piles. From the standpoint of a wave equation analysis the unloading quake is also of significant importance because under dynamic loading the motion of the soil with respect to the pile may change directions several times before the energy causing the displacement of the pile-soil system has dissipated.

In an earlier laboratory research investigation (which was not part of this study) Dunlap (4) conducted triaxial tests on sand samples using various initial relative densities and moisture contents. The samples were subjected to cyclic loading at constant confining pressure and at constantly varying confining pressure. The stress versus strain data indicated that the secant modulus of the unloading curve is higher than the secant modulus of the loading curve. The unloading secant modulus was not significantly affected by confining pressure. For a constant confining pressure, the unloading secant modulus remained essentially constant throughout the cyclic loading although there was some tendency for the modulus to increase with repeated loading. From the stress versus strain data obtained from Dunlap's work, it was indicated that the unloading quake for the soil surrounding a pile may be constant though not necessarily equal to the loading quake.

From the static load test data obtained throughout this study it was possible to obtain some indication of the unloading quake under field conditions. Gross settlement at the head of the pile was

recorded with maximum load applied. The pile was unloaded and allowed to rebound, whereupon gross settlement was again recorded. The difference between the settlements from maximum load to no-load yields a measure of the elastic recovery of the pile-soil system. The elastic recovery, or quake, of the soil can then be deduced by subtracting the elastic compression of the pile from the total elastic rebound, in a manner similar to that used for computing the movement for the load transfer curves.

From the data obtained during this study, an unloading quake of 0.1 in. was determined to be representative of both sands and clays. An unloading quake of 0.1 in. was used for all analyses reported herein. The wave equation computer program was modified to incorporate the ability to use a loading quake which differs from the unloading quake for analyses of piles in sand. For piles in clay, the loading quake equals the unloading quake as had been assumed for prior investigations.

Soil Damping. - Having established the proper soil quake values for each soil type, the next step in the procedure was to determine the proper soil damping values. This step was accomplished by conducting a parameter study using known force-time data as input along with the established soil quake values. All reasonable combinations of soil damping values were used as input to the computer program and the calculated pile stresses and blow counts were correlated with the measured pile stresses and blow counts.

This study was basically concerned with piles in sands because

there was essentially no change in the input data for clays from what Foye (7) had used in his investigation. However, a limited study was conducted in order to determine the point damping for piles in clays. Previously, the point damping was considered to be zero because the measured static and dynamic forces at the point of the piles were essentially equal. A parameter study was conducted for clays using small values of point damping. Other input values used in the analysis were the measured force-time data, soil quake values of Q -point = Q -side = 0.1 in. and side damping - J' of 0.2 seconds per foot. The results showed that when a point damping - J value of 0.01 seconds per foot was used there was a better correlation between the calculated pile stresses and the measured pile stresses and the calculated blow counts were in closer agreement with the measured blow counts.

An analysis of the Corpus Christi test pile was then conducted to determine the side and point damping values for piles in sand. A parameter study was made using as input the force versus time data measured at the head of the pile and the loading and unloading values of Q determined from the static load tests (Q -side = 0.2, Q -point = 0.4, Q -unloading = 0.1). Having the measured force wave shape applied to the top of the pile, the side damping and point damping values were the only unknowns associated with the pile-soil system remaining to be evaluated. Reasonable combinations of J and J' were selected and used to compute the pile stresses at the location of the strain gage bridges and the corresponding blow count. A partial tabulation of

the parameter study results is given in Table 3 (see next page).

The side damping and point damping values that were determined to be the most representative for piles in sand and piles in clay are given in Table 4. The damping values in Table 4 were selected because their use produced the best overall agreement between computed and measured stresses and blow counts.

TABLE 4.

SUMMARY OF SOIL DAMPING VALUES FOR ALL FIVE TEST PILES

Soil Type	Friction Damping J'	Point Damping J
Sand	0.5	0.15
Clay	0.2	0.01

Pile Stresses. - The procedure for determining the side and point damping values utilized the measured force-time data and the measured static bearing capacity to compute the predicted pile stresses and blow count. Elimination of hammer uncertainties by use of force-time data allowed a better determination of damping values by resolving the problem to one involving only the pile-soil system, and within that system the damping values were the only unknowns. However, in most cases where wave equation analysis is used the force-time data will not be available and the hammer-pile system simulation must be utilized. For that reason, the five test piles were also analyzed with hammer input data along with the proper quake and damping parameters to ascertain the agreement between computed and measured stresses.

TABLE 3.

SUMMARY OF PILE STRESSES AND BLOW COUNTS FOR CORPUS CHRISTI INITIAL USING
DIFFERENT SOIL DAMPING VALUES, FORCE-TIME DATA AND Q-SIDE = 0.2, Q-POINT = 0.4

Side Damping	Point Damping	Gage No.	Experimental		Force-Time Input	
			dynamic peak force (kips)	blow counts (blows/in.)	dynamic peak force (kips)	blow counts (blows/in.)
0.40	0.15	1	505.6		502.3	
		2	504.4	4.0	495.1	3.84
		3	218.1		292.6	
0.50	0.10	1	505.6		502.6	
		2	504.4	4.0	493.6	3.83
		3	218.1		277.4	
0.50	0.15	1	505.6		502.8	
		2	504.4	4.0	493.7	3.95
		3	218.1		177.7	

As mentioned previously, Foye's analyses of the Port Arthur and Corpus Christi test piles disclosed that predicted stresses were much higher than measured stresses when the stiffness values ($\frac{AE}{L}$) were computed from a generally accepted value of Young's modulus-E for the material and the specified cross section area-A. To obtain reasonable stress agreements Foye had to apply a reduction factor to the computed stiffness value. For this investigation, the average stiffness value developed by Foye of 182 $\frac{\text{kips}}{\text{in.}}$ for the Port Arthur piles was used because the soil quake and soil friction damping values for clay remained unchanged. Table 5 presents a summary of the peak dynamic stresses at each gage point for the Port Arthur pile tests. In general, a better overall stress agreement was obtained with the force-time input data. This was particularly true for the top two gages.

For the analysis of the Corpus Christi pile, a new stiffness value had to be determined because different soil quake and point damping values were used. The stiffness value for the cushion plus the first pile segment for the Corpus Christi pile was determined to be 900 kips/in.

For the Harlingen piles, the cushion stiffness was determined to be 1400 kips/in. for the pile at bent 99R and 1000 kips/in. for the pile at bent 4L. This difference in the two stiffness values is attributed to the differences in the driving conditions at the two sites which were located approximately one-half mile apart.

Tables 6 & 7 summarize the experimental, force-time input, and hammer input dynamic peak compressive forces for the Corpus Christi

TABLE 5.
SUMMARY OF DYNAMIC PEAK COMPRESSIVE
FORCES FOR PORT ARTHUR PILES

Pile No.	Gage No.	Experimental dynamic peak force (kips)	Force-Time Input dynamic peak force (kips)	Hammer Input dynamic peak force AE/L = 182 (kips)
PA 1-Initial	1	182.4	182.4	237.7
	3	147.5	142.5	176.2
	4	55.5	74.5	94.7
	5	28.5	37.6	46.1
PA 1-Final	1	294.4	294.4	274.7
	3	180.6	208.2	160.4
	4	82.5	77.2	45.9
	5	56.6	36.7	22.5
PA 2-Initial	1	215.0	215.0	241.3
	2	190.8	196.9	217.7
	4	117.8	91.5	118.2
	5	36.0	31.9	39.0
PA 2-Final	1	240.1	240.1	270.2
	2	273.8	269.8	295.3
	4	122.3	100.1	123.5
	5	23.0	36.7	39.4

TABLE 6.
SUMMARY OF DYNAMIC PEAK COMPRESSIVE
FORCES FOR CORPUS CHRISTI TEST PILE

Pile No.	Gage No.	Experimental dynamic peak force (kips)	Force-Time Input dynamic peak force (kips)	Hammer Input dynamic peak force AE/L = 900 (kips)
CC Initial	1	505.6	505.6	475.7
	2	504.4	495.4	383.2
	3	218.1	193.2	379.4
CC Final	1	517.2	517.2	484.7
	2	511.6	453.7	395.5
	3	248.0	251.4	345.3

TABLE 7.
SUMMARY OF DYNAMIC PEAK COMPRESSIVE
FORCES FOR HARLINGEN TEST PILES

Pile No.	Gage No.	Experimental dynamic peak force (kips)	Force-Time Input dynamic peak force (kips)	Hammer Input dynamic peak force (kips) AE/L = 1400
99R Initial	1	507	507.0	385.1
	2	456	484.5	453.2
	3	249	201.8	349.1
99R Final	1	526	526.0	381.8
	2	486	483.0	448.9
	3	203	199.0	341.3
Pile No.	Gage No.	Experimental dynamic peak force (kips)	Force-Time Input dynamic peak force (kips)	Hammer Input dynamic peak force (kips) AE/L = 1000
4L Initial	1	453	453.0	355.6
	2	366	328.9	394.5
	3	183	178.6	236.1
4L Final	1	442	442.0	354.3
	2	377	350.9	418.7
	3	180	198.9	277.1

and Harlingen piles, respectively. Inspection of the values tabulated in Tables 6 & 7 reveal that, in general, the force-time input data gave a better force prediction than the hammer input data.

Bearing Capacity. - In the analyses for determination of the proper soil damping values and the proper stiffness values, the measured static bearing capacity was used as input to the wave equation program and a single predicted blow count was computed. This allowed a comparison between predicted and measured blow counts which were generally in good agreement. However, the requirement of obtaining a predicted bearing capacity from a measured blow count could not be met under those circumstances. In order to obtain a predicted bearing capacity, a bearing graph has to be developed by assuming several values for the bearing capacity and allowing the program to compute a corresponding blow count. The data are plotted and the predicted bearing capacity obtained by entering the bearing graph with the measured blow count.

The computed blow count is obtained by taking the reciprocal of the permanent set of the pile per blow. The standard method used in the existing computer program to compute the permanent set is to subtract the soil quake from the maximum computed displacement at the pile tip. An alternative method for obtaining the permanent set is also available in the existing computer program. For each time interval of computation, the program computes the displacement of the last segment of the pile. If the program is allowed to continue computations until the calculated pile tip displacement remains nearly

constant, the final calculated value may be a better representation of the permanent set. During this past year both methods were used. It was found that the two methods gave approximately the same bearing graph. The alternate method will generally yield a slightly larger permanent set (smaller blow count) for the same soil resistance. The bearing graphs presented in this report are based on the alternate method. In practice, the decision regarding which method to use will be somewhat dependent on the degree of refinement required and the amount of computer time available. Generally speaking, the alternate method represents a greater degree of refinement and requires the greater amount of computer time.

For piles in sand, the use of a loading quake different from the unloading quake requires that a new interpretation be given to the static soil resistance symbolically denoted by RUT. Before the introduction of different quakes, in order to obtain a bearing graph several values of RUT were selected. Each value of RUT represented an assumed potential of the soil to resist load. When the assumed RUT was less than the resistance which the hammer was capable of overcoming, the hammer could cause the soil at the tip of the pile to fail plastically and cause some amount of permanent set. This is illustrated in Fig. 19a where the assumed load resisting potential of the soil is RUT_1 and the hammer causes soil deformation at the tip to follow the path OAB to point B, and the soil rebounds along BC to point C. The permanent set is then OC. When the assumed RUT was greater than the capability of the hammer, the hammer could not cause a plastic failure at the tip, i.e., the tip displacement would be

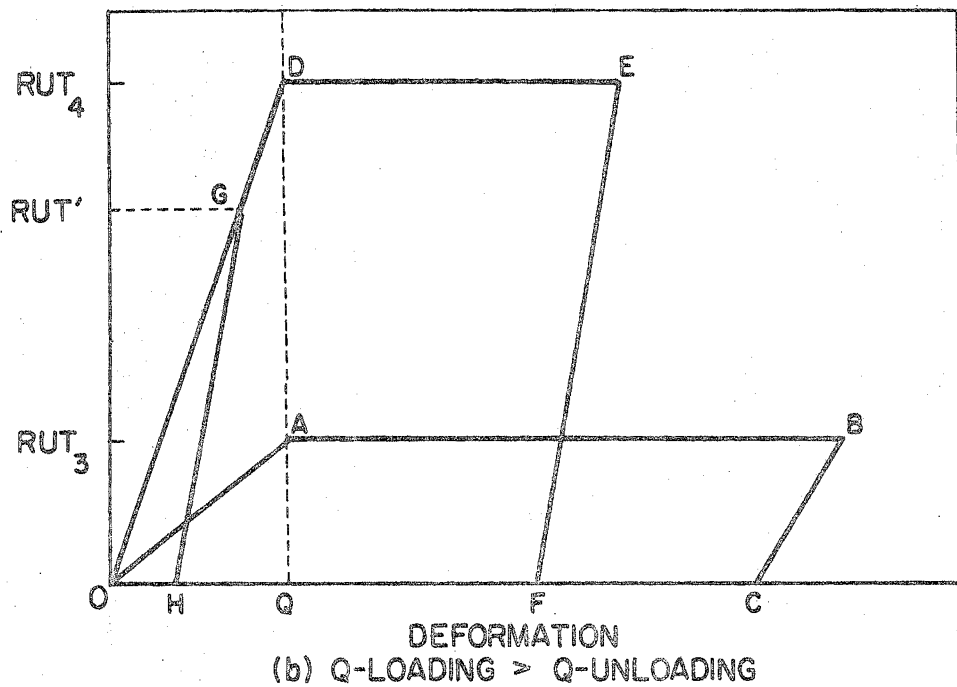
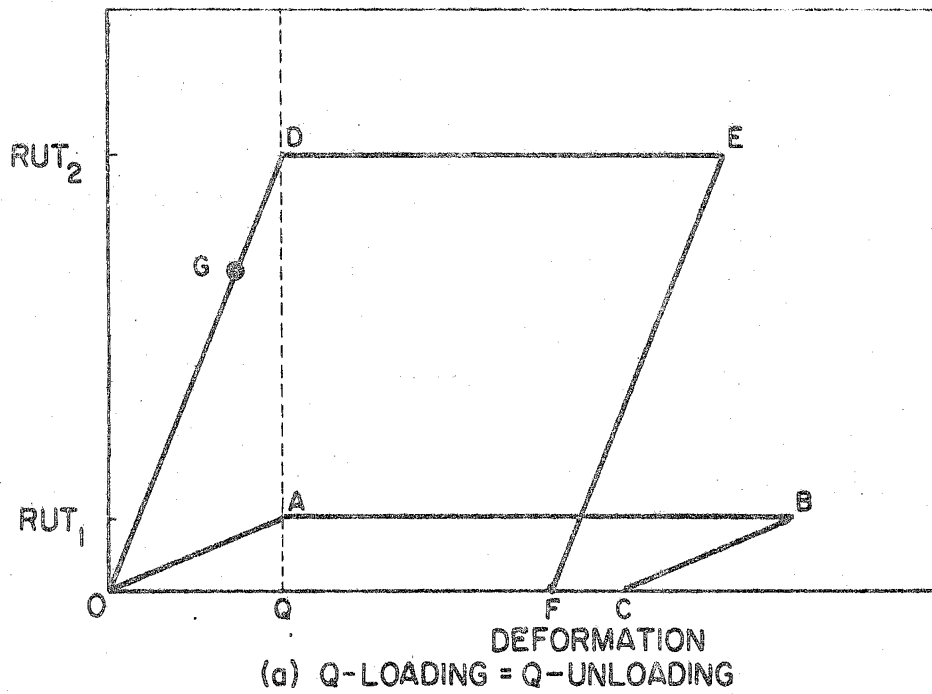


FIG.19—SOIL LOADING vs DEFORMATION CURVES

equal to or less than the quake at the tip. With Q loading = Q unloading, the soil at the tip would rebound completely, or regain all its elastic deformation. Consequently, no permanent set was obtainable and an infinitely large blow count was the result. This is illustrated in Fig. 19a where, with RUT_2 assumed, the hammer causes the soil to deform only to point G, whereupon the soil rebounds along line GO back to point O with no resulting permanent set.

With the assumption of a loading quake greater than the unloading quake, some amount of permanent set is always obtained. RUT again represents the potential of the soil to resist load. When the assumed RUT is less than the capability of the hammer, the conditions are basically the same as for the previous case as the hammer can cause plastic failure in the soil. When the assumed RUT is greater than the capability of the hammer the soil does not fail plastically but some permanent set is obtained. This is represented in Fig. 19b where, with the soil potential assumed to be RUT_4 , the soil is displaced to point G. Upon unloading, the soil does not rebound along the loading path GO, but instead rebounds along GH to point H. The resultant permanent set is then OH. In this case the assumed value for RUT_4 is not the actual soil resistance "seen" or overcome by the hammer. In fact, the resistance overcome by the hammer is only a fraction of the full potential of the soil, RUT_4 , the actual amount depending on how near the soil came to a plastic failure. In order to obtain a meaningful bearing graph the computed blow count must be plotted versus the amount of soil resistance overcome which is RUT' .

To predict the bearing capacity of the piles tested during this investigation the piles were analyzed using hammer simulation data. Values of 182, 900, 1400, and 1000 kips/in. were used as the stiffness at the head of the PA1 and PA2, Corpus, Harlingen 99R, and Harlingen 4L piles respectively. The bearing graphs are presented in Figs. 20 through 24. Table 8 presents a summary of the measured bearing capacity for each pile test and the predicted capacities obtained with hammer simulation data. It has been pointed out that the use of force-time input yields a better agreement between stresses. This is also true for bearing capacity prediction. For example, wave equation analysis of the Port Arthur No. 1 final test pile with force-time input gave a predicted bearing capacity of 105 tons. This value differs from the measured pile capacity by 5%, whereas a 7% difference was obtained when the hammer simulation data were used. Similarly, for the Corpus Christi final test a difference of 5% was obtained with force-time, as compared to 32.5% with hammer simulation. It has been stated that the use of unadjusted stiffness values at the head of a pile would yield higher computed stresses. As a matter of interest, the PA1 final test pile was analyzed using the stiffness value based on the commonly accepted modulus for the cushion material and the specified cross-sectional area. This resulted in a bearing capacity prediction which was 53% larger than the measured value, as compared to the 5% error obtained with force-time input.

It is also of interest to note in Table 8 that the predicted bearing capacities are larger than the load test capacities in all

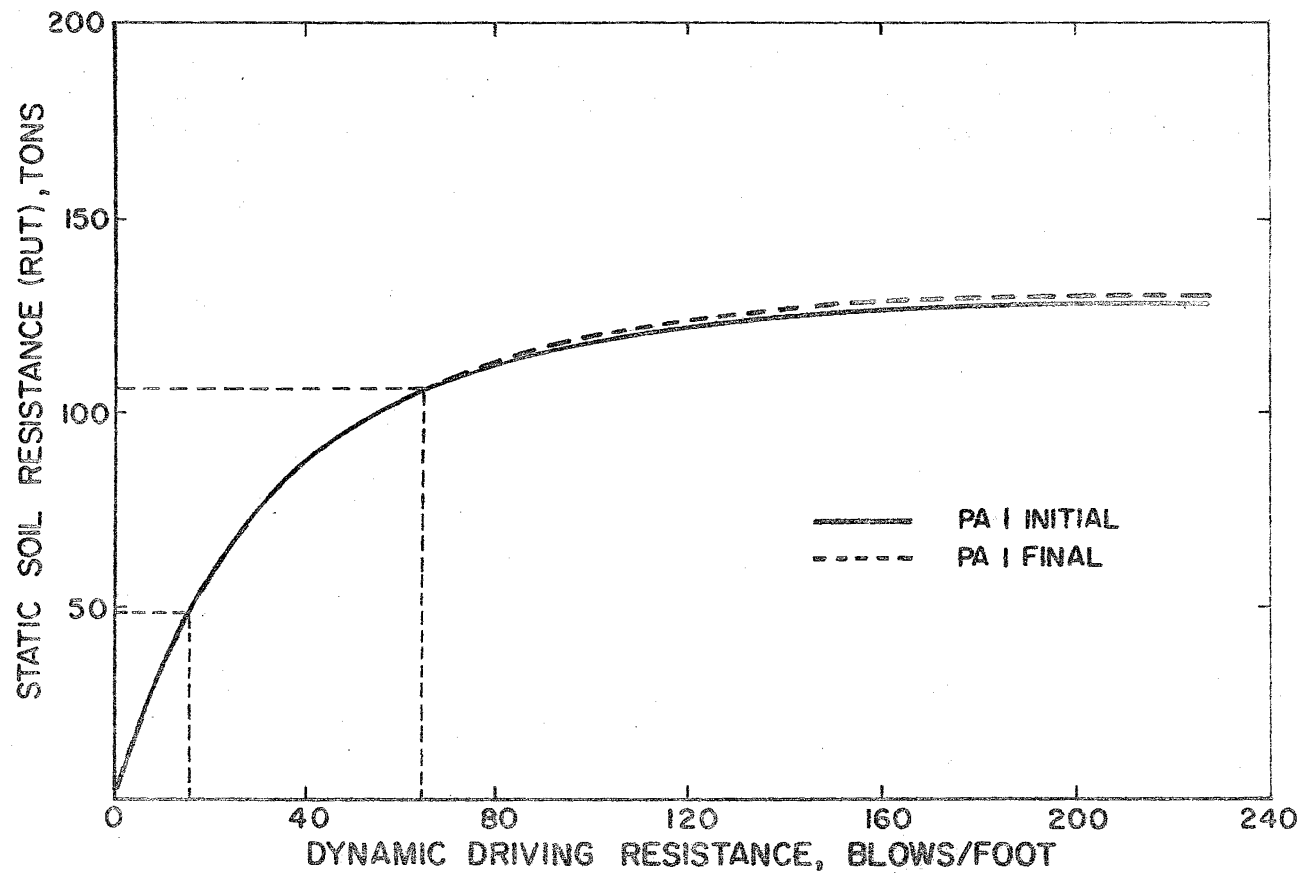


FIG. 20 - RUT vs. BLOW COUNT CURVES FOR PORT ARTHUR No. 1

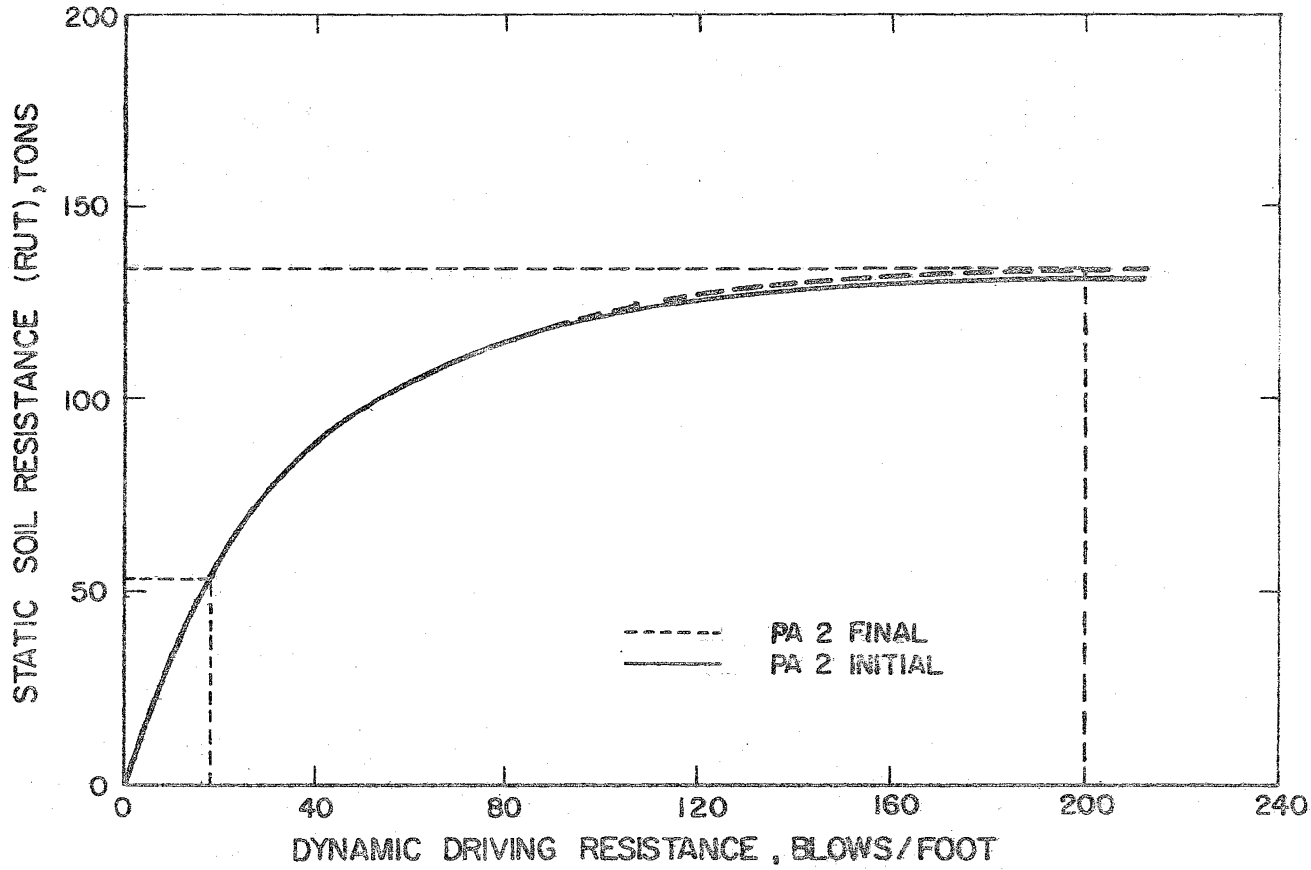


FIG.21 - RUT vs. BLOW COUNT CURVES FOR PORT ARTHUR NO.2

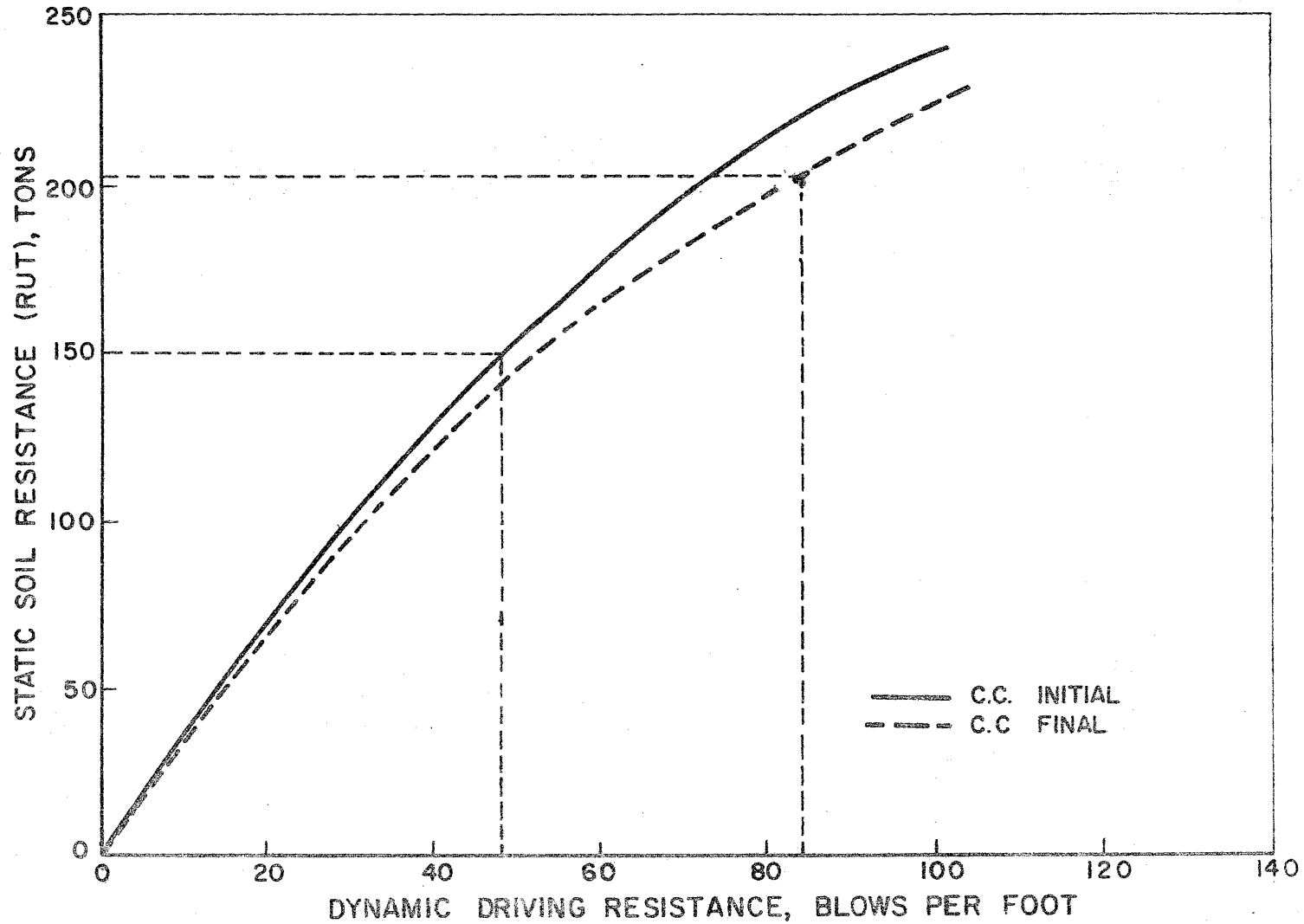


FIG. 22 - RUT vs. BLOW COUNT CURVES FOR CORPUS CHRISTI TEST PILE

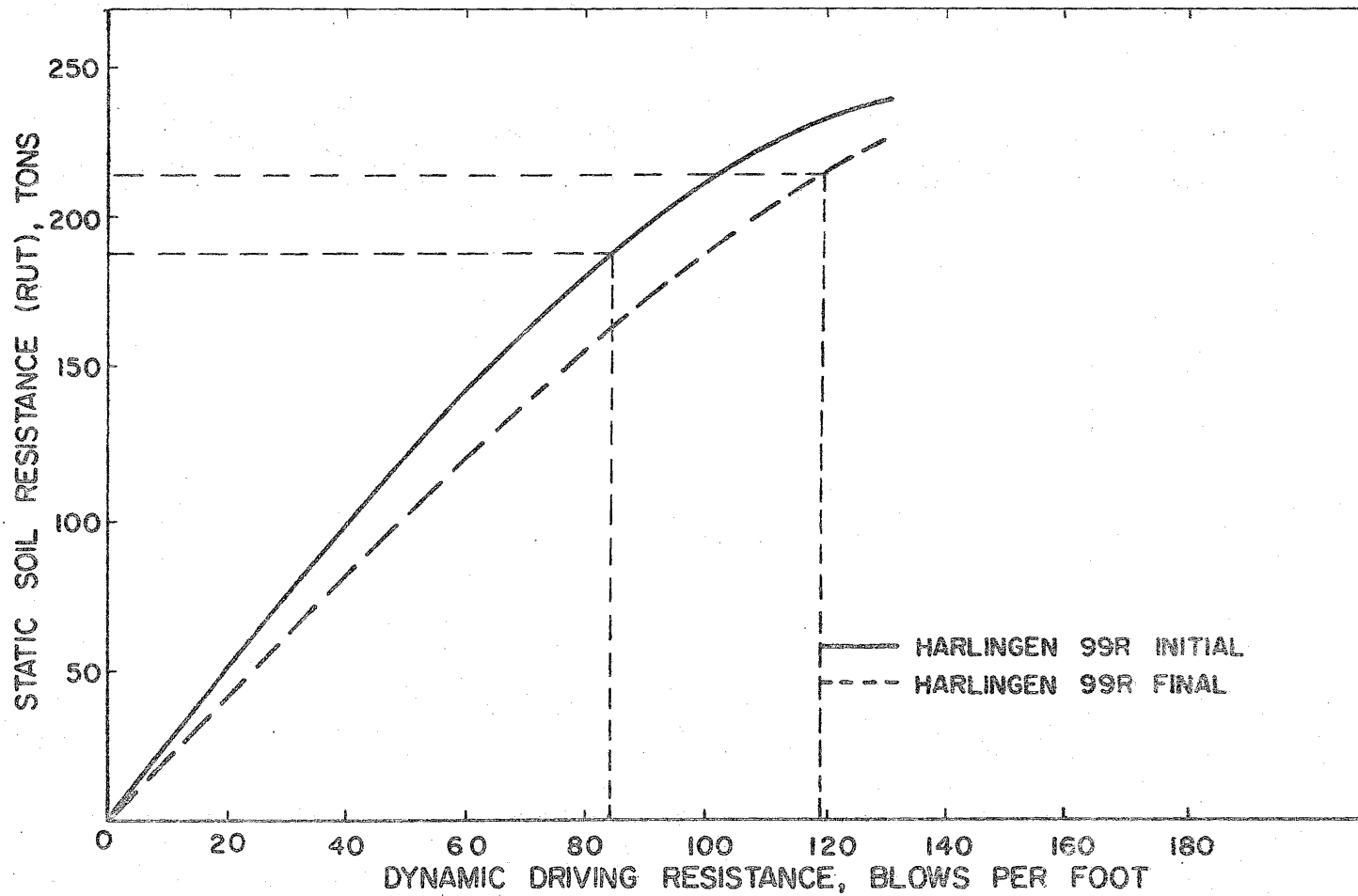


FIG.23 - RUT vs. BLOW COUNT CURVES FOR HARLINGEN 99R

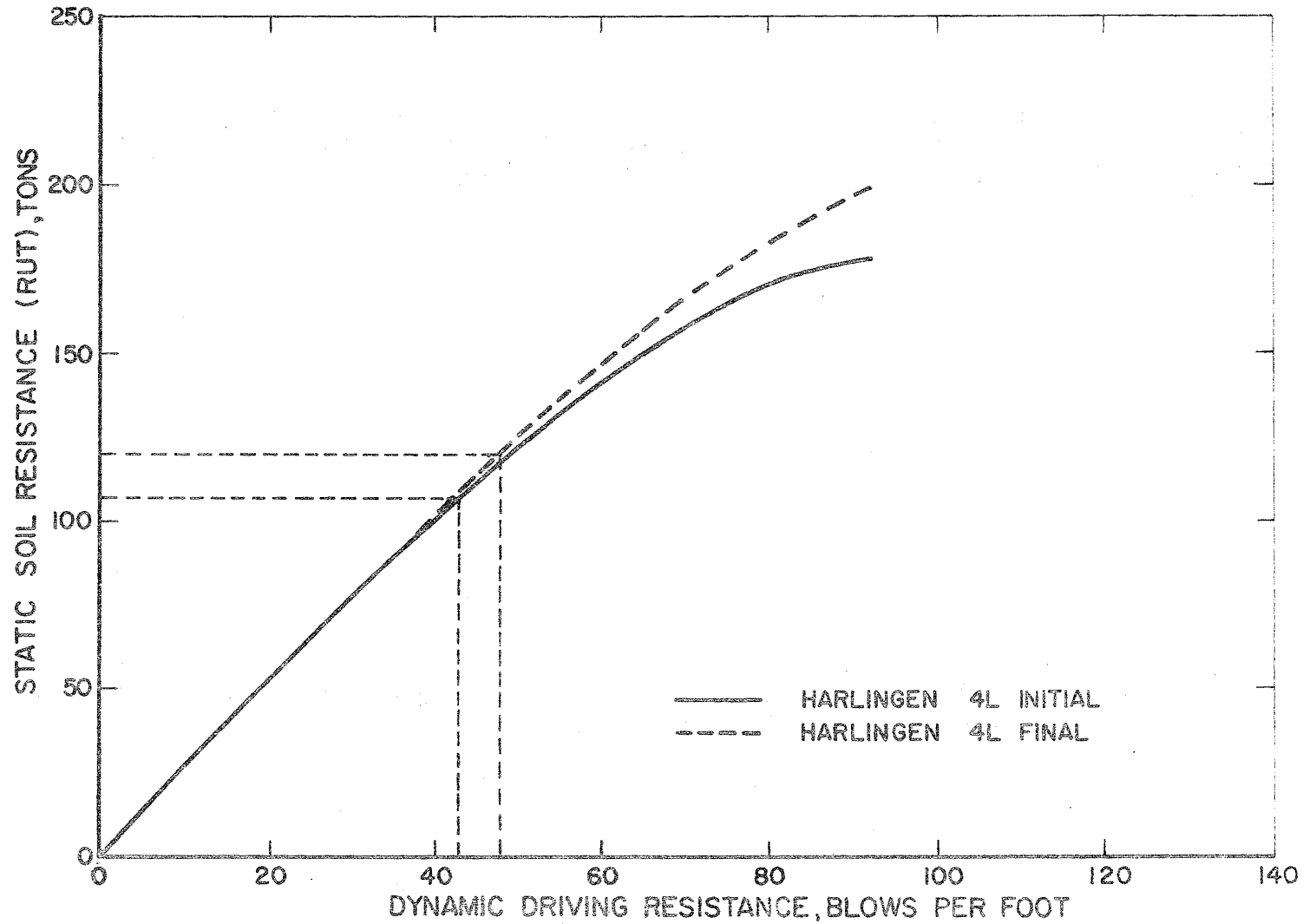


FIG.24-RUT vs. BLOW COUNT CURVES FOR HARLINGEN 4L

TABLE 8.

SUMMARY OF PREDICTED BEARING CAPACITY RESULTS FOR TEST PILES

File No.	Stiffness value, k_p or $k_c + p$ (kips/in.)	Capacity by load test, RUT_{LT} (tons)	Capacity by wave equation RUT_{WE} (tons)	% Error $\left(\frac{RUT_{WE} - RUT_{LT}}{RUT_{LT}} \right) (100)$
PA1 - Initial	182	46	48	+ 4.3
PA1 - Final	182	100	107	+ 7.0
PA2 - Initial	182	54	55	+ 1.8
PA2 - Final	182	131	135	+ 3.1
CC - Initial	900	134	150	+11.9
CC - Final	900	157	208	+32.5
99R - Initial	1400	185	189	+ 2.2
99R - Final	1400	199	215	+ 8.0
4L - Initial	1000	129	108	-16.3
4L - Final	1000	133	121	- 9.0

cases except for Harlingen 4L. In the case of the Port Arthur piles in clay the load test capacity would be higher due to additional set-up if the piles were tested at 15 days or 30 days. The Corpus Christi pile and Harlingen 99R pile were not tested to plunging failure as indicated by the load-settlement curves in Appendix II. Therefore, the load test capacity could be higher. This is particularly true in the case of Corpus Christi Final where the percent error is +32.5. Fig. II-3 in Appendix II indicates that the 10-day load test could not be completed because of reaction beam flexure. The 157 tons given in Table 8 for CC-Final is based on the 7-day test and is obviously low. In the case of Harlingen 4L the predicted capacities are low compared to the load test capacities. This is probably due to the problem encountered in determining the proper blow count for these tests. If this test pile had been driven deeper until a gradually increasing blow count had occurred, the predicted capacity would probably have been greater than the load test capacity.

APPLICATIONS OF WAVE EQUATION ANALYSIS

The wave equation has been demonstrated to be a useful tool in the design and analysis of pile foundations (5, 14). Piling behavior, being the complex problem that it is, necessarily involves a large number of variables associated with the overall hammer-pile-soil system. The so-called dynamic bearing capacity formulas all involve simplifying assumptions concerning many of the variables known to affect the problem. It has been shown (13) that under certain specific conditions regarding pile length, pile type, depth of embedment, soil type, hammer type, etc., one of the many formulas available will yield very good predictions of pile bearing capacity; however, under different conditions the formula is quite inadequate. The wave equation is perhaps the only method capable of accounting for most of the significant variables under any given set of conditions. Moreover, the dynamic bearing capacity formulas were derived for and are capable of predicting only one major item of interest connected with pile driving, i.e., bearing capacity. They cannot provide information concerning other factors which may be of interest, i.e., pile stresses.

One of the objectives of this investigation has been to determine soil parameters for clays and sands which will increase the accuracy and enhance the application of the wave equation method. In this report it has been shown how the wave equation has been used to determine damping parameters and stiffness values from data obtained

during testing of several instrumented piles. Previous investigations (14, 15) have shown how the wave equation can be used to select the optimum driving accessories (cushion, capblock, etc.) for a given hammer-pile-soil system, and to determine the effect of various significant parameters on the problem, such as the effect of pile dimensions and coefficient of restitution on the rate of penetration. These applications may be considered as part of the design and/or analysis of pile foundations, but the usefulness of the wave equation does not stop at the design and analysis level. Beyond this, the problem of field control of the driving of piles is encountered.

One of the major problem areas connected with field control of driven piles occurs when concrete piles are being installed. The Texas Highway Department had at one time been experiencing pile damage due to tension cracks. Because of this problem, the cooperative research program was established in 1962 between the Texas Highway Department and the Texas Transportation Institute to investigate the cause and find a solution. The research disclosed (14) five basic causes of tension cracks which are summarized briefly as follows:

1. Stress waves of high magnitude and short duration caused by an insufficient amount of cushion material.
2. High magnitude stress waves caused by high ram impact velocities, or a very high ram drop.
3. Tensile strength of concrete too low.
4. Little or no soil resistance at the point of long piles, causing critical tensile stresses near the bottom or middle of the pile.

5. Hard driving at the point of long piles, causing critical tensile stresses in the upper half of the pile due to reflected tensile stresses from the pile head.

Generally speaking, the probability of critical tensile stresses existing in short concrete piles is small in comparison with long piles. Provided that adequate cushioning material is used, and reasonable precautions are taken to reduce driving stresses during easy driving (i.e., reducing ram velocity or using a smaller stroke), tension cracks will generally not be much of a problem except when little or no resistance is present at the point of a long pile.

To illustrate how wave equation analysis can be applied to the problem of field control of driving stresses, assume that a 100 ft long concrete pile was to be driven through clay with a Link-Belt 520 double-acting diesel hammer. This problem was chosen for illustrative purposes for two reasons: (1) compared to a single-acting steam hammer of comparable energy rating, the double-acting diesel hammer produces a high-magnitude, short duration stress wave due to the relatively high impact velocity of the comparatively lightweight ram; and (2) very little point soil resistance is encountered throughout the entire driving operation when driving through soft clay. These two conditions are most likely to cause a potential tensile crack problem.

The problem was analyzed by the wave equation to determine the relationship between pile penetration, blow count, and maximum tensile stress for pile penetrations of 10, 50, and 90 percent. At a pile

penetration of 10%, the ratio of point-to-total soil resistance (RUP/RUT) was assumed to be 90%; at a penetration of 50%, the ratio was taken as 50%; and a ratio of 10% was assumed at 90% penetration. Maximum soil resistances of 50, 100, and 200 tons were assumed for penetrations of 10, 50, and 90 percent, respectively. The data obtained are presented in Fig. 25. The maximum tensile stress was plotted versus the soil resistance, and the blow count was also plotted versus soil resistance. The maximum tensile stress allowable in the concrete was assumed to be 1500 lb per sq in. To determine the blow count at which critical tensile stresses may occur, the tensile stress versus blow count curve was entered with the allowable stress and the corresponding soil resistance was determined. The soil resistance value thus determined was used to enter the soil resistance versus blow count curve for the same penetration, and the corresponding blow count was determined. Proceeding in a similar manner for the two remaining values of penetration, three points were obtained which were then used to plot the curve shown in Fig. 26. This curve may be used to determine the blow count, for any penetration, below which critical tensile stresses are most likely to occur. For example, if the blow count becomes equal to or less than 23 blows per foot when the pile is 1/3 of the way into the ground, the driving operation ought to be altered in some manner (i.e., reduce ram velocity) to prevent pile damage.

Another application of wave equation analysis concerns the development of a bearing capacity versus depth curve which is being used for

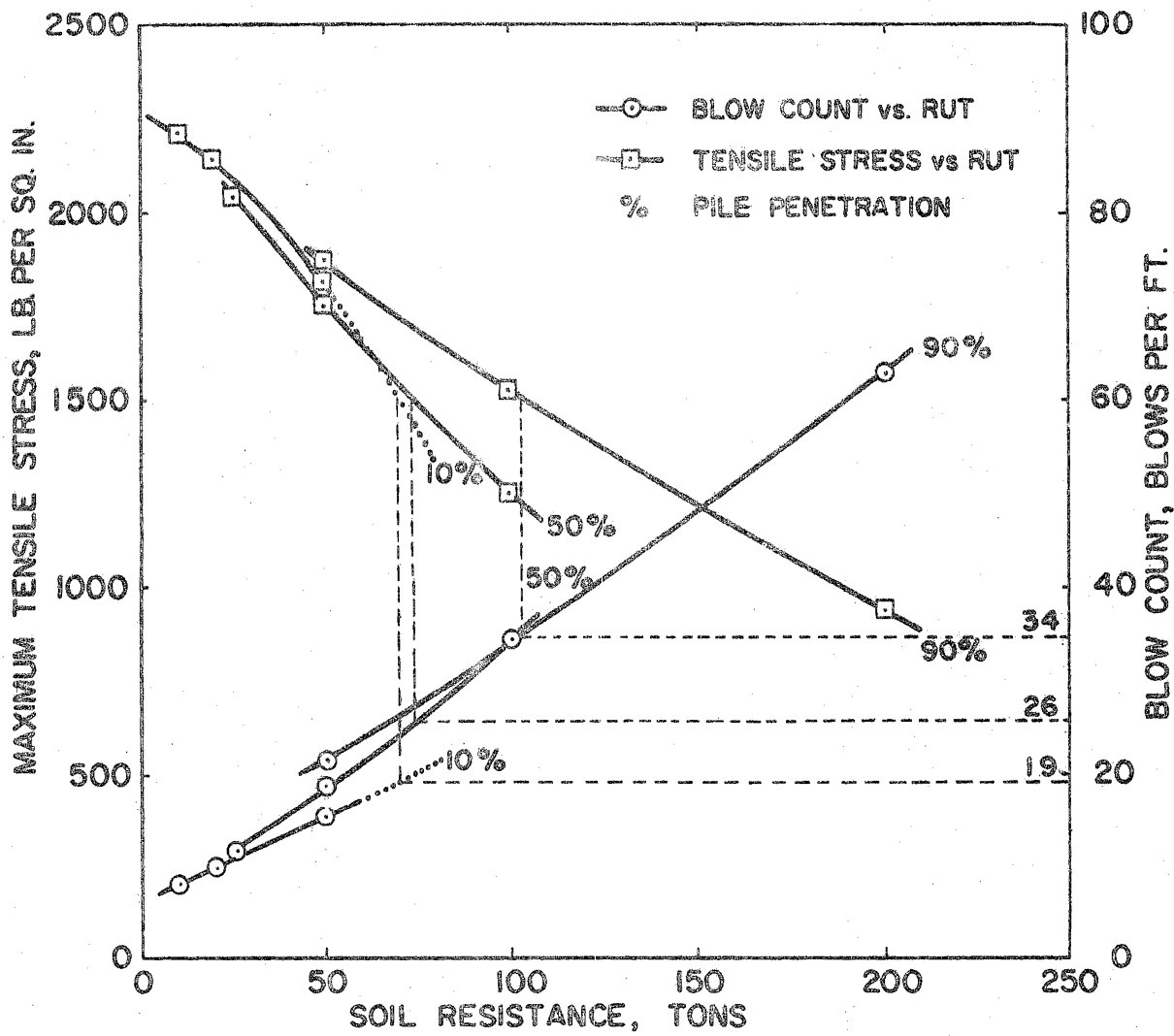


FIG. 25 — MAXIMUM TENSILE STRESS AND BLOW COUNT vs. SOIL RESISTANCE

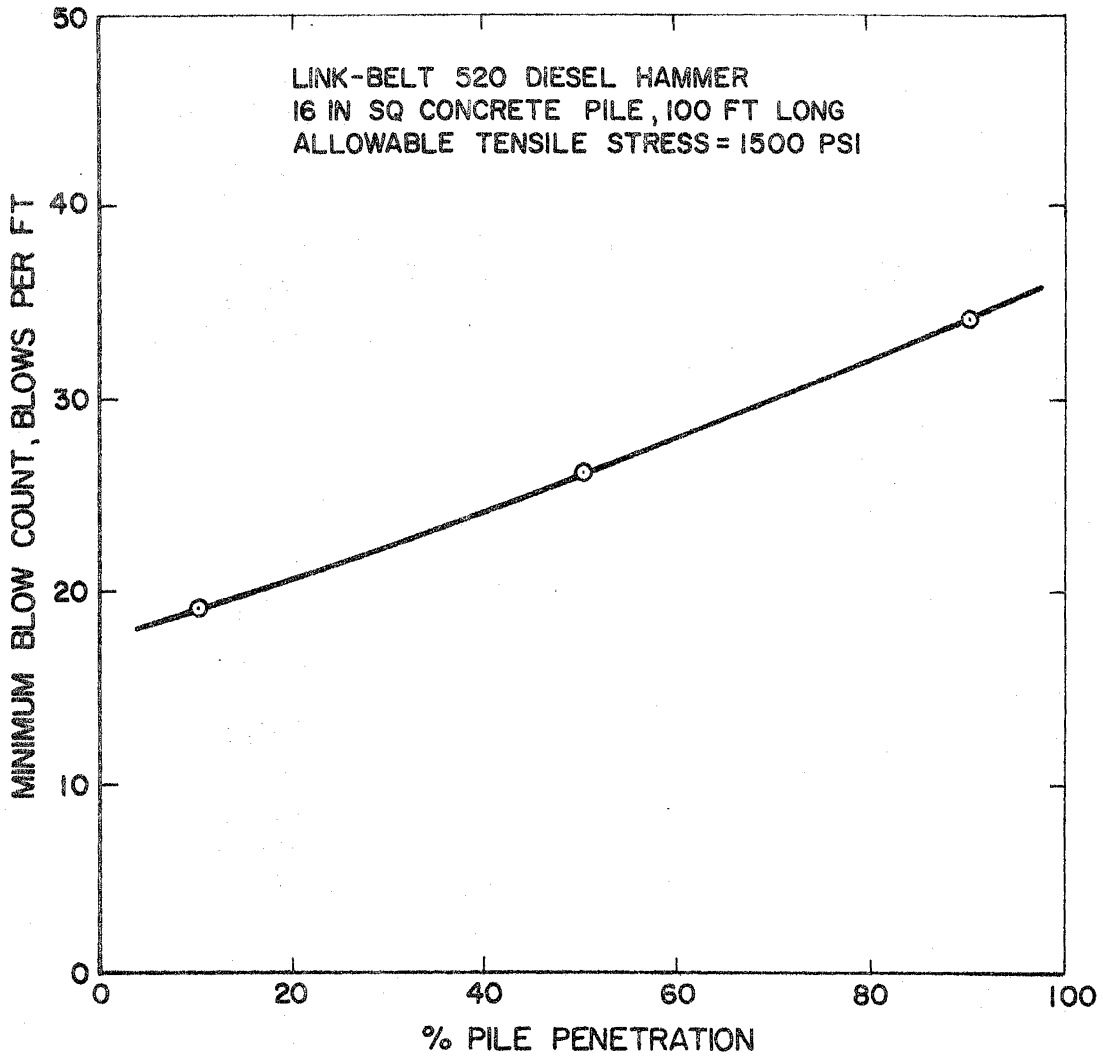
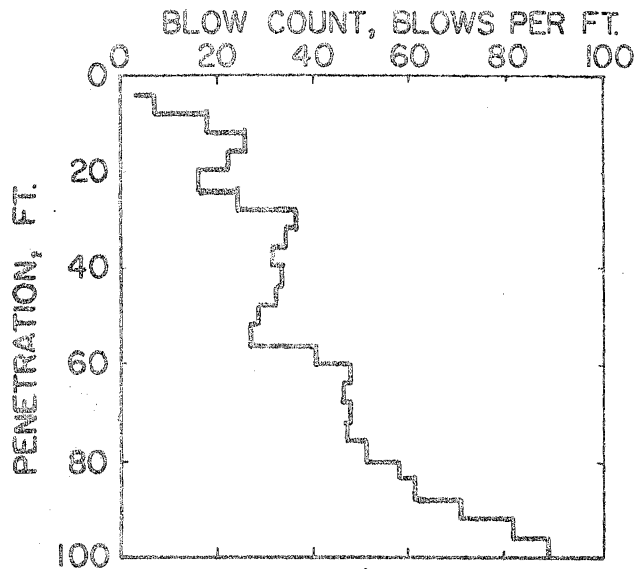


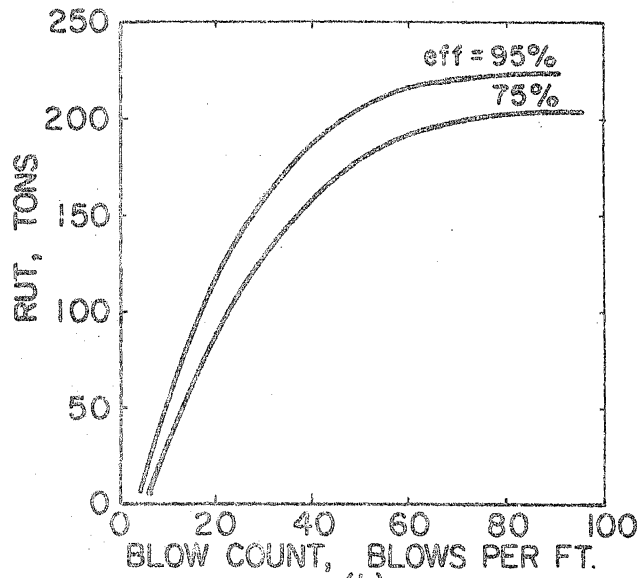
FIG 26 - MINIMUM ALLOWABLE BLOW COUNT FOR PREVENTION OF CRITICAL TENSILE STRESS

determination of pile length. One of the dynamic formulas is normally used to compute the bearing capacity of a pile at selected intervals of depth, the usual interval being every foot or two. It is known that the ratio of point load to side load affects the rate of penetration of the pile into the ground, due to the effect of the soil resistance, or lack of it, on the stress wave. Generally speaking, the dynamic formulas are not capable of accounting for this effect, whereas the wave equation has such a capability. The wave equation can be used to compute a soil resistance versus blow count curve (bearing graph) for selected intervals of depth, using the ratio of point to total load encountered throughout the particular stratum under investigation. The ratio can be predicted on the basis of soil shear strength data, or an approximate choice can be made from a knowledge of the general character of the soil profile down to that point. For each stratum investigated, a series of curves can be generated with a different hammer efficiency being used for each individual curve if it is suspected that the hammer efficiency will vary over a relatively large range.

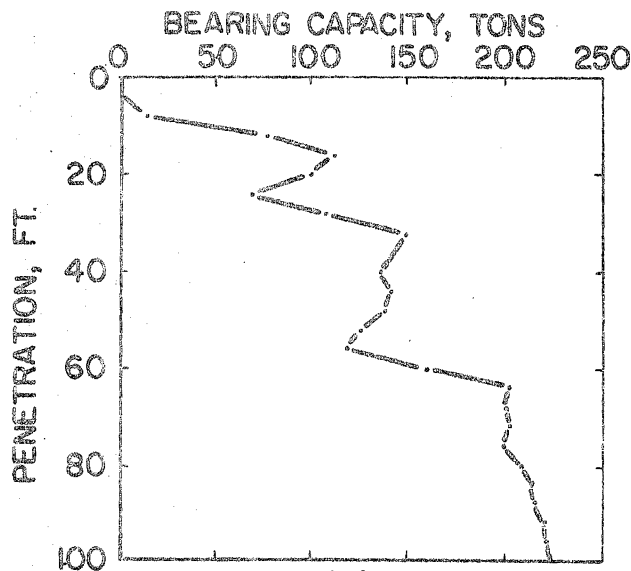
The procedure is illustrated by the curves shown in Fig. 27. Fig. 27 (a) shows a typical driving record for a 100 ft pile. Fig. 27 (b) shows the bearing graphs obtained from a wave equation analysis, where it has been assumed that the hammer efficiency is expected to vary between 75% and 95%. For this example, it is further assumed that the variation in the ratio of point-to-total load during driving will not significantly affect the bearing graph. The plot of predicted



(a)



(b)



(c)

FIG. 27—DETERMINATION OF BEARING CAPACITY vs DEPTH FROM DRIVING RECORD

bearing capacity versus depth, shown in Fig. 27(c), from 0 to 60 ft penetration was obtained from the 75% hammer efficiency bearing graph; the 95% efficiency bearing graph was used to develop the curve from 60 to 100 ft penetration. For example, while driving from 56 to 60 ft of penetration, the average blow count was 40 blows per foot, which yields a predicted bearing capacity of 160 tons with the hammer operating at 75% efficiency. Other points are obtained in a similar manner.

Although the data of Fig. 27 are hypothetical and are not intended to be typical of all driving conditions, they are helpful in describing an important detail regarding the interpretation of a driving record and bearing graph. A rather large increase in blow count is not necessarily indicative of a correspondingly large increase in static bearing capacity. As shown in Fig. 27(a), the blow count increased from 48 to 88 blows per foot, or nearly doubled, between 64 and 100 ft penetration. Fig. 27(c) shows that the predicted bearing capacity increased by only 20 tons, from 200 to 220 tons, as the driving capacity of the hammer was approached.

In cases where the ratio of point-to-total load does not change significantly after the pile is driven, the bearing graph which is valid at the time of driving may be used to predict the bearing capacity after soil set-up has occurred. Set-up is not likely to occur for piles in sand, but an appreciable amount of set-up may develop in some clays. Stiff or over-consolidated and normally consolidated clays may exhibit considerable set-up, while under-consolidated clays may

exhibit very little, if any, set-up. To predict an "after set-up" bearing capacity, a pile should be redriven an additional three to five feet, or until a relatively constant redriving blow count is obtained and the pile is moving relative to the soil. The blow count then obtained is used to determine the bearing capacity from the bearing graph in the usual manner. For piles which are driven in clay, the point load generally will not vary greatly as these piles are predominantly friction piles. This is evidenced by the data obtained from the Port arthur test piles where the load at the tip of the piles decreased from 7 to 15 percent between driving and redriving. Data are not available for other conditions, i.e., a pile driven through soft clay to bearing on a dense sand or a pile driven through dense sand into a soft clay. For these conditions or others which differ from those observed in this study, the "time-of-driving" bearing graph may not be valid for redriving data, and the applicability should be verified by at least one load test. The wave equation should be used to determine set-up where possible, and especially on large jobs, as a substantial dollar-savings can be realized from a reduction in pile length which can be obtained by utilizing the increased capacity due to set-up.

Notwithstanding the simplicity and ease of operation of diesel hammers, the importance of the wave equation should not be overlooked concerning a comparison of various hammers. Considering a diesel and a steam hammer of near the same energy rating, the diesel hammer will have a comparatively lightweight ram operating at a higher impact

velocity. The two hammers may appear equivalent on an energy-rating basis, but the comparative operating characteristics (ability to drive a pile under given conditions) may be quite different. As a general rule, a steam hammer will apply a stress wave of moderate intensity to the head of the pile. The larger mass of the ram causes the stress wave to act on the pile for a relatively long time period, all the while causing the pile to penetrate further into the soil. Under light to moderate soil resistance, the long duration stress wave of the steam hammer causes a much larger penetration per hammer blow than does the diesel hammer. On the other hand, under hard driving conditions, the magnitude of the steam hammer stress wave is insufficient to overcome the soil resistance, whereas the high intensity, short duration stress wave of the diesel hammer can overcome the soil resistance and set the pile into motion. The penetration per blow will be relatively smaller, but the pile can be driven against larger resistances. These tendencies are evident in the bearing graphs obtained from wave equation analyses utilizing the two types of hammers. Consequently, the wave equation can be extremely valuable in selecting a particular hammer for a specific job when the alternative is between steam or diesel hammers.

When the alternative is solely between diesel hammers, the wave equation can effectively be used to evaluate or rate one hammer against another, or compare hammers of various energy ratings at different operating efficiencies. Ram height of fall for steam or open-end diesel hammers, and bounce chamber pressure for closed-end diesel hammers, are

relatively good indicators of operating efficiency. With a family of wave equation bearing graph curves available in the field, each curve representing a different efficiency, the driving operation can constantly be assessed with regard to bearing capacity.

The problem encountered while driving the pile at bent 4L near Harlingen, Texas, provides another illustration of how wave equation bearing graphs can be helpful when unusual driving conditions are encountered. While the pile was being driven with approximately 20 ft of pile embedded, the observed blow count suddenly decreased from 40 to 12 blows per foot, whereupon driving was terminated. In instances such as this, it would have been wise to continue driving the pile an additional two to three feet to ascertain whether the decreased blow count was due to a temporary condition, such as the pile passing through a very thin seam of loose material, or if the condition was more permanent in nature. With bearing graphs available, it would have been possible to obtain a good indication of the bearing capacity at that time, both before the blow count decreased and at the time the count was unusually low. The bearing graph would have been helpful in determining if driving could have been stopped while the blow count was low and still have achieved the design capacity of the pile, or if additional driving was in fact necessary to attain the design load.

CONCLUSIONS AND RECOMMENDATIONS

Conclusions. - Instrumented piles were tested under three field conditions: (1) all in clay; (2) all in sand; and (3) in clay with tip in sand. Based on these conditions the following conclusions are made:

1. Wave equation analysis can be used effectively to predict static bearing capacity of axially loaded piles and to predict driving stresses which occur during driving.

2. The accuracy of the predicted bearing capacity and driving stress is directly related to the accuracy of the computer input parameters used for the hammer-pile system as follows:

- a. If measured force-time data is input at the head of the pile, the predicted values are very accurate.
- b. If an adjusted stiffness value ($\frac{AE}{L}$) is input at the head of the pile by matching computed and measured peak forces, the predicted values are sufficiently accurate for use in practice.
- c. If adjusted stiffness values are not input at the head of the pile, the predicted values may not be reliable enough for use in practice.

3. Accurate predictions of bearing capacity and driving stress will be obtained by using the computer input parameters developed in this study for the pile-soil system as follows:

- a. For piles in clay use loading quake values of $Q_{-side} = Q_{-}$

point = 0.1; unloading quake values of Q-side = Q-point = 0.1; and damping values of J-side = 0.2, J-point = 0.01.

- b. For piles in saturated sand use loading quake values of Q-side = 0.2, Q-point = 0.4; unloading quake values of Q-side = Q-point = 0.1; and damping values of J-side = 0.5, J-point = 0.15.

4. A single bearing graph curve can be used for bearing capacity prediction at initial driving and final re-driving as long as the static load distribution (primarily the ratio of RUP to RUT) does not change appreciably. Any increase in pile capacity due to soil "set-up" is reflected at final re-driving by an increased blow count, and any decrease in pile capacity due to soil "relaxation" is reflected at final re-driving by a reduced blow count.

Recommendations. - Based on the findings of this research study, the following recommendations are offered:

1. A simple device for measuring the dynamic peak force at the pile head during initial driving or final re-driving is being developed so that an adjusted top pile segment stiffness can be determined. This will reduce the uncertainties associated with the present procedure for simulating the hammer-pile system and will insure that predicted bearing capacity and driving stresses will be sufficiently accurate for practical usage.

2. After the simple dynamic peak force measuring device is developed, it should be field tested at least one time with an instrumented test pile. This will provide a complete field verification of the new device.

3. Instrumented test piles should be driven and load tested in other soil types, particularly silts and unsaturated sand, and when the soil profiles differ basically from those encountered in this study, i.e., clay underlying sand. The tests should be conducted according to the procedure developed in this study. This will allow the determination of soil quake and soil damping values for these soil types and geologic conditions.

4. At least one additional instrumented pile test should be conducted and dynamic force-time data recorded when the test pile is embedded $1/4$, $1/2$, and $3/4$ of the total pile penetration. This will allow the measurement of reflected tensile forces and a comparison with wave equation computed tensile forces can be made. This test could be performed at the same time that the field verification test is conducted on the dynamic peak force device.

5. A standard procedure should be developed for determining blow counts in the field, so that the problem which occurred during the test at Harlingen 4L will not be repeated. This problem can probably be resolved by requiring that test piles be driven until a constant blow count or a slightly increasing blow count is achieved over several feet of driving.

6. The present method of static analyses should be refined so that accurate determination of pile load distribution can be made when instrumented pile data are not available. This could be accomplished by establishing better correlation of penetrometer test data with soil strength parameters; which in turn can be used to establish better pile load distribution for wave equation analyses.

APPENDIX I. - REFERENCES

1. Bartoskewitz, R. E. and Coyle, H. M., "Wave Equation Prediction of Pile Bearing Capacity Compared with Field Test Results," Texas Transportation Institute Research Report 125-5, Texas A&M University, December, 1970.
2. Coyle, H. M. and Sulaiman, I. H., "Skin Friction for Steel Piles In Sand," Journal of the Soil Mechanics and Foundations Division, ASCE Vol. 93, No. SM6, Proc. Paper 5590, November, 1967, pp. 261-278.
3. Cummings, A. E., "Dynamic Pile Driving Formulas," Journal of the Boston Society of Civil Engineers, January, 1940.
4. Dunlap, D. D., "The Effects of Repetitive Loadings on the Shearing Strength of a Cohesionless Soil," Thesis submitted to the Graduate College of the Agricultural and Mechanical College of Texas, May, 1959, unpublished.
5. Forehand, P. W. and Reese, J. L., Jr., "Prediction of Pile Capacity by the Wave Equation," Journal of the Soil Mechanics and Foundations Division, ASCE Vol. 90, No. SM2, Part 1, Proc. paper 3820, March, 1964, pp. 1-25.
6. Fox, E. N., "Stress Phenomona Occurring in Pile Driving," Engineering, (London), Vol. 134, 1932.
7. Foye, R. Jr., Coyle, H. M., Hirsch, T. J., Bartoskewitz, R. E. and Milberger, L. J., "Wave Equation Analysis of Full-Scale Test Piles Using Measured Field Data," Texas Transportation Institute Report 125-7, Texas A&M University, August, 1972.
8. Fuller, F. M. and Hoy, H. E., "Pile Load Tests Including Quick-Load Test Method and Interpretations," Highway Research Record No. 333, 1970, pp. 74-86.
9. Gibson, G. C. and Coyle, H. M., "Soil Damping Constants Related to Common Soil Properties in Sands and Clays," Texas Transportation Institute Research Report 125-1, Texas A&M University, September, 1968.
10. Glanville, W. H., Grime, G., Fox, E. N. and Davies, W. W., "An Investigation of the Stresses in Reinforced Concrete Piles During Driving," British Bldg. Research Board Technical Paper No. 20, D.S.I.R., 1938.
11. Issacs, D. V., "Reinforced Concrete Pile Formula," Transactions of the Institution of Engineers, Australia, Vol. 12, 1931, pp. 312-323.

12. Korb, K. W. and Coyle, H. M., "Dynamic and Static Field Tests on a Small Instrumented Pile," Texas Transportation Institute Research Report 125-2, Texas A&M University, February, 1969.
13. Lowery, L. L., Jr., Finley, J. R., Jr., and Hirsch, T. J., "A Comparison of Dynamic Pile Driving Formulas with the Wave Equation," Texas Transportation Institute Research Report 33-12, Texas A&M University, August, 1968.
14. Lowery, L. L., Jr., Hirsch, T. J., Edwards, T. C., Coyle, H. M., and Samson, C. H., "Pile Driving Analysis - State of the Art," Texas Transportation Institute Research Report 33-13, Texas A&M University, January, 1969.
15. Lowery, L. L., Jr., Hirsch, T. J., and Samson, C. H., "Pile Driving Analysis - Simulation of Hammers, Cushions, Piles and Soils," Texas Transportation Institute Research Report 33-9, Texas A&M University, August, 1967.
16. Perdue, G. W. and Coyle, H. M., "In-Situ Measurements of Friction and Bearing Correlated with Instrumented Pile Tests," Texas Transportation Institute Research Report 125-4, Texas A&M University, June 1970.
17. Rehmet, J. D. and Coyle, H. M., "Preliminary Study of In-Situ Measurements of Friction and Bearing In Clay," Texas Transportation Institute Research Report 125-3, September, 1969.
18. Smith, E. A. L., "Pile Driving Analysis by the Wave Equation," Journal of the Soil Mechanics and Foundation Division, ASCE Vol. 86, No. SM4, Proc. Paper 2574, August, 1960, pp. 35-61.
19. Smith, E. A. L., "Pile Driving Impact," Proceedings, Industrial Computation Seminar, September, 1950, International Business Machines Corp., New York, N. Y., p. 44.
20. Van Reenen, D. A., Coyle, H. M. and Bartoskewitz, R. E., "Investigation of Soil Damping on Full-Scale Test Piles," Texas Transportation Institute Research Report 125-6, Texas A&M University, August, 1971.

APPENDIX II - FIELD TEST AND COMPUTER INPUT DATA

PORT ARTHUR TEST PILE NO. 1

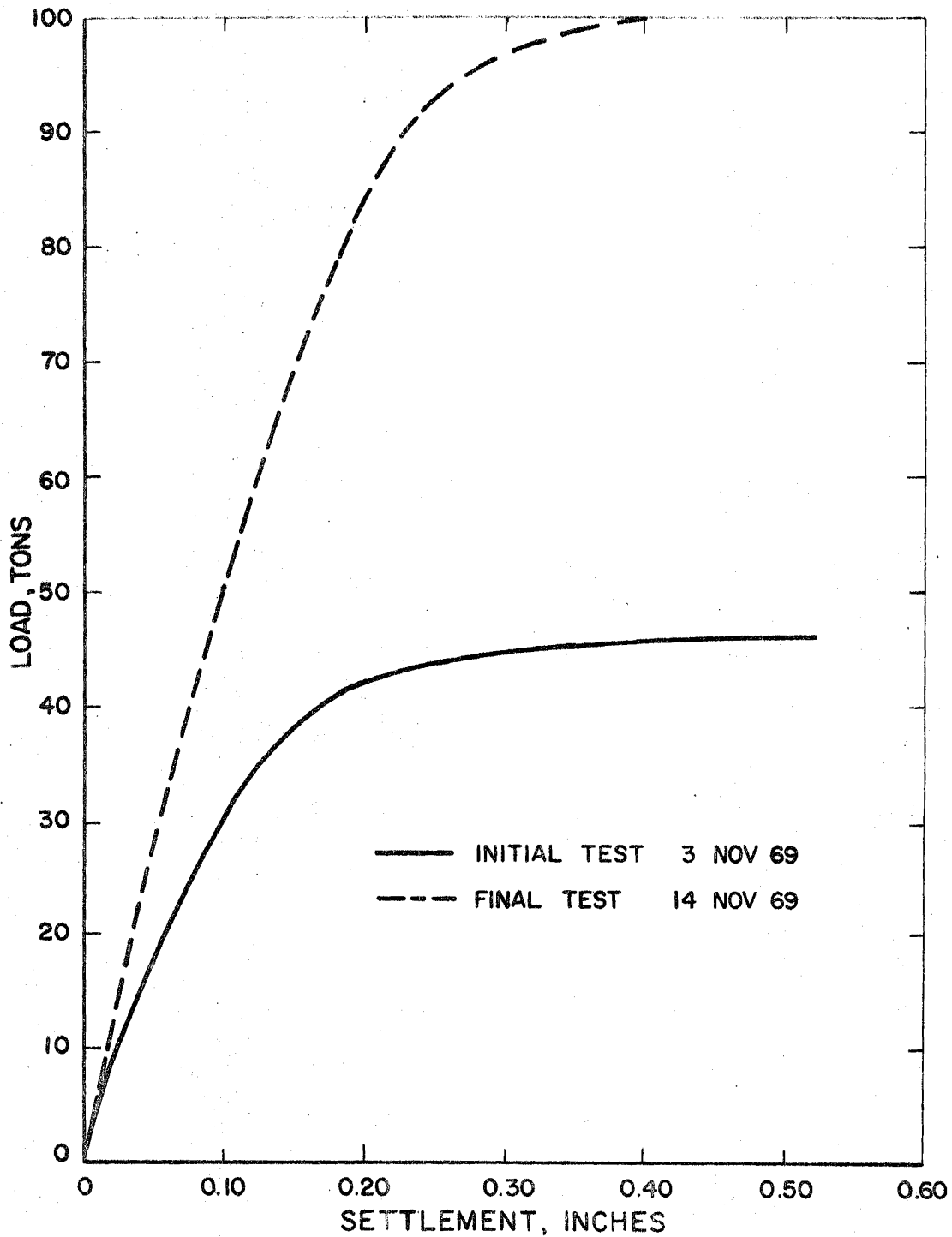


FIG. II-1 - LOAD vs. SETTLEMENT CURVES FOR PORT ARTHUR TEST PILE NO. 1

TABLE II-1 - PORT ARTHUR PILE LOAD TEST DATA

Test Pile No. 1 Initial Test 3 Nov 69

Jack Load (Tons)	Load Cell (Tons)	Gage 1 (Tons)	Gage 3 (Tons)	Gage 4 (Tons)	Gage 5 (Tons)
10	8.39	10.3	5.95	2.15	.85
20	16.2	17.3	11.55	5.15	1.75
30	22.9	24.95	18.25	9.25	2.9
40	31.2	34.7	27.35	15.1	4.65
50	38.3	41.9	34.1	20.85	6.85
57	45.8	46.15	37.65	22.9	9.05

TABLE II-2 - PORT ARTHUR PILE LOAD TEST DATA

Test File No. 1 Final Test 14 Nov 69

Jack Load (Tons)	Load Cell (Tons)	Gage 1 (Tons)	Gage 3 (Tons)	Gage 4 (Tons)	Gage 5 (Tons)
10	10.5	8.9	3.15	.8	.15
20	14.7	17.15	7.1	1.85	.3
30	21.2	25.25	10.65	2.75	.75
40	29.4	34.1	14.85	3.75	.9
50	52.1	42.9	18.55	4.9	.8
60	45.4	51.05	24.45	7.5	1.45
70	54.3	59.65	30.6	7.8	1.45
80	63.9	67.2	35.15	9.35	2.3
85	68.0	71.35	38.0	10.25	2.4
90	73.6	76.05	41.3	11.25	2.65
95	78.2	79.85	43.7	12.15	2.75
100	81.4	83.8	46.2	12.75	2.85
105	86.5	87.0	48.4	13.05	3.15
110	91.1	91.4	51.2	14.7	3.35
115	95.3	94.85	52.65	15.7	3.65
120	100.0	99.99	54.6	17.15	4.55

TABLE II-3 - PA1 INITIAL PILE DRIVING DATA

Pile Tip Elevation (ft)	Depth of Pile in Ground (ft)	Energy of Hammer (ft-lb)	Number of Blows	Total Penetration (inches)	Blows Per Foot
3.20 to -18.80	22	Weight of Hammer Not Within Range of Manufacturer's Energy Rating Chart for P.S.I.G.			
-18.80 to -30.80	34				
-31.80	35	15,000	10	12	10
-32.80	36	15,000	10	12	10
-33.80	37	15,000	11	12	11
-34.80	38	15,000	11	12	11
-35.80	39	15,000	11	12	11
-36.80	40	15,000	11	12	11
-37.70	41	15,000	11	12	11
-38.80	42	15,000	10	12	10
-39.80	43	15,000	11	12	11
-40.80	44	15,000	11	12	11
-41.80	45	15,000	11	12	11
-42.80	46	15,000	10	12	10
-43.80	47	15,000	11	12	11
-44.80	48	15,000	11	12	11
-45.80	49	15,000	11	12	11
-46.80	50	16,750	12	12	12
-47.80	51	18,000	13	12	13
-48.80	52	18,000	12	12	12
-49.80	53	18,000	12	12	12
-50.80	54	18,000	12	12	12
-51.80	55	19,125	12	12	12
-52.80	56	19,125	13	12	13
-53.80	57	20,250	14	12	14
-54.80	58	20,250	14	12	14
-55.80	59	20,250	14	12	14
-56.80 ^a	60	21,250	15	12	15
-57.80 ^b	61	21,250	15	12	15
-58.80 ^b	62	19,125	20	12	20
-59.80 ^b	63	20,250	18	12	18
-60.55 ^b	63.75	20,250	13	9	17

^aLast blow without cushion. Stopped 1 hour.

^bDriven with cushion. Final blow count without cushion extrapolated to be 16 blows per foot.

TABLE II-4 - PA1 FINAL PILE DRIVING DATA

Pile Tip Elevation (ft)	Depth of Pile in Ground (ft)	Energy of Hammer (ft-lb)	Number of Blows	Total Penetration (inches)	Blows Per Foot
-60.55 ^a	63.75	21,200	36	1	432
-60.72 ^a	63.92	19,500	114	2	684
-60.97 ^b	64.17	24,250	21	3	84
-61.22 ^c	64.42	24,250	18	3	72
-61.47 ^c	64.67	24,250	18	3	72
-61.72 ^c	64.92	24,250	18	3	72
-61.97 ^c	65.17	24,250	18	3	72
-62.22	65.42	24,250	19	3	76
-62.47	65.67	24,250	16	3	64
-62.72	65.92	24,250	18	3	72
-62.97	66.17	24,250	18	3	72
-63.22	66.42	24,250	18	3	72
-63.47	66.67	24,250	17	3	68
-63.72	66.92	24,250	18	3	72
-63.97	67.17	24,250	18	3	72
-64.22	67.42	24,250	18	3	72
-64.47	67.67	24,250	16	3	64
-64.72	67.92	24,250	17	3	68
-64.97	68.17	24,250	18	3	72
-65.22	68.42	24,250	19	3	76

^aDriven with cushion.

^bFirst blow without cushion.

^cBlow count without cushion averaged to be 72 blows per foot.

TABLE II-5 - COMPUTER INPUT DATA FOR PA1 INITIAL

Hammer Properties

Type: Link Belt 520
Rated energy: 26,300 ft-lb
Hammer efficiency (%): 100
Explosive force: 98 kips
Ram velocity: 14.70 fps
Ram weight: 5.07 kips
Ram stiffness: 108,500 kips/in.,
e = 0.6 (steel on steel impact)
Anvil weight: 1.179 kips
Adapter weight: 1.05 kips
Capblock: Alternating aluminum and plastic
disks (enclosed). $K_c = 18,600$ kips/in., e = 0.8
Cushion: None

Pile Properties

Type: 16 in. OD, 3/8 in. wall, closed end steel pipe
Segment length: 2 ft
Segment weight: 0.1252 kip
Segment stiffness: 22,700 kips/in., e = 1.0

Soil Distribution

RUT: 92.0 kips
RUP: 18.0 kips
Load distribution: 0.805 RUT uniform side load,
0.195 RUT at pile tip

TABLE II-6 - COMPUTER INPUT DATA FOR PA1 FINAL

Hammer Properties

Type: Link Belt 520
Rated energy: 26,300 ft-lb
Hammer efficiency (%): 100
Explosive force: 98 kips
Ram velocity: 15.92 fps
Ram weight: 5.07 kips
Ram stiffness: 108,500 kips/in.,
e = 0.6 (steel on steel impact)
Anvil weight: 1.179 kips
Adapter weight: 1.05 kips
Capblock: Alternating aluminum and plastic
disks (enclosed). $K_c = 18,600$ kips/in., e = 0.8
Cushion: None

Pile Properties

Type: 16 in. OD, 3/8 in. wall, closed end steel pipe
Segment length: 2 ft
Segment weight: 0.1252 kip
Segment stiffness: 22,700 kips/in., e = 1.0

Soil Distribution

RUT: 200 kips
RUP: 10 kips
Load distribution: 0.95 RUT uniform side load,
0.05 RUT at pile tip

PORT ARTHUR TEST PILE NO. 2 .

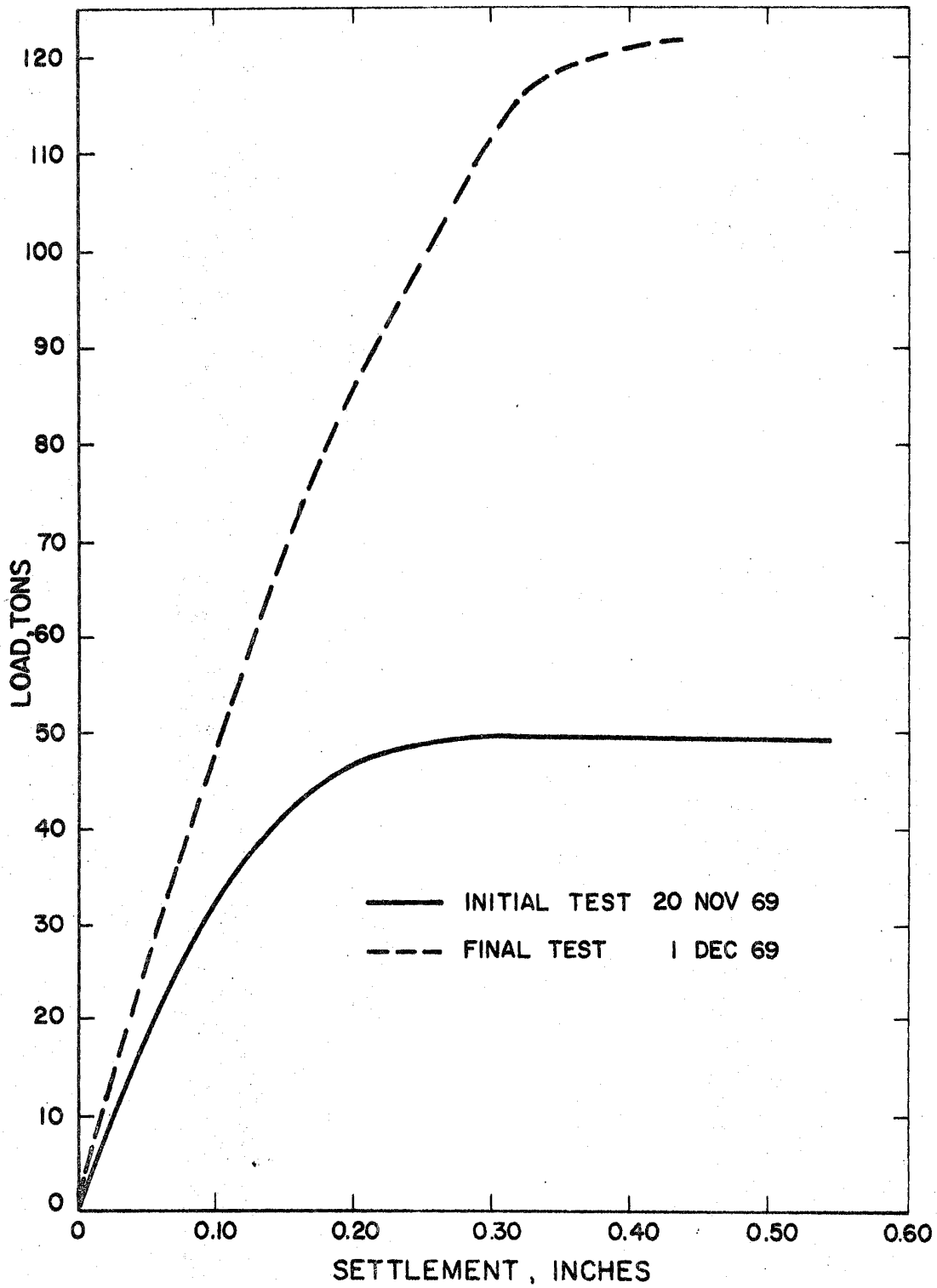


FIG. II-2- LOAD vs.SETTLEMENT CURVES FOR PORT ARTHUR TEST PILE NO.2

TABLE II-7 - PORT ARTHUR PILE LOAD TEST DATA

Test File No. 2 Initial Test 20 Nov 69

Jack Load (Tons)	Load Cell (Tons)	Gage 1 (Tons)	Gage 2 (Tons)	Gage 4 (Tons)	Gage 5 (Tons)
10	13.8	9.45	7.35	4.3	.45
20	21.3	18.5	27.1	6.15	1.0
30	30.3	28.3	23.2	10.15	1.85
40	40.7	38.05	32.4	16.0	3.45
45	44.9	33.9	36.35	19.5	4.1
50	49.3	46.2	40.0	20.0	5.35
55	54.4	50.1	44.0	24.05	8.1

TABLE II-8 - PORT ARTHUR PILE LOAD TEST DATA

Test Pile No. 2 Final Test 1 Dec 69

Jack Load (Tons)	Load Cell (Tons)	Gage 1 (Tons)	Gage 2 (Tons)	Gage 4 (Tons)	Gage 5 (Tons)
10	6.73	5.98	4.26	.67	.06
20	20.7	17.21	12.71	2.56	.33
30	30.8	27.53	21.50	4.06	.61
40	39.9	37.63	29.34	6.12	.95
50	43.2	45.97	36.53	8.01	1.23
60	60.7	55.86	45.02	10.52	1.74
70	70.9	65.69	53.74	13.03	2.19
80	80.4	74.30	61.43	15.59	2.52
90	89.8	83.71	70.02	18.54	3.03
95	93.4	87.88	74.23	20.53	3.37
100	98.1	92.10	78.19	22.25	3.75
105	103.4	96.75	82.49	24.33	4.10
110	107.5	100.44	85.94	26.44	4.49
115	112.1	104.34	89.50	28.79	4.94
120	116.8	108.83	93.86	31.34	5.61
125	121.1	113.26	98.09	33.90	6.46
130	126.0	117.87	102.42	36.97	7.63
135	130.8	121.45	106.18	41.31	10.44

TABLE II-9 - PA2 INITIAL PILE DRIVING DATA

Pile Tip Elevation (ft)	Depth of Pile in Ground (ft)	Energy of Hammer (ft-lb)	Number of Blows	Total Penetration (inches)	Blows Per Foot
3.00 to -28.00	31	Weight of Hammer Not Within Range of Manufacturer's Energy Rating Chart for P.S.I.G.			
-28.00 to -38.00	41				
-39.00	42	15,000	8	12	8
-40.00	43	15,000	8	12	8
-41.00	44	15,000	8	12	8
-42.00	45	15,000	8	12	8
-43.00	46	15,000	10	12	10
-44.00	47	15,000	9	12	9
-45.00	48	15,000	10	12	10
-46.00	49	15,000	12	12	12
-47.00	50	15,000	12	12	12
-48.00	51	18,000	12	12	12
-49.00	52	19,125	12	12	12
-50.00	53	18,000	11	12	11
-51.00	54	18,000	10	12	10
-52.00	55	18,000	12	12	12
-53.00	56	16,750	12	12	12
-54.00	57	15,000	16	12	16
-55.00	58	16,750	14	12	14
-56.00	59	18,000	16	12	16
-57.00	60	16,750	15	12	15
-58.00	61	16,750	14	12	14
-59.00	62	16,750	15	12	15
-60.00	63	18,000	12	12	12
-61.00	64	20,250	12	12	12
-62.00	65	20,250	13	12	13
-63.00	66	21,250	13	12	13
-64.00	67	21,250	15	12	15
-65.00	68	21,250	16	12	16
-66.00	69	22,250	16	12	16
-67.00 ^a	70	22,250	21	12	21
-68.00 ^b	71	22,250	23	12	23
-69.00 ^b	72	22,250	23	12	23
-70.00 ^b	73	22,250	22	12	22
-71.00 ^b	74	22,250	22	12	22

^aLast blow without cushion. Stopped 45 minutes.

^bDriven with cushion. Final blow count without cushion extrapolated to be 18 blows per foot.

TABLE II-10 - PA2 FINAL PILE DRIVING DATA

Pile Tip Elevation (ft)	Depth of Pile in Ground (ft)	Energy of Hammer (ft-lb)	Number of Blows	Total Penetration (inches)	Blows Per Foot
-71.00 ^a	74.00	Stopped Here on PA2-Initial			
-71.08 ^a	74.08	22,750	60	1	720
-71.17 ^b	74.17	22,750	44	1	528
-71.25	74.25	22,000	44	1	528
-71.33	74.33	22,750	60	1	720
-71.42	74.42	22,750	50	1	600
-71.50	74.50	22,000	40	1	480
-71.75	74.75	23,500	98	3	392
-72.00 ^c	75.00	23,500	50	3	200
-72.25 ^c	75.25	23,500	50	3	200
-72.50 ^c	75.50	23,500	45	3	180
-72.75 ^c	75.75	22,750	45	3	180
-73.00 ^c	76.00	22,750	52	3	208
-73.25 ^c	76.25	22,000	55	3	220
-73.50 ^c	76.50	22,000	48	3	192
-73.75 ^c	76.75	22,000	53	3	212
-74.00 ^c	77.00	22,000	50	3	200
-74.25	77.25	22,000	50	3	200
-74.50	77.50	22,000	50	3	200
-74.75	77.75	21,200	54	3	216
-75.00	78.00	21,200	58	3	232
-75.25	78.25	23,500	50	3	200
-75.50	78.50	23,500	25	3	100
-75.75	78.75	23,500	31	3	124
-76.00	79.00	23,500	30	3	120
-76.25	79.25	22,750	31	3	124
-76.50	79.50	22,750	35	3	140

^aDriven with cushion.

^bFirst blow without cushion.

^cBlow count without cushion averaged to be 200 blows per foot.

TABLE II-11 -- COMPUTER INPUT DATA FOR PA2 INITIAL

Hammer Properties

Type: Link Belt 520
Rated energy: 26,300 ft-lb
Hammer efficiency (%): 100
Explosive force: 98 kips
Ram velocity: 15.16 fps
Ram weight: 5.07 kips
Ram stiffness: 108,500 kips/in.,
e = 0.6 (steel on steel impact)
Anvil weight: 1.179 kips
Adapter weight: 1.05 kips
Capblock: Alternating aluminum and plastic
disks (enclosed). $K_c = 18,600$ kips/in., e = 0.8
Cushion: None

Pile Properties

Type: 16 in. OD, 3/8 in. wall, closed end steel pipe
Segment length: 2 ft
Segment weight: 0.1252 kip
Segment stiffness: 22,700 kips/in., e = 1.0

Soil Distribution

RUT: 108 kips
RUP: 16.0 kips
Load distribution: 0.85 RUT uniform side load,
0.15 RUT at pile tip

TABLE II-12 - COMPUTER INPUT DATA FOR PA2 FINAL

Hammer Properties

Type: Link Belt 520
Rated energy: 26,300 ft-lb
Hammer efficiency (%): 100
Explosive force: 98 kips
Ram velocity: 15.62 fps
Ram weight: 5.07 kips
Ram stiffness: 108,500 kips/in.,
 $e = 0.6$ (steel on steel impact)
Anvil weight: 1.179 kips
Adapter weight: 1.05 kips
Capblock: Alternating aluminum and plastic
 disks (enclosed). $K_c = 18,600$ kips/in., $e = 0.8$
Cushion: None

Pile Properties

Type: 16 in. OD, 3/8 in wall, closed end steel pipe
Segment length: 2 ft
Segment weight: 0.1252 kip
Segment stiffness: 22,700 kips/in., $e = 1.0$

Soil Distribution

RUT: 262 kips
RUP: 20 kips
Load distribution: 0.92 RUT uniform side load,
 0.08 RUT at pile tip

CORPUS CHRISTI TEST FILE

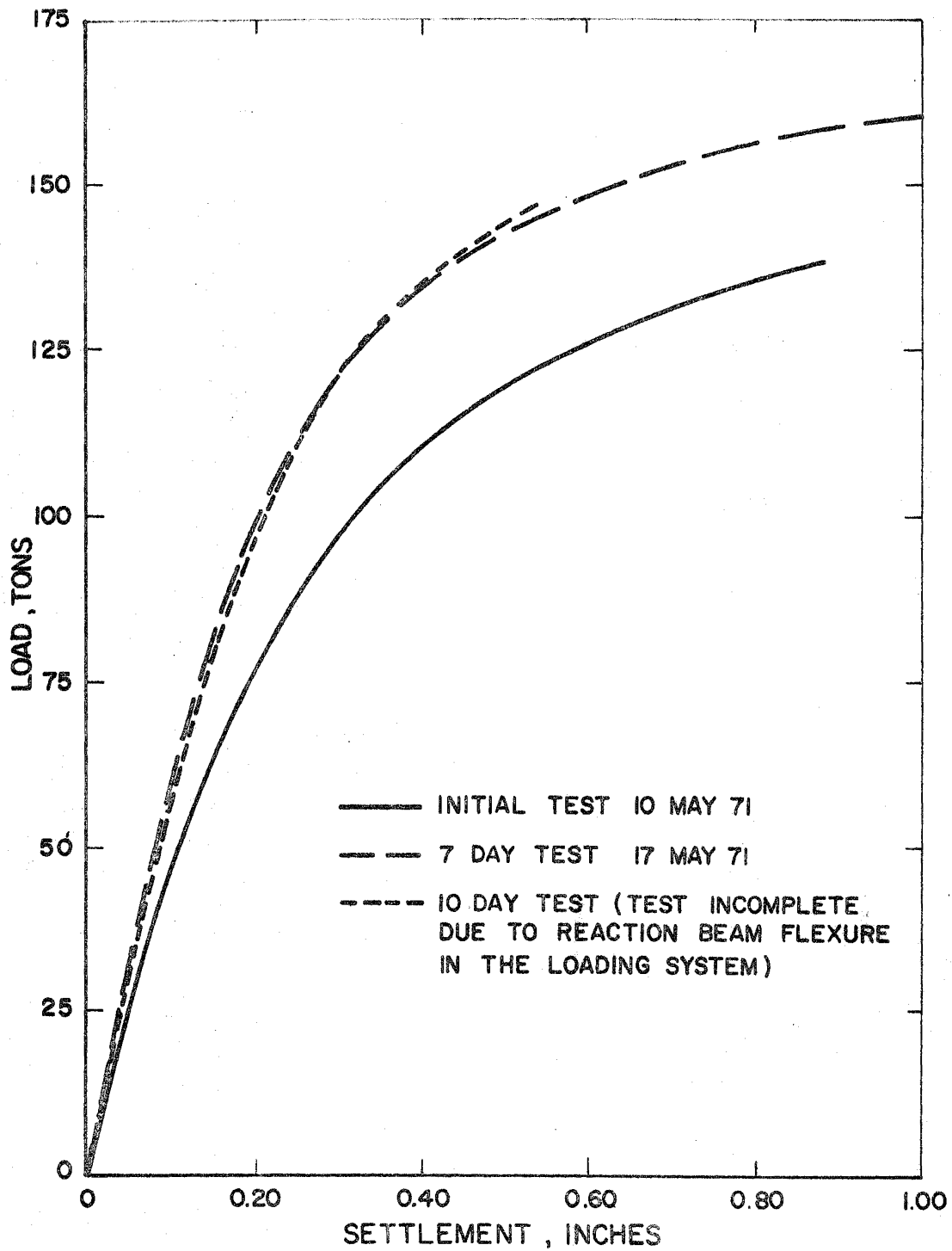


FIG. II-3- LOAD vs. SETTLEMENT CURVES FOR CORPUS CHRISTI TEST PILE

TABLE II-13 - CORPUS CHRISTI PILE LOAD TEST DATA

Initial Test 10 May 71

Jack Load (Tons)	Load Cell (Tons)	Gage 1 (Tons)	Gage 2 (Tons)	Gage 3 (Tons)
20	14.2	12.92	12.40	6.37
40	29.5	28.80	24.09	17.20
60	49.5	49.23	43.47	31.42
80	68.6	68.43	61.10	46.09
90	81.7	80.84	73.49	56.21
100	92.8	92.87	84.14	66.42
110	101.8	104.04	95.32	75.50
120	111.6	114.34	103.52	83.01
130	119.0	121.68	111.20	89.64
140	127.7	131.10	119.23	98.20
147	133.7	138.26	127.26	106.40

TABLE II-14 - CORPUS CHRISTI PILE LOAD TEST DATA

Final Test 17 May 71

Jack Load (Tons)	Load Cell (Tons)	Gage 1 (Tons)	Gage 2 (Tons)	Gage 3 (Tons)
20	18.0	17.18	12.89	7.34
40	37.4	35.44	28.82	18.88
60	54.8	53.88	42.25	30.88
80	75.6	74.65	61.40	44.75
90	85.5	84.31	71.42	52.09
100	93.8	93.26	78.94	58.18
110	103.0	102.39	86.82	64.35
120	111.0	111.52	96.84	70.89
130	120.0	121.90	105.62	77.51
140	129.5	130.50	113.13	84.49
150	140.0	142.31	123.52	93.29
160	149.6	152.69	131.39	103.02
170	157.0	161.11	139.27	112.15

TABLE II-15 - CORPUS CHRISTI INITIAL PILE DRIVING DATA

Pile Tip Elevation (ft)	Depth of Pile in Ground (ft)	Stroke of Hammer (ft)	Number of Blows	Total Penetration (inches)	Blows Per Foot
- 6.5	9.5	Approximately 5 ft. alignment hole			
-15.0	18.0	5.00	24	102	3
-16.0	19.0	4.50	18	12	18
-17.0	20.0	4.50	18	12	18
-18.0	21.0	4.50	19	12	19
-19.0	22.0	4.75	19	12	19
-19.5	22.5	5.00	10	6	20
-20.0	23.0	4.50	10	6	20
-20.5	23.5	4.50	11	6	22
-21.0	24.0	5.00	9	6	18
-21.5	24.5	4.75	12	6	24
-22.0	25.0	4.75	8	6	16
-22.5	25.5	4.75	11	6	22
-23.0	26.0	4.75	11	6	22
-23.5	26.5	5.00	10	6	20
-24.0	27.0	5.00	10	6	20
-24.5	27.5	4.75	11	6	22
-25.0	28.0	5.00	10	6	20
-25.5	28.5	5.00	11	6	22
-25.7 ^a	28.7	5.00	8	3	32
-26.2	29.2	5.25	13	3	52
-26.6 ^b	29.6	5.00	7	3.75	22
-26.9 ^c	29.9	5.00	12	4	36
-27.1	30.1	5.50	7	2.25	37
-27.5 ^d	30.5	5.25	16	5	38
-28.0	31.0	5.00	18	6	36
-28.5	31.5	5.25	20	6	40
-28.9 ^e	31.9	5.50	14	4.5	37
-29.0 ^e	32.0	5.50	5	1.5	40
-29.3	32.3	5.50	12	3.5	41
-29.5 ^f	32.5	5.75	9	2.5	43
-30.0 ^f	33.0	5.75	23	6	46
-30.2 ^f	33.2	5.75	13	3	52
-30.5 ^f	33.5	5.50	11	3	44
-30.7 ^f	33.7	5.50	9	2	54

^aStopped 33 minutes.

^bStopped 10 minutes.

^cStopped 7 minutes.

^dStopped 6 minutes.

^eStopped 2 minutes.

^fBlow count averaged to be 48 blows per foot.

TABLE II-16 - CORPUS CHRISTI FINAL PILE DRIVING DATA

Pile Tip Elevation (ft)	Depth of Pile in Ground (ft)	Stroke of Hammer (ft)	Number of Blows	Total Penetration (inches)	Blows Per Foot
-30.86	33.9				
-30.9 ^a	33.9	6.00	18	1	216
-31.0 ^b	34.0	6.50	7	1	84
-31.1 ^{b,c}	34.1	6.25	8	1	96
-31.2 ^b	34.2	6.00	6	1	72
-31.3 ^b	34.3	6.00	7	1	84
-31.4 ^b	34.4	5.75	7	1	84
-31.4	34.4	5.50	7	1	84
-31.5	34.5	5.25	8	1	96
-31.6	34.6	5.50	9	1	108
-31.7	34.7	5.50	8	1	96
-31.8	34.8	5.50	8	1	96
-31.9	34.9	5.25	9	1	108
-32.1	35.1	5.50	19	2	114
-32.3	35.3	5.50	33	3	132
-32.6 ^d	35.6	5.50	31	3	124
-32.9	35.9	6.25	33	3	132
-33.1	36.1	6.25	32	3	128
-33.4	36.4	6.00	34	3	136
-33.6 ^e	36.6	6.50	44	3	176
-33.9	36.9	6.50	39	3	156
-34.1	37.1	6.25	41	3	164
-34.4	37.4	6.25	46	3	184
-34.6	37.6	6.00	43	3	172
-34.9	37.9	6.25	54	3	216
-35.0	38.0	6.00	46	3	184

^a9 blows with no explosion. Stopped 2 minutes.

^bBlow count averaged to be 84 blows per foot.

^cStopped 10 minutes.

^dStopped 3 minutes.

^eStopped 5 minutes.

TABLE II-17 - COMPUTER INPUT DATA FOR CC INITIAL

Hammer Properties

Type: Delmag D-22
Rated energy: 39,700 ft-lb
Hammer efficiency (%): 100
Explosive force: 158.7 kips
Ram velocity: 17.1 fps
Ram weight: 4.85 kips
Ram stiffness: 49,700 kips/in.,
e = 0.6 (steel on steel impact)
Anvil weight: 1.576 kips
Helmet weight: 1.3 kips
Capblock: Oak block, 18 in. x 18 in. x 9 in. thick
(grain vertical), $K_c = 23,800$ kips/in., e = 0.8
Cushion: 7 sheets of 3/4 in. plywood fir, $K_c = 1,705$
kips/in., $K_c + p = 1.595$ kips/in., e = 0.5

File Properties

Type: 16 in. square prestressed concrete
Segment length: 2 ft
Segment weight: 0.516 kip
Segment stiffness: 59,750 kips/in., e = 1.0

Soil Distribution

RUT: 268 kips
RUP: 212 kips
Load distribution: 0.209 RUT uniform side load,
0.791 RUT at pile tip

TABLE II-18 - COMPUTER INPUT DATA FOR CC FINAL

Hammer Properties

Type: Delmag D-22
Rated energy: 39,700 ft-lb
Hammer efficiency (%): 100
Explosive force: 158.7 kips
Ram velocity: 17.3 fps
Ram weight: 4.85 kips
Ram stiffness: 49,700 kips/in.,
e = 0.6 (steel on steel impact)
Anvil weight: 1.576 kips
Helmet weight: 1.3 kips
Capblock: Oak block, 18 in. x 18 in. x 9 in. thick
(grain vertical), $K_c = 23,800$ kips/in., e = 0.8
Cushion: 7 sheets of 3/4 in. plywood fir, $K_c = 1,705$
kips/in., $K_{c+p} = 1,595$ kips/in., e = 0.5

File Properties

Type: 16 in. square prestressed concrete
Segment length: 2 ft
Segment weight: 0.516 kip
Segment stiffness: 59,750 kips/in., e = 1.0

Soil Distribution

RUT: 314 kips
RUP: 224 kips
Load distribution: 0.287 RUT uniform side load,
0.713 RUT at pile tip

HARLINGEN TEST PILE NO. 99R

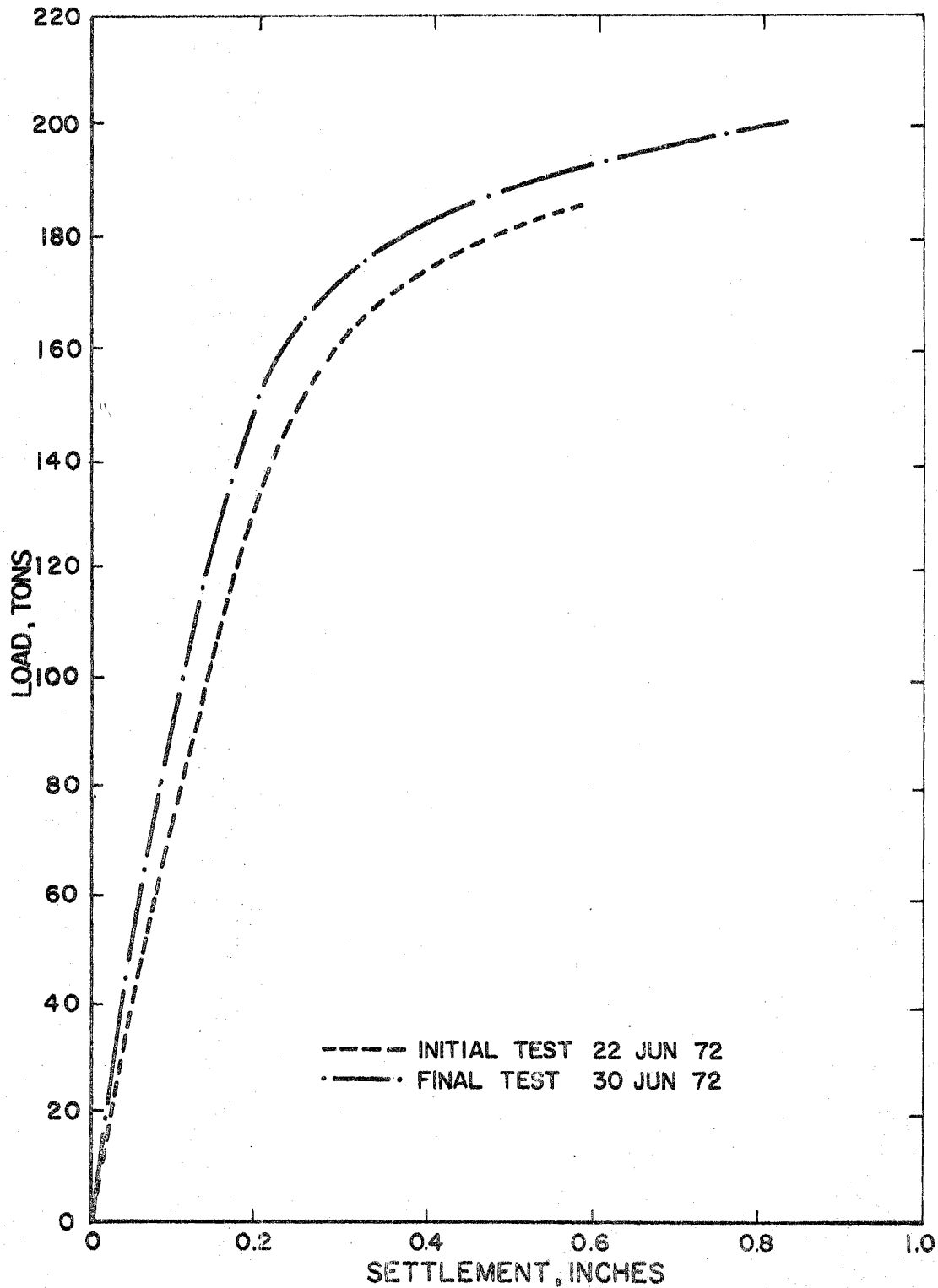


FIG. II-4- LOAD vs. SETTLEMENT CURVES FOR HARLINGEN PILE LOAD TEST AT BENT 99R

TABLE II-19 - HARLINGEN PILE LOAD TEST DATA

No. 99R 22 Jun 72 Initial Load Test

Jack Load (Tons)	Load Cell (Tons)	Gage 1 (Tons)	Gage 2 (Tons)	Gage 3 (Tons)
0	00	0	0	0
10	---	---	---	---
20	16.3	17.1	14.0	5.3
			21.9	
30	25.8	26.3	21.9	9.2
40	35.0	35.0	30.7	13.2
50	45.3	44.7	39.5	18.0
60	53.8	53.0	47.3	22.4
70	65.1	65.3	57.9	28.9
80	75.9	76.7	68.8	35.9
90	85.1	85.9	76.3	40.8
100	94.9	97.8	87.7	47.3
110	106.3	107.8	97.3	54.5
120	114.7	115.7	105.2	59.6
130	125.0	126.3	115.3	67.5
140	135.0	136.8	125.4	75.0
150	146.0	147.3	135.9	83.3
160	155.9	156.9	146.9	92.1
170	164.3	166.6	157.4	98.6
180	173.9	176.7	166.6	107.0
185	178.6	180.6	171.9	112.2
190	184.9	186.8	177.1	115.7

TABLE II-20 - HARLINGEN PILE LOAD TEST DATA

No. 99R 30 Jun 72 Final Load Test

Jack Load (Tons)	Load Cell (Tons)	Gage 1 (Tons)	Gage 2 (Tons)	Gage 3 (Tons)
0	0	0	0	0
10	6.78	6.1	5.3	1.8
20	18.1	17.1	14.9	5.7
30	26.9	24.6	21.0	8.8
40	35.5	33.3	29.8	12.7
50	45.3	42.5	36.8	16.7
60	54.3	51.3	45.2	21.0
70	64.1	60.1	53.5	26.3
80	75.7	72.3	63.6	32.0
90	85.3	82.0	73.2	37.3
100	96.4	92.1	82.9	43.0
110	105.6	101.7	91.6	48.7
120	114.8	110.5	101.3	54.8
130	126.4	121.0	111.4	61.4
140	137.1	132.4	122.3	68.4
150	146.7	141.6	131.5	74.5
160	155.8	150.8	140.7	81.5
170	165.1	161.3	150.8	88.1
180	175.0	169.2	159.6	95.6
190	183.0	178.9	168.8	103.5
195	188.5	182.8	173.6	109.2
200	195.8	190.7	181.1	114.0
205	199.0	192.5	184.1	118.4
200	---	---	---	---

TABLE II-21 - HARLINGEN 99R INITIAL PILE DRIVING DATA

Pile Tip Elevation (ft)	Depth of Pile in Ground	Energy of Hammer (ft-lb)	Number of Blows	Total Penetration (inches)	Blows Per Foot
37.31	3.94		20	16.5	14
35.94	5.31	17250	20	14.5	16
34.73	6.52	18250	20	17.0	14
33.31	7.94	18250	20	22.0	11
31.48	9.77	19500	20	17.0	14
30.06	11.19	22870	20	12.0	20
29.06	12.19	24375	20	7.5	32
28.44	12.81	24750	20	7.25	33
27.83	13.42	24750	20	7.25	33
27.23	14.02	25150	20	7.75	31
26.58	14.67	25150	20	7.75	31
25.94	15.31	24375	20	4.5	53
25.56	15.69	24375	20	3.0	80
25.31	15.94	24375	19	1.75	130
25.17	16.08	24750	20	3.25	74
24.90	16.35	24750	20	4.75	51
24.50	16.75	24375	20	4.00	60
24.17	17.08	25150	20	3.75	64
23.85	17.40	24750	20	3.25	74
23.58	17.67	24750	14	.75	224
23.52	17.73	24375	12	1.25	115
23.42	17.83	25150	20	2.25	107
23.23	18.02	25150	20	3.00	80
22.98	18.27	25150	20	3.25	74
22.71	18.54	24750	20	2.75	87
22.48	18.77	24750	20	2.75	87
22.29	18.96	25150	20	2.25	107
22.00	19.85	25150	20	3.5	69

TABLE II-22 - HARLINGEN 99R FINAL PILE DRIVING DATA

Pile Tip Elevation (ft)	Depth of Pile in Ground	Energy of Hammer (ft-lb)	Number of Blows	Total Penetration (inches)	Blows Per Foot
21.82	19.15				
21.74	19.23	24425	20	1	240
21.65	19.32	25500	12	1	144
21.57	19.40	24750	18	1	216
21.49	19.48	25500	15	1	180
21.40	19.57	25125	10	1	120
21.32	19.65	25125	10	1	120
21.24	19.73	25500	10	1	120
21.15	19.82	25125	10	1	120
21.07	19.90	25500	10	1	120
20.98	19.98	25125	10	1	120
20.90	20.07	25125	10	1	120
20.82	20.15	25500	10	1	120
20.57	20.40	25500	28	3	112
20.32	20.65	25125	26	3	104
20.07	20.90	25500	44	3	176
19.82	21.15	25750	34	3	136
19.57	21.40	25750	34	3	136
19.32	21.65	25750	34	3	136
19.20	21.77	25750	17	1.5	136

TABLE II-23 - COMPUTER INPUT DATA FOR HARLINGEN 99R INITIAL

Hammer Properties

Type: Link Belt 520
Rated energy: 26,300 ft-lb
Hammer efficiency (%): 100
Explosive force: 98 kips
Ram velocity: 16.35 fps
Ram weight: 5.07 kips
Ram stiffness: 108,500 kips/in.,
e = 0.6 (steel on steel impact)
Anvil weight: 1.179 kips
Helmet weight: 1.85 kips
Capblock: $K_C = 18,600$ kips/in., e = 0.65
Cushion: 2 1/4 in. of 3/4 in. x 16 in. x 16 in. Pine Plywood
e = 0.4

Pile Properties

Type: 16 in. square prestressed concrete
Segment length: 2 ft
Segment weight: 0.534 kips
Segment stiffness: 73,100 kips/in., e = 1.0

Soil Distribution

RUT: 370 kips
RUP: 232 kips
Load distribution: 0.043 RUT uniform side load on upper
5 ft, 0.330 RUT uniform side load on lower 10 ft,
0.627 RUT at pile tip

TABLE II-24 - COMPUTER INPUT DATA FOR HARLINGEN 99R FINAL

Hammer Properties

Type: Link Belt 520
Rated energy: 26,300 ft-lb
Hammer efficiency (%): 100
Explosive force: 98 kips
Ram velocity: 16.20 fps
Ram weight: 5.06 kips
Ram stiffness: 108,500 kips/in.,
e = 0.6 (steel on steel impact)
Anvil weight: 1.1790 kips
Helmet weight: 1.850 kips
Capblock: $K_c = 18,600$ kips/in., e = 0.65
Cushion: 2 1/4 in. of 3/4 in. x 16 in. x 16 in. Pine Plywood
e = 0.4

File Properties

Type: 16 in. square prestressed concrete
Segment length: 2 ft
Segment weight: 0.534 kips
Segment stiffness: 73,100 kips/in., e = 1.0

Soil Distribution

RUT: 398 kips
RUP: 236 kips
Load distribution: 0.075 RUT uniform side load on upper
5 ft, 0.332 RUT uniform side load on lower 10 ft,
0.593 RUT at pile tip

HARLINGEN TEST PILE NO. 4L

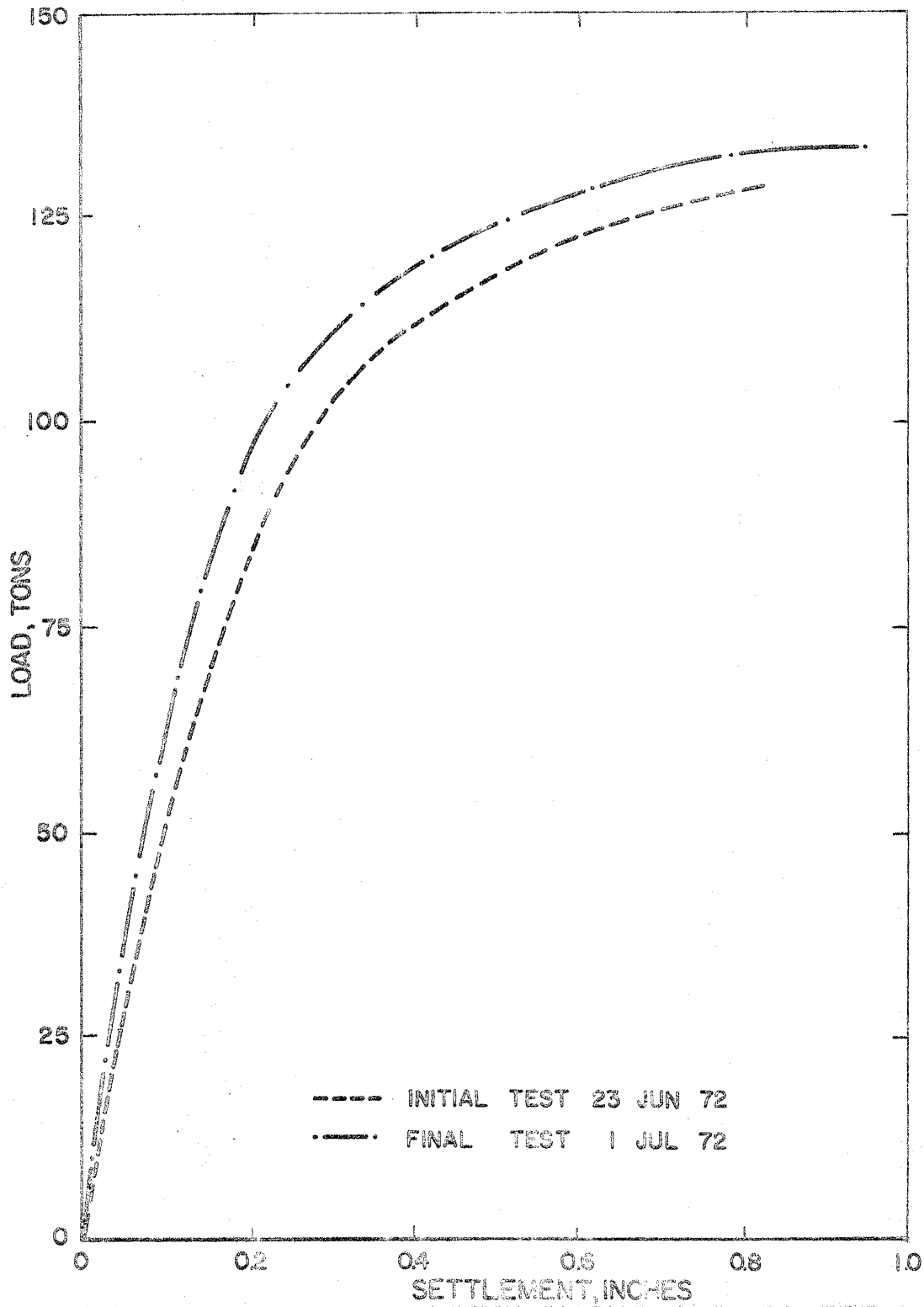


FIG. II- 5- LOAD vs. SETTLEMENT CURVES FOR HARLINGEN PILE LOAD TEST AT BENT 4L

TABLE II-25 - HARLINGEN PILE LOAD TEST DATA

No. 4L 23 Jun 72 Initial Load Test

Jack Load (Tons)	Load Cell (Tons)	Gage 1 (Tons)	Gage 2 (Tons)	Gage 3 (Tons)
0	0	0	0	0
10	6.78	7.9	4.4	2.6
20	18.4	18.9	14.5	7.9
30	26.7	27.2	21.9	11.8
40	37.0	36.0	31.6	18.0
50	46.2	44.7	40.3	23.2
60	54.7	52.2	48.2	28.1
70	64.6	60.5	56.6	32.9
80	76.1	71.0	67.5	39.5
90	86.5	81.1	79.8	47.8
100	96.8	91.2	88.6	54.4
105	101.7	91.4	92.1	58.7
110	106.1	101.7	97.8	62.7
115	110.7	107.0	102.6	66.6
120	115.0	111.8	107.4	70.6
125	119.3	116.6	112.2	74.5
130	124.9	122.8	115.7	78.5
135	128.6	127.1	119.2	81.5

TABLE II-26 - HARLINGEN PILE LOAD TEST DATA

No. 4L 1 Jul 72 Final Load Test

Jack Load (Tons)	Load Cell (Tons)	Gage 1 (Tons)	Gage 2 (Tons)	Gage 3 (Tons)
0	0	0	0	0
10	4.83	4.8	3.5	2.2
20	15.4	14.9	12.3	6.6
30	25.2	25.4	21.5	11.0
40	34.8	34.6	30.7	16.2
50	44.6	43.8	39.9	21.9
60	53.7	52.2	47.8	28.1
70	63.8	60.5	57.9	29.8
80	74.3	71.5	68.4	36.4
90	83.8	81.5	79.4	45.6
100	94.9	93.8	89.0	53.9
105	98.8	99.1	93.4	57.4
110	104.5	104.3	98.2	60.5
115	107.9	108.7	103.5	64.0
120	112.7	113.1	108.7	69.3
125	118.2	118.4	112.2	72.3
130	123.0	124.5	117.1	78.0
135	127.1	128.0	123.2	82.9
140	132.8	132.8	128.9	87.7
137	131.1	133.3	125.4	85.9

TABLE II-27 - HARLINGEN 4L INITIAL PILE DRIVING DATA

Pile Tip Elevation (ft)	Depth of Pile in Ground	Energy of Hammer (ft-lb)	Number of Blows	Total Penetration (inches)	Blows Per Foot
39.0	5.8		13	12	13
38.0	6.8		11	12	11
37.0	7.8		10	12	10
36.0	8.8		10	12	10
35.0	9.8		10	12	10
34.0	10.8	16750	9	12	9
33.0	11.8	18125	9	12	9
32.0	12.8	17700	9	12	9
31.0	13.8	18200	9	12	9
30.0	14.8	18200	13	12	13
29.0	15.8	20300	12	12	12
28.4	16.4	22000	19	7.25	31
28.0	16.8	22800	12	4.75	30
27.5	17.3	24000	8	6	16
27.0	17.8	24375	13	6	26
26.5	18.3	24375	17	6	34
26.0	18.8	24750	17	6	34
25.5	19.3	24750	17	6	34
25.2	19.6	24375	10	3.5	34
25.0	19.8	24375	9	2.5	43
24.4	20.4	24375	12	6	24
23.9	20.9	24750	9	6	18
23.7	21.1	24750	3	3	12
	Using last 20 blows		8	4	24
23.7	21.1	24750	9	6	18
			3	3	12

TABLE II-28 - HARLINGEN 4L FINAL PILE DRIVING DATA

Pile Tip Elevation (ft)	Depth of Pile in Ground	Energy of Hammer (ft-lb)	Number of Blows	Total Penetration (inches)	Blows Per Foot
23.39	21.41	24425	6	1	72
23.30	21.50	24425	6	1	72
23.22	21.58	24425	6	1	72
23.14	21.66	24425	6	1	72
23.05	21.75	24425	12	1	144
22.97	21.83	24425	12	1	144
22.89	21.91	24425	12	1	144
22.80	22.00	24425	12	1	144
22.72	22.08	24425	12	1	144
22.64	22.16	24425	12	1	144
22.55	22.25	24425	12	1	144
22.47	22.33	24425	12	1	144
22.22	22.58	24750	24	3	96
21.97	22.83	24425	12	3	48
21.72	23.08	25125	12	3	48
21.47	23.33	24750	14	3	56
21.22	23.58	24425	12	3	48
20.97	23.83	24750	11	3	44
20.72	24.08	25125	12	3	48
20.47	24.33	25500	12	3	48

TABLE II-29 - COMPUTER INPUT DATA FOR HARLINGEN 4L INITIAL

Hammer Properties

Type: Link Belt 520
Rated energy: 26,300 ft-lb
Hammer efficiency (%): 100
Explosive force: 98 kips
Ram velocity: 16.15 fps
Ram weight: 5.07 kips
Ram stiffness: 108,500 kips/in.
 $e = 0.6$ (steel on steel impact)
Anvil weight: 1.179 kips
Helmet weight: 1.850 kips
Capblock: $K_c = 18,600$ kips/in., $e = 0.65$
Cushion: 2 1/4 in. of 3/4 in. x 16 in. x 16 in. Pine Plywood
 $e = 0.4$

File Properties

Type: 16 in. square prestressed concrete pile
Segment length: 2 ft
Segment weight: 0.534 kips
Segment stiffness: 73,100 kips/in., $e = 1.0$

Soil Distribution

RUT: 258 kips
RUP: 162 kips
Load distribution: 0.077 RUT uniform side load on upper
 10 ft, 0.295 RUT uniform side load on lower 8 ft,
 0.628 RUT at pile tip

TABLE II-30 - COMPUTER INPUT DATA FOR HARLINGEN 4L FINAL

Hammer Properties

Type: Link Belt 520
Rated energy: 26,300 ft-lb
Hammer efficiency (%): 100
Explosive force: 98 kips
Ram velocity: 16.00 fps
Ram weight: 5.07 kips
Ram stiffness: 108,500 kips/in.,
 $e = 0.6$ (steel on steel impact)
Anvil weight: 1.1790 kips
Helmet weight: 1.850 kips
Capblock: $K_c = 18,600$ kips/in., $e = 0.65$
Cushion: 2 1/4 in. of 3/4 in. x 16 in. x 16 in. Pine Plywood
 $e = 0.4$

File Properties

Type: 16 in. square prestressed concrete
Segment length: 2 ft
Segment weight: 0.534 kips
Segment stiffness: 73,100 kips/in., $e = 1.0$

Soil Distribution

RUT: 266 kips
RUP: 176 kips
Load distribution: 0.030 RUT uniform side load on upper
 10 ft, 0.308 RUT uniform side load on lower 8 ft,
 0.662 RUT at pile tip